Universidad Politécnica de Madrid

Escuela Técnica Superior de Ingenieros de Telecomunicación


POLITÉCNICA

**PhD DISSERTATION**

# CONTRIBUTION TO THE IMPROVEMENT OF COMMUNICATION SERVICES IN NANOSATELLITE CONSTELLATIONS USING DELAY AND DISRUPTION TOLERANT NETWORKING BASED ARCHITECTURES

Author

**Héctor Manuel Bedón Monzón**

*MSc Telematics Engineering*

Advisor

**Carlos Miguel Nieto**

*Professor in Department of Telematics Engineering (DIT-UPM) at Technical University of Madrid (UPM)*

2016

**Título de la Tesis**: *CONTRIBUTION TO THE IMPROVEMENT OF COMMUNICATION SERVICES IN NANOSATELLITE CONSTELLATIONS USING DELAY AND DISRUPTION TOLERANT NETWORKING BASED ARCHITECTURES*
**Autor**: Héctor Manuel Bedón Monzón
**Director**: Carlos Miguel Nieto

Tribunal nombrado por el Excmo. y Magfco. Sr. Rector de la Universidad Politécnica de Madrid, el día ___ de _____ de 2016

**Presidente**: _____

**Vocal**: _____

**Vocal**: _____

**Vocal**: _____

**Secretario**: _____

**Suplente**: _____

**Suplente**: _____

Realizado el acto de defensa y lectura de Tesis el día ___ de _____ de 2016 en la E.T.S. de Ingenieros de Telecomunicación de Madrid.

**Calificación:**

EL PRESIDENTE LOS VOCALES

EL SECRETARIO

*A mi linda esposa Elizabeth y a mis hijos Job, Ana, Emmy, Juan Pablo, Maria Gracia, Almudena y Francisco un regalo de Dios que hace posible lo imposible.*

# Acknowledgement

I want to thank you first to God for allowing me to come to complete this long journey of doctoral studies that a colleague told me it looks like a long-winded career. In this process, I have often hesitated to continue and have had difficulties, but thanks to that I have a great partner in this journey, my wife Elizabeth, now I appreciate and share the joy of completing the work begun several years ago. I also thank very especially my mentor Carlos Miguel who took me into his lab and trust me when I asked him to be my tutor and has continued since then to encourage me, support me and allowing me to work on research projects over the years.

I also want to thank my great friends there in the lab GISAI DIT, Ramon Alcarria, Augusto Morales, Edwin Cedeño, Diego Martin, Alvaro Sanchez and Sergio Miranda with whom I have shared joys, sorrows, jokes, famous coffees in the morning and lunch and who always carry in my heart for all those moments lived there in Madrid.

I want to thank the teachers ETSIT-UPM, Prof. Tomas Robles, Prof. Francisco Ruiz, Prof. Angel Fernandez, Prof. Ramon Martinez and Prof. Leon Vidaller who in some way or another have supported me in this process and those I am very grateful because they have been there when I needed them. I would also like to thank Prof. Salvador Landeros UNAM of Mexico for its many tips in this field. Prof. Fernando Aguado from the University of Vigo, which inspired me to continue in this line of research. Prof. Jong Sou Park of Korea University for their support to get started in this field.

I also thank the entire project team Chasqui at the National University of Engineering and especially to Margarita Mondragon, Glen Rodriguez and Jose Oliden who have been a source of constant motivation to initiate and continue these studies. I also thank prof. Doris Rojas for his confidence placed in me and her constant support.

I also thank my parents Amanda y Fermin and my brothers for always being there to share my joys and failures and always supporting me. I would also like to thank my brothers in the community of St. James the Apostle in Madrid who welcomed me and gave me his full support when I arrived to Madrid with my family to make this stay doctorate. Finally thank my children Job, Ana, Emmy, Juan Pablo, Maria Gracia, Francisco and Almudena that although children still have had to accompany me to Madrid and spend your little sufferings to adapt and then another to return.

Madrid, December 2015

# Agradecimientos

Quiero dar gracias en primer lugar a Dios por haberme permitido llegar a culminar este largo recorrido de los estudios de doctorado que un compañero me decía se parece a una carrera de largo aliento. En este proceso, muchas veces he vacilado en continuar y he tenido dificultades, pero gracias a que tengo una gran aliada en este viaje, mi esposa Elizabeth, hoy le agradezco y comparto esta gran alegría de culminar lo iniciado hace algunos años. Agradezco también muy en especial a mi tutor Carlos Miguel quien me acogió en su laboratorio y confió en mi cuando le solicité que sea mi tutor y no ha dejado desde entonces de animarme, apoyarme y permitirme trabajar en los proyectos de investigación durante todos estos años.

Quiero agradecer también a mis grandes amigos allá en el laboratorio del GISAI del DIT, a Ramón Alcarria, Augusto Morales, Edwin Cedeño, Diego Martin, Álvaro Sánchez y Sergio Miranda con quienes he compartido alegrías, tristezas, bromas, los famosos cafecitos de mañana y de almuerzo y a quienes llevo siempre en el corazón por todos esos momentos vividos allá en Madrid.

Quiero agradecer también a los profesores del ETSIT-UPM, Prof. Tomas Robles, Prof. Francisco Ruiz, Prof. Ángel Fernández, Prof. Ramón Martínez y Prof. León Vidaller quienes de alguna u otra manera me han apoyado en este proceso y de quienes estoy muy agradecido porque han estado allí cuando yo los necesitaba. Asimismo quiero agradecer al Prof. Salvador Landeros de la UNAM de México por sus muchos consejos en este campo. Al Prof. Fernando Aguado de la Universidad de Vigo, que me inspiro a seguir en esta línea de investigación. Al Prof. Jong Sou Park de la Universidad de Corea por su apoyo al iniciarme en este campo.

Agradezco también a todo el equipo del proyecto Chasqui en la Universidad Nacional de Ingeniería y en especial a Margarita Mondragón, Glen Rodríguez y José Oliden quienes han sido una fuente de motivación constante para iniciar y seguir estos estudios. También agradezco a la Prof. Doris Rojas por su confianza depositada en mí y su apoyo contante.

También agradezco a mis padres Fermín y Amanda y hermanos por siempre estar ahí compartiendo mis alegrías y fracasos y apoyándome siempre. Quiero agradecer también a mis hermanos de comunidad de la parroquia san Jaime Apóstol en Madrid que me acogieron y me brindaron todo su apoyo cuando llegue con mi familia a realizar esta estancia de doctorado. Agradezco finalmente a mis hijos Job, Ana, Emmy, Juan Pablo, María Gracia, Almudena y Francisco que aunque niños todavía han tenido que acompañarme a Madrid y pasar sus pequeños sufrimientos para adaptarse y luego otros al regresar.

Madrid, Diciembre 2015

# Keywords

DTN, aloha, nanosatellites networks, sensor networks, cubesats, waposat, ALOHAGP.

# Abstract

This thesis is developed within the framework of satellite communications in the innovative field of small satellites also known as nanosatellites (<10 kg) or CubeSats, so called from their cubic form. These nanosatellites are characterized by their low cost because they use commercial components called COTS (commercial off-the-shelf), and their small size and mass, such as 1U Cubesats (10cm * 10cm * 10cm) with approximately 1 kg mass.

This thesis is based on a proposal made by the author of the thesis to put into orbit the first Peruvian satellite in his country called Chasqui I, which was successfully launched into orbit from the International Space Station in 2014. The experience of this research work led me to propose a constellation of small satellites named Waposat to provide water quality monitoring sensors worldwide, scenario that is used in this thesis.

In this scenario and given the limited features of nanosatellites, both power and data rate, I propose to investigate a new communications architecture that allows solving in an optimal manner the problems of nanosatellites in orbit LEO due to the disruptive nature of their communications by putting emphasis on the link and application layers.

This thesis presents and evaluates a new communications architecture to provide services to terrestrial sensor networks using a space Delay/Disruption Tolerant Networking (DTN) based solution. In addition, I propose a new multiple access mechanism protocol based on extended unslotted ALOHA that takes into account the priority of gateway traffic, which we call ALOHA multiple access with gateway priority (ALOHAGP) with an adaptive contention mechanism. It uses satellite feedback to implement the congestion control, and to dynamically adapt the channel effective throughput in an optimal way. We assume a finite sensor population model and a saturated traffic condition where every sensor always has frames to transmit. The performance was evaluated in terms of effective throughput, delay and system fairness. In addition, a DTN convergence layer (ALOHAGP-CL) has been defined as a subset of the standard TCP-CL (Transmission Control Protocol-Convergence Layer). This thesis reveals that ALOHAGP/CL adequately supports the proposed DTN scenario, mainly when reactive fragmentation is used.

Finally, this thesis investigates an optimal DTN message (bundles) transfer using proactive fragmentation strategies to give service to a ground sensor network using a nanosatellite communications link which uses a multi-access mechanism with priority in downlink traffic (ALOHAGP). The effective throughput has been optimized by adapting the protocol parameters as a function of the current number of active sensors received from satellite. Also, there is currently no method for advertising or negotiating the maximum size of a bundle which can be accepted by a bundle agent in satellite communications for storage and delivery, so that bundles which are too large can be

dropped or which are too small are inefficient. We have characterized this kind of scenario obtaining a probability distribution for frame arrivals to nanosatellite and visibility time distribution that provide an optimal proactive fragmentation of DTN bundles. We have found that the proactive effective throughput (goodput) reaches a value slightly lower than reactive fragmentation approach. This contribution allows to use the proactive fragmentation optimally with all its advantages such as the incorporation of the security model of DTN and simplicity in protocol implementation for computers with many CPU and memory limitations.

The implementation of these contributions was initially contemplated as part of the payload of the nanosatellite QBito, which is part of the constellation of 50 nanosatellites envisaged under the QB50 project.

# Resumen

Esta tesis se desarrolla dentro del marco de las comunicaciones satelitales en el innovador campo de los pequeños satélites también llamados nanosatélites o cubesats, llamados así por su forma cubica. Estos nanosatélites se caracterizan por su bajo costo debido a que usan componentes comerciales llamados COTS (commercial off-the-shelf) y su pequeño tamaño como los Cubesats 1U (10cm*10 cm*10 cm) con masa aproximada a 1 kg.

Este trabajo de tesis tiene como base una iniciativa propuesta por el autor de la tesis para poner en órbita el primer satélite peruano en mi país llamado chasqui I, actualmente puesto en órbita desde la Estación Espacial Internacional. La experiencia de este trabajo de investigación me llevo a proponer una constelación de pequeños satélites llamada Waposat para dar servicio de monitoreo de sensores de calidad de agua a nivel global, escenario que es usado en esta tesis.

Es ente entorno y dadas las características limitadas de los pequeños satélites, tanto en potencia como en velocidad de datos, es que propongo investigar una nueva arquitectura de comunicaciones que permita resolver en forma óptima la problemática planteada por los nanosatélites en órbita LEO debido a su carácter disruptivo en sus comunicaciones poniendo énfasis en las capas de enlace y aplicación.

Esta tesis presenta y evalúa una nueva arquitectura de comunicaciones para proveer servicio a una red de sensores terrestres usando una solución basada en DTN (Delay/Disruption Tolerant Networking) para comunicaciones espaciales. Adicionalmente, propongo un nuevo protocolo de acceso múltiple que usa una extensión del protocolo ALOHA no ranurado, el cual toma en cuenta la prioridad del trafico del Gateway (ALOHAGP) con un mecanismo de contienda adaptativo. Utiliza la realimentación del satélite para implementar el control de la congestión y adapta dinámicamente el rendimiento efectivo del canal de una manera óptima. Asumimos un modelo de población de sensores finito y una condición de tráfico saturado en el que cada sensor tiene siempre tramas que transmitir. El desempeño de la red se evaluó en términos de rendimiento efectivo, retardo y la equidad del sistema. Además, se ha definido una capa de convergencia DTN (ALOHAGP-CL) como un subconjunto del estándar TCP-CL (Transmission Control Protocol-Convergency Layer). Esta tesis muestra que ALOHAGP/CL soporta adecuadamente el escenario DTN propuesto, sobre todo cuando se utiliza la fragmentación reactiva.

Finalmente, esta tesis investiga una transferencia óptima de mensajes DTN (Bundles) utilizando estrategias de fragmentación proactivas para dar servicio a una red de sensores terrestres utilizando un enlace de comunicaciones satelitales que utiliza el mecanismo de acceso múltiple con prioridad en el tráfico de enlace descendente (ALOHAGP). El rendimiento efectivo ha sido optimizado mediante la adaptación de los parámetros del protocolo como una función del número actual de los sensores activos

recibidos desde el satélite. También, actualmente no existe un método para advertir o negociar el tamaño máximo de un "bundle" que puede ser aceptado por un agente DTN "bundle" en las comunicaciones por satélite tanto para el almacenamiento y la entrega, por lo que los "bundles" que son demasiado grandes son eliminados o demasiado pequeños son ineficientes. He caracterizado este tipo de escenario obteniendo una distribución de probabilidad de la llegada de tramas al nanosatélite así como una distribución de probabilidad del tiempo de visibilidad del nanosatélite, los cuales proveen una fragmentación proactiva óptima de los DTN "bundles". He encontrado que el rendimiento efectivo (goodput) de la fragmentación proactiva alcanza un valor ligeramente inferior al de la fragmentación reactiva. Esta contribución permite utilizar la fragmentación activa de forma óptima con todas sus ventajas tales como permitir implantar el modelo de seguridad de DTN y la simplicidad al implementarlo en equipos con muchas limitaciones de CPU y memoria.

La implementación de estas contribuciones se han contemplado inicialmente como parte de la carga útil del nanosatélite QBito, que forma parte de la constelación de 50 nanosatélites que se está llevando a cabo dentro del proyecto QB50.

# Contents

# List of figures

# Lists of tables

## Tables

# Acronyms

| | |
|---|---|
| DTN | Delay/Disruption Tolerant Networking |
| LEO | Low Earth Orbit |
| ISS | International Space Station |
| ALOHAGP | Aloha Gateway Priority Protocol |
| COTS | Commercial Off-The-Shelf |
| TCP | Transport Control Protocol |
| UDP | User Datagram Protocol |
| WAPOSAT | Global Water Pollution Nanosatellite Constellation |
| AMSS | Automated Multi-Sensor System |
| GMS | Ground Monitoring Station |
| GW | Gateway |
| BER | Bit Error Rate |
| GS-DGT | Ground Station for Data Gathering |

# 1 Introduction

There is currently great interest in developing low-cost small satellites (< 50 Kg) in LEO orbit, called nanosatellites or CubeSats, first developed by Stanford University and California Technical University [1]. Today a large number of projects at universities and research centers are developing this type of small satellite [2]. Currently, many ideas for nanosatellite constellations mission have been proposed [3] but in particular there are already initiatives under way to implement a nanosatellite constellation for space monitoring, such as QB50 [4] or ground sensors monitoring as is the case of HUMSAT [5].

Hence, these nanosatellites become key elements to provide effective communication services between sensors located inside the nanosatellite as QB50 or distributed in ground places like HUMSAT to terrestrial gateways and from there to the mission control center using Internet network. I research these general scenarios in this thesis. Nanosatellites are mainly located in LEO (Low Earth Orbit), either alone or in network, forming a swarm type constellation that provides very intermittent and disruptive communication links.

The search for a solution to provide efficient communication in such a context offers interesting challenges in nanosatellite based technology. This is due primarily to the low data rate and the intrinsic characteristics of LEO satellite links such as limited contact time, satellite multiple access complexity, link error rates and store-forward mechanisms. However, in turn they have favorable characteristics such as low attenuation loss and low delay in communication with the ground segment due to their short propagation path. The impact on performance also depends on the design of the link (type of constellation, link margin, coding and modulation) and operational conditions (link obstructions, weather conditions, fading, energy constraint, etc.) that are not part of our research work.

Currently, a few solutions have emerged from a global perspective of a communication infrastructure that allows using the great potential of these nanosatellite constellations to provide efficient simple data transmission with multiple access in a highly disruptive environment as appears in these scenarios and be transparently

integrated into the Internet network. In this dissertation, in order to address some of these nanosatellite communication services, I study this new nanosatellite technology, application scenarios, Internet technologies limitations and propose a new architecture based on DTN [6], using a new multiple access strategy (ALOHAGP) [7] and finally an efficient message transfer using a proactive fragmentation strategy is investigated.

## Document structure

This dissertation is structured as follows:

Chapter 2, Motivation, Goals and Objectives, describes the motivation of the thesis, the goals to achieve and the particular objectives to achieve the goals.

Chapter 3, State of the art analyzes related work regarding the proposed contributions and how these contributions fulfill the objectives stated in Chapter 2.

Chapter 4, Nanosatellite Networks and Internetworking, identifies nanosatellite technologies, proposes use case of nanosatellite networks studied in this thesis and finally conventional Internet protocols to provide communication services using this use case are analyzed.

Chapter 5, Definition of Delay/Disruption Tolerant Network Architecture, proposes a new DTN architecture that supports the scenarios identified in Chapter 4.

Chapter 6, Multiple Access Design and Analysis, proposes a new multiple access protocol (ALOHAGP) with an adaptive contention mechanism to provide an efficient and fair channel use of ground wireless sensor networks.

Chapter 7, Delay/Disruption Tolerant Networking Optimization, investigates an optimal DTN message transfer using a proactive fragmentation strategy to give service to ground wireless sensor networks.

Finally, Chapter 8, Conclusions and Future Works, summarizes the achievements of the contributions of this thesis work and describes future and current research lines continuing the work of this dissertation.

# 2 Motivation, goals and objectives

In this section, we describe the motivation of the thesis and the goals to achieve. In addition, how these goals turn into particular objectives.

## 2.1 Motivation

This thesis is motivated by the need to explore and propose contributions that enhance satellite communication services between a constellation of nanosatellites and ground stations (sensors, gateways) in a simple, efficient, optimal way, automatically and transparently integrated into Internet.

The new small satellite technology started by the universities of Stanford and Calpoly as mentioned above, has awakened a great interest in development research centers, universities and companies mainly for its low-cost implementation due to its small size and the use of commercial off the shelf components (COTS). This is the case of Chasqui I nanosatellite, currently in orbit, proposed and developed in the initial phase by me as part of this thesis as it is described in chapter 4. The identification of the limitations and advantages of this new nanosatellite technology is a key aspect that I have achieved in this thesis through direct participation in the development of this nanosatellite.

The ability of nanosatellites to access areas with limited infrastructure as it exists in the regions of developing countries opens great opportunities for the application of this technology, which allows me to propose a solution based on the use of nanosatellites to monitor a network of ground sensors for environmental monitoring.

Using existing conventional Internet protocols is also explored in this thesis to address the problems arising in this new type of application scenario.

Nanosatellites in LEO orbit have limited access time with the ground segment ranging from several seconds to minutes, so it is necessary to propose a new communication architecture that supports disruptive communications.

The necessity to provide access to limited nanosatellite resources such as bandwidth, power and storage capacity to service a group of ground sensors within the nanosatellite

coverage leads us to explore a multiple access mechanism that is efficient, fair and takes into account the priority of the nanosatellite downlink data.

Optimizing message transfer takes us to evaluate different strategies of message fragmentation in the DTN layer in this new type of architecture.

## 2.2 Goals and Objectives

*The goal of this thesis is to contribute to the improvement of satellite communication services between a constellation of nanosatellites and ground stations (sensors, gateways) in a simple, efficient, optimal manner, and automatically and transparently integrated into Internet. This is achieved through the study of this new technology, potential application scenarios, the limitations of the current Internet technology and the proposal of a new architecture of communications, a new multiple access protocol and a new fragmentation strategy for efficient message transfer.*

Contributing to the improvement of communication services involves a study of this new technology, potential applications and the limitations of current Internet mechanisms. I have started characterizing and identifying the limitations and advantages of this new nanosatellite technology, proposing potential scenarios where this new technology may have applications like a constellation of nanosatellites aimed to provide communication services to a network of ground or space sensors and studying the limitations of current Internet technology applied to this new scenario. Finally, nanosatellites into LEO orbit exhibit disruptive communications with the ground segment mainly because this is outside the coverage of the nanosatellite, causing loss of information, so a solution that takes into account the nature of such satellite communication should be proposed and should be automatically and transparently integrated into Internet. These considerations lead me to propose the following specific objective:

**Objective #1** To propose a new communication architecture that supports the type of application scenario identified in this thesis, which allows automatic and transparently disruptive communications to be integrated into Internet.

Nanosatellites resources are quite limited especially concerning satellite channel, power and storage capacity of the satellite. Therefore, it is necessary to propose a simple mechanism for multiple access in order to provide service to a network of sensors located within the satellite coverage, taking into account the priority of the nanosatellites downlink data due to their limited storage capacity and energy. In this sense, I establish the following objective:

**Objective #2** To propose a new multiple access protocol to provide communication services to a network of ground sensors, which will take into account the limited storage

capacity, energy of nanosatellite and the priority in downlink data from the nanosatellite.

Finally, in order to optimize the satellite resource I propose to study a fragmentation mechanism that takes into account features such as the distribution of visibility and frequency of contacts between the satellite and the ground segment. From here, I can set the following specific objective:

**Objective #3** To explore a new fragmentation strategy that enables optimal transfer of messages within the DTN architecture proposed in **Objective #1**.

# 3 State of the Art

This section discusses the status of the work related to the proposed contributions in this thesis.

I will start this chapter showing a review of current initiatives in the field of small satellites also called nanosatellites or CubeSats. In addition, I include those that have been developed in Latin America specifically in Peru through the Chasqui I project; an initiative that has been proposed to me and that has served as an initial framework for the development of this thesis.

Real scenarios where this new small satellite technology is used are then displayed. Then, the multiple access protocols used for communication satellites are analyzed targeting those that are simpler to implement in the case of CubeSats, given its limited processing capacity. Given the disruptive nature of satellites communications in LEO orbit, I analyze architectures that have been proposed to address this type of disruptive scenarios. Finally, we show the current fragmentation mechanisms that optimize this type of disruptive satellite communications.

## 3.1 Nanosatellites

From the initial ideas of nanosatellites development made mainly by the universities of Stanford and the University of California in 2000 [1], in recent years, the number of projects involving the development of low-cost small satellites that make use of COTS (Commercial Off-The-Shelf) components has been increasing very fast like an exponential curve having actually more than 375 CubeSats launched [2]. Particularly in Latin America we have successfully experience with the Libertad I [3] CubeSat project. Specifically in my country due to enormous importance of the satellite technology in various application fields such as telecommunications, earth observation, environmental monitoring and urban planning among other and the little experience on Aerospace field the National University of Engineering (UNI by Spanish acronym) started in 2008 a first

country nanosatellite project proposed by me and called Chasqui I [4], to acquire knowledge in aerospace technology. Chasqui I was launched successfully on august 2014 from the International Space Station (ISS). Additionally other two Peruvian universities have launched two CubeSats called PUCP-SAT 1 and UAPSAT built by Universidad Catolica del Peru [5] and Universidad Alas Peruanas [6] respectively.

## 3.2 Application sceneries

The great potential utility of nanosatellites both individually as forming constellations for monitoring ground sensors, earth observation, providing Internet access to areas with limited communications infrastructure and the study of outer space are some of the major applications which today are already being implemented and others are even proposals, but they are changing the rules in the field of satellite technology. Following are the initiatives that are being implemented:

- Terrestrial Monitoring

In the field of terrestrial monitoring using small satellites we have the HumSAT [7] system currently in implementation. The main purpose of the HumSAT system is the development of a satellite based system for connecting a set of users with a network of worldwide-distributed sensors that they have previously deployed. Sensors will be responsible for acquiring user data and for transmitting it to the satellites through a standard radio interface. Users will be able to define their own sensors, for monitoring different types of parameters; for example, water temperature or wind speed. A specific application of the Humsat concept for water quality monitoring terrestrial sensors in rivers and lakes using 40 nanosatellites is the WAPOSAT project proposed by me as part of my thesis research [8].

- Space and atmospheric research

Applications for atmospheric research are given by projects currently in implementation as the QB50 project [9]. QB50 has the scientific objective to study in-situ the temporal and spatial variations of a number of key parameters in the lower thermosphere (between 330 and 90 km of altitude) with a network of 50 CubeSats, separated by a few hundred kilometers and carrying identical sensors. It will also study the re-entry process by measuring a number of key parameters during re-entry and by comparing predicted and actual CubeSat trajectories and orbital lifetimes. MARCO [10] is another initiative where two NASA nanosatellites were first sent into deep space. If

this flyby demonstration is successful, the technology will provide NASA the ability to quickly transmit status information about the main spacecraft after it lands on Mars. In the field of scientific research of deep space, also exist a very interesting mission idea called XSOLANTRA [11] to detect exoplanets with an array of CubeSats.

- Internet Access

The task of providing Internet access to areas with limited telecommunications infrastructure through low cost technologies have already been initiated by large technology companies such as Google through the LOON [12] project using hot air balloon as masts radiator, Facebook through the Internet.org [13] project proposes the use of drones to bring connectivity to places with limited communications infrastructure. Samsung also intends to provide Internet access through an initiative to put thousands of nanosatellites in space [14].

- Earth Observation

In the field of Earth observation, there are initiatives such as the company Planet Labs [15]. Planet Labs, is an American Earth imaging private company that designs and manufactures Triple-CubeSat miniature satellites called Doves that are then delivered into orbit as passengers on other missions. Each Dove Earth observation satellite continuously scans Earth, sending data once it passes over a ground station. Actually, Doves form a satellite constellation that provides a complete image of Earth at 3-5 m optical resolution and open data access. The images gathered by Doves provide up-to-date information relevant to climate monitoring, crop yield prediction, urban planning, and disaster response. Planet Labs has a constellation of 87 nanosatellites in orbit.

## 3.3 Multiple Access Protocols

With regard to multiple access mechanism used in a communications environment between the nanosatellites and the sensor network, both with limited processing power and connection speed it has been considered using a variant of a simple protocol to implement as Aloha. Aloha is a widely used multiple random access protocol, mainly due to its simplicity and adequate working capability for distributed wireless nodes having bursty traffic [16]. In conventional ALOHA systems, the performance of

exponential backoff algorithm in terms of measures such as throughput, delay [17], stability [18] and fairness [19] has been extensively studied. In addition, studies considering finite population model for ALOHA systems have been done in [20]. Additionally, considering traffic saturated conditions, in [21]. Finally, the maximum throughput obtained using ALOHA with multiple power level for ad hoc networks has been studied in [22] and the effect of jamming for sensor network is studied in [23].

## 3.4 Disruptive satellite communications

A common problem with communications satellite into orbit LEO stage regardless of the type of application for which it is used is the disruptive nature of communications so it is necessary to explore a communications architecture that supports disruptive communications.

Delay and Disruption Tolerant Networking is a new communications architecture designed to provide data communication services as an automated store and forward mechanism in networks, which are characterized by frequent and prolonged temporary disconnections, long delays in signal propagation and a diversity of supporting protocols below the application layer. The origin of these concepts emerged in response to the requirements set for the Interplanetary Internet (IPN) [24]. Experiments are currently being conducted using commercial satellites in orbit to validate the DTN technology and infrastructure. Such is the case of the experiments performed using Disaster Monitoring Constellation (DMC), a satellite constellation built by Surrey Satellite Technology Ltd (SSTL). Satellite images produced on the satellite are downloaded to ground stations using the DTN Bundle Protocol, which also enables proactive fragmentation [25]. NASA JPL (Jet Propulsion Laboratory) at the University of California has also carried out an experiment that uses the Deep Impact satellite in the role of relay orbiter to connect three stations located at NASA JPL, emulating space stations located in Earth, Mars and Phobos to transmit images and evaluate the performance of DTN infrastructure [26]. Finally, an experiment was performed that involves sending data from a biological experiment module at the International Space Station to a ground station using DTN architecture [27].

## 3.5 Fragmentation in disruptive satellite communications

Fragmentation studies for similar environments to the space scenario, such as the VDTN, have been developed by [28] where it has been established that the use of fragmentation allows the transfer of messages larger than the typically short contacts between vehicles, resulting in an increased delivery ratio and decreased delivery latency. Also, if the fragments of the proactive fragmentation are well adjusted to the contact opportunity, this may perform slightly better than reactive fragmentation. The effect of the fragmentation on the message delivery success have been studied on [29] showing

that the fragmentation could increase overall connectivity but it is prerequisite to know a message size and contact duration distribution. Also in [30] several fragmentation algorithms have been studied for different land scenarios. Problems of the fragmentation effect in DTN networks in space have been identified in [31]; one of them is that currently there is no method for advertising or negotiating the maximum size of a bundle that can be accepted by a bundle agent for storage or delivery. A proactive and reactive DTN fragmentation using two ground stations in order to transfer large files from space was realized in [32]. In this scenario, [33] considers that there is a strong correlation between the DTN layer and the lower layers.

# 4 Nanosatellite Networks and Internetworking

In this section I will show the main components that constitute a nanosatellite based on work done in the nanosatellite Chasqui I [4], launched into orbit from the International Space Station (ISS). Let us start with a description of the objectives of the mission, then an overview of the satellite and a brief description of the subsystems. Additionally, the characteristics of a typical ground station for these satellites are shown. In addition, in this chapter I will propose a network of nanosatellites call WAPOSAT [8] that was selected as a semifinalist in a competition of ideas of mission MIC conducted by the Japanese organization UNISEC [34] and was awarded first place as an idea Business in the competition organized by the Telecommunications ETSIT UPM. Finally, in the proposal of nanosatellite constellations populating outer space with a variety of applications, such as the one proposed above, the concern of using these topologies to allow connection between two or more terrestrial points exploring the use of standard Internet protocols arises through intersatellites links between nanosatellites [35]. For this purpose, I will consider a work I have done on [36] using a topology for the QB50 project proposal, [9] an initiative of the von Karman Institute for Fluids Dynamics (VKI) that is currently running.

## 4.1 Nanosatellite technology

### 4.1.1 Mission overview

The Chasqui I will have an LEO orbit (~400 km). The projected lifetime is between 1 and 4 months. The main payloads are two CMOS cameras in the visible and near infrared spectrum. The communication is using Amateur UHF radio. The key components are highly-efficient solar cells not proven even in space.

The satellite will be operated from the mission control center at UNI. Initially the satellite has a Launch mode where variables are initialized and sensor data acquisition

starts after requested by the onboard computer. Next it has a Control mode where the satellite is stabilized and oriented towards the Earth, for example to take pictures. Finally, the satellite has a Safe mode where basic function is activated.

### 4.1.2 Satellite overview

Chasqui I is based on CubeSat standard. The satellite configuration consisting of five stacked electronic cards which use the PC/104 standard for communicating between them as shown in Figure 1. Onboard computer card is at the bottom, then comes the Thermal and Power card connected to the batteries covered by a package specially constructed for them. Then comes this Attitude Control card and the Communication card is above it. Finally at the top is the card that supports both satellite CMOS cameras. The satellite uses coils located on the sides of the satellite and a magnet to control the attitude of the satellite.

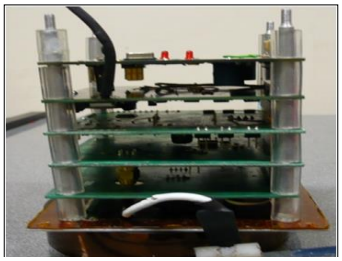

**Figure 1. Chasqui I Engineering Model**

### 4.1.3 Satellite Subsystem

#### *4.1.3.1 Power Subsystem*

The Power and Thermal Control Module (PCT) generates, regulates and distributes energy to the satellite; and maintains the temperature of the satellite components within their operation ranges. It will use for first time a high efficient solar cell in space. This subsystem uses multilayer photovoltaic cells, 28% efficiency and a rechargeable Li-Ion Batteries.

It will supply 1W average to the satellite, the outputs are 3.3V and 5.0V DC regulated. Also has a battery packing at 10 to 20ºC (50 to 68 ºF) with an active (heater) and passive (insulator) system.

#### *4.1.3.2 Attitude Determination and Control*

Chasqui I must be equipped with an attitude determination and control subsystem (SDCA) in order to perform its objectives of aiming the antenna towards the ground station, for communication, and acquiring a desired spatial orientation, for Earth photographing. SDCA is not only used to orient gradually the satellite in the desired direction despite its attitude in space but also it is used to reduce the satellite rotational kinetic energy after deployment or when necessary. High angular velocities are

undesired as they limit the use of the on-board electronics. A total rotation rate is therefore required to have to stay between 0.2 and 10 degrees per second. With the most stringent design constraints being mass, volume and power, SDCA is limited to 15% of the total satellite mass and volume, together with a maximum allocated power of 1W. An additional demand of low costs is present since Chasqui I is a university project. SDCA configuration is presented in Figure 2. Sensors for the attitude determination subsystem (SDA) are mini-GPS, magnetometers, photodiodes and gyrometers, all of them connected and housed on the ADCS board. Data are collected by a microcontroller that executes both the attitude determination and the stabilization/orientation algorithms which then sends to CCMI module. Corrections to the attitude are sent to the coil actuators. For orienting the satellite, the attitude control subsystem (SCA) will use an active LQR with magnetic actuation through magnetorquers, and two permanent magnets on the x-axis (parallel to the antenna). For dissipation of the satellite's angular velocities, SCA will use an active B-dot algorithm and hysteresis materials, the latter placed along perpendicular axes to the antenna. Preliminary results obtained with both algorithms are shown in Figure 2. SDA will use the TRIAD method to initialize an EKF (Extended Kalman Filter), which will be used to improve the accuracy of the attitude determination. The microcontroller used is the 32 bits MCF51QE128 from Freescale. The programming of the QE128 is based on the modes of operation. SPI and I2C are the protocols used by the QE128 to communicate with the sensors. The I2C protocol is also used for communication with the CCMI when SDCA data uplink or downlink is required. Elemental communication with the CCMI is performed using 4 bits. Attitude estimation will also be performed on the control center by recalculations based on the sensor data received from the satellite. A Matlab/Simulink model of the satellite and its space environment has been developed to permit an initial evaluation of the determination and control subsystems. Furthermore, a hardware-in-the-loop (HIL) simulator was implemented. The HIL simulator will run in real time and include the SDCA's hardware inside the control loop. In order to make a redundant system, additional stabilization and orientation algorithms such as a sliding mode control algorithm was implemented.

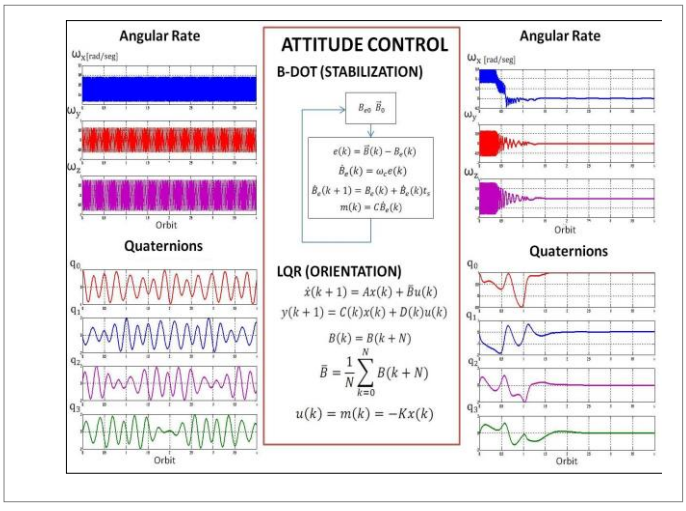


**Figure 2. Angular Velocities and Quaternions Controlled Responses.**

#### *4.1.3.3 Onboard Computer*

The onboard computer manages the satellite operations and communications between the other modules. It uses MC9S08QE128 processor (Ultra Low Power) at 4MHz with two I²C Buses, one SPI Bus and two UART Buses.

#### *4.1.3.4 Communications Subsystem*

The Communication subsystem is in charge of the communication process between the satellite and the ground station. It receives commands and transmits information to Earth. It uses a Texas Instruments MSP430 processor with Modem/transceptor Radio Unit in UHF frequency range (435 - 438 MHz) using a FSK modulation. This subsystem has been developed in collaboration with NCKU University in Taiwan.

#### *4.1.3.5 Structure and Mechanism*

The mechanical structure of Chasqui I is a hollow cube of 10 cm. edge, use made of aircraft aluminum 6061 - T6. The cube is manufactured by fusion welding the parts, using the TIG process without the addition of electrode. An exploded view is shown in Figure 3.

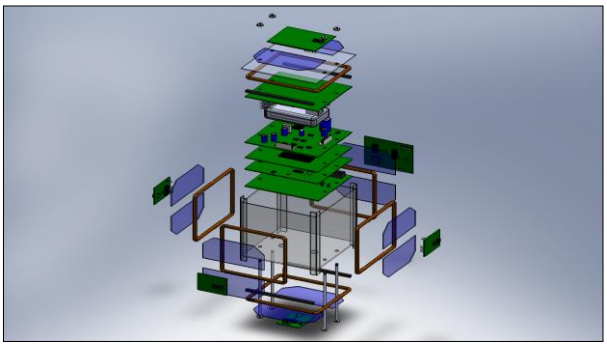

**Figure 3. Chasqui I exploded view**

The technological support is based on modal analysis, random vibrational, thermal and mechanical behavior under both the launch and in orbit and finite element modeling with a load of 16 gravities.

#### *4.1.3.6 Payload*

The payload is based on a system for image acquisition (SIMA). The main objective of SIMA is to obtain Earth images in two bands of the electromagnetic spectrum, Visible (VIS) and near infrared (NIR). As far as we know, no previous academic CubeSat mission had NIR imaging capabilities.

The SIMA system is based on two commercial CMOS digital camera modules (C328, COMedia Ltd.) and a multiplexor (HD74LS157P). Each module has an embedded JPG coder than enables to obtain JPG images with a max resolution of 640x480 pixels.

The control of SIMA is made directly by the Central Control and Information Management (CCMI, on board computer), where the algorithms to turn on/off a specific camera, picture resolution configuration, and shooting control are embedded.

Physically SIMA and CCMI share the same board, and electrically they are connected through two control signals (Select and Enable), and a serial data communication signal (UART).

The optics for each camera is based on composed lenses with 1090FOV. In the VIS camera, a band-pass filer (400nm-700nm) is placed between the lenses and the CMOS sensor while a low-pass filter (800nm-1000nm) is used for the NIR camera. The spatial resolution of the system is 1.878Km /pixel, considering the satellite is at 350Km on the targeted surface. In order to avoid CMOS sensor degradation due cosmic rays, a gold thin film (Figure 4) has been fabricated using a sputtering deposition system (Electron Microscopy Sciences model 550). The electrical consumption of SIMA is 63mA when a camera is taking pictures and less than 1mA while the system is hibernating. Tests show that the system can easily take pictures at -40 ◦C and at pressures around $10^{-2}$ bar.

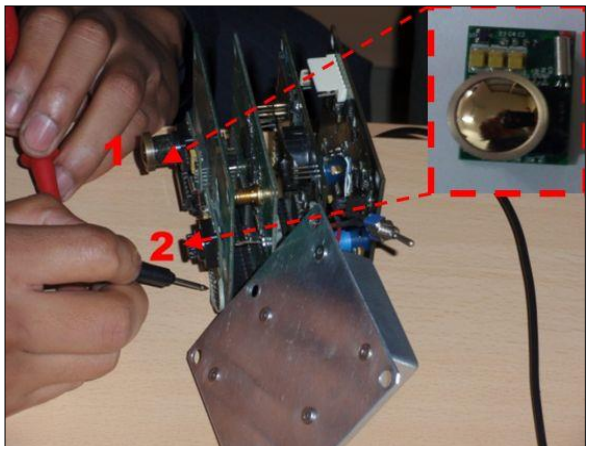


**Figure 4. Position of the cameras (1, 2) in Chasqui-I detailing the lenses with gold thin film.**

### 4.1.4 Ground Station

A Ground Station consists of a set of equipment, facilities and software for wireless communication between human users in the ground and the satellite. The satellite can be our own CubeSat or any other satellite using one of the frequency bands supported by the equipment.

The main functions of a Ground Station are:

-Tracking: to hear the satellite's beacon in order to know its position and identity.

-Telemetry: state variables acquisition (temperature, voltage, etc.) in order to monitoring the satellite and determine its operational parameters.

-Command: to issue orders to the satellite, such as system reset, taking pictures, etc.

A block diagram with the main components of or Ground Station is shown in the Figure 5.

Core components of the Ground Station:

-Transceiver ICOM IC-910H (VHF and UHF)

-Power supply for the transceiver PS-125.

-Two pre amplifiers (one for VHF, other for UHF)

-Antenna rotor YAESU G-5500

-ARS-El interface for the rotor

-A Power meter.

-Two X-Quad antennas, one for VHF (2 m), other for UHF (70 cm)

-Two lightning arrestors

-Two phasing harnesses

-Cables and connectors

-Personal computers with network adapter.

-TNC (own design)

-Amplifier "Mini Circuits".

Additional equipment:

-Two LCD displays for orbit visualization and other uses.

-Fast Ethernet Switches and Cat5e cables for network access.

-UPS (Uninterruptible power supply)

The calculations of the link budget was made in the most difficult setting (download, because the transmitter is the CubeSat, and it will have low power available for transmission).

We assume that the satellite will be able to communicate when it is above 10 degrees of elevation. For non-coherent FSK we have a margin of more than 5 dB for a BER=$10^{-5}$; that is, the communication will be quite successful. But for AFSK (coherent FSK in audio frequencies and then FM-modulated), even with less demanding BER=$10^{-3}$, the margin is almost zero, so communication will be very error-prone.

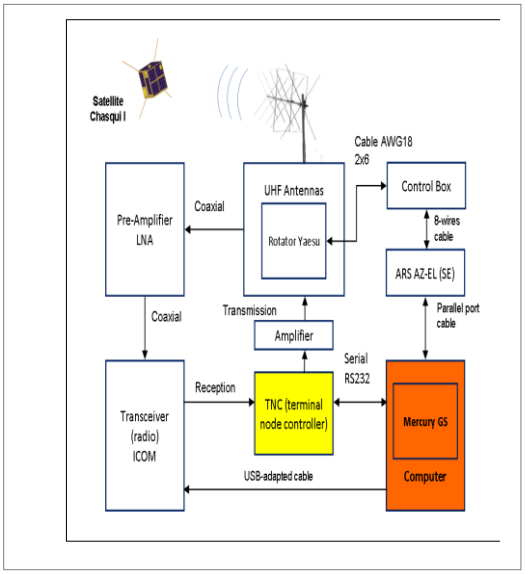


**Figure 5. Block diagram of the Ground Station**

The ground station may monitor other university CubeSat satellite as part of a network similar to GENSO.

**Table 1. Link budget calculations (download)**

| | |
|---|---|
| Frequency | 435 MHz |
| Wavelength | $\lambda$= 0.6892 m |
| TX power | P=2W =3.01 dBW |
| Tx Antenna Gain (ideal) | 2.15dBi |
| Tx Ant. Gain (real, no perfect alignment) | -7.85dBi |
| Tx line loss | 0.2 dB |
| Equivalent isotropic Radiated power | EIRP=-5.04dBW |
| Max. propagation path length | 1932.245 Km |
| Free Space Loss | 150.931dB |
| Atm. propagation loss | 0.2 dB |
| Polarization loss | 3 dB |
| Rx Antenna gain | 12.8dBd = 14.95dBi |
| Rx line loss (antenna to pre-amp) | 0.3 dB |
| Rx power at the pre-amp | -114.521 dBm |

| | |
|---|---|
| Rx line loss (pre-amp to transceiver) | 4.25 dB |
| Data rate | 1200 bps |
| Spectral factor | 1.25 |
| Eff. noise temperature | 266K |
| Spectral Noise (No) | -174.33 dBm/Hz |
| Noise in Rx | -142.57 dBm/Hz |
| Carrier pow. /noise pow. | C/N=28.049 dB |
| Fading margin (multipath) | 10 dB |
| Eb/No | 19.0181 dB |
| Required Eb/No (FSK, BER=10-5) | 13.8 dB |
| Required Eb/No (AFSK, BER=10-3) | 19 dB |

The operation of the Ground Station will need not only hardware, but also one or more software products with these characteristics:

-Direct human control for console or GUI.

-Remote control or tele-operation enabled.

-Advanced commands available

-Ability to receive files and format data.

-Ability to read telemetry data.

-Ability to configure and monitor the equipment (especially transceiver and rotor)

-Radio tuning, to correct Doppler Effect.

-If possible, some form of automatic control or "automatic pilot"

One interesting aspect of our Ground Station is it good location. There is no other academic Ground Station in the Central-Western part of the south Pacific. For any satellite coming NW to SE and leaving the Western Coast of USA, the Ground Station of Lima will be the first contact point. For any satellite coming NW to SE, it will be the last point of contact before crossing the South Pacific.

### 4.1.5 Launch

Nanosatellites are usually placed in space through containers housing one or more satellites. The containers travel as a secondary load in the rockets which carry a main load, so that the launch position is defined by the primary payload carrying the rocket. Another scheme launch that is being used lately is throwing from the International Space Station (ISS). This latest release is the scheme that has been used for the Chasqui I, being launched from the Russian module of the ISS (Figure 6).

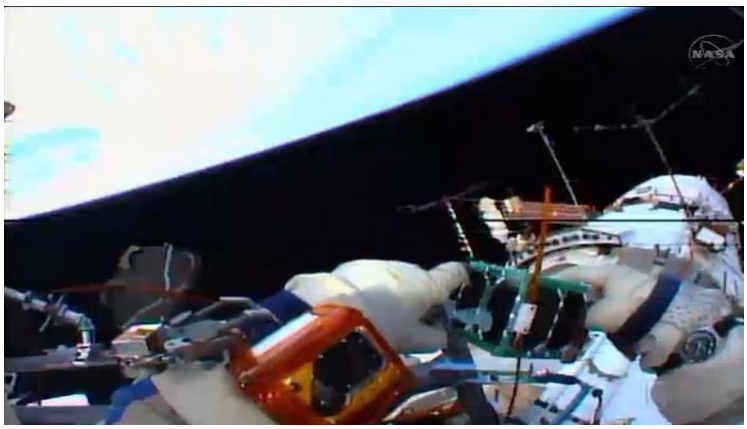


**Figure 6. Chasqui I launch from ISS**

## 4.2 Nanosatellite networks

A single CubeSat is simply too small to also carry payloads or sensors for significant scientific research. Hence, for the universities the main objective of developing, launching and operating a CubeSat is educational. However, when combining a large number of CubeSats with identical sensors into a network, in addition to the educational value, fundamental scientific questions can be addressed, which are inaccessible otherwise. A double (10x10x20 cm3) or triple (10x10x30 $cm^3$) unit CubeSat can include more sophisticated payloads and higher power budget that can be considered as a powerful probe to perform in-situ measurements. Networks of CubeSats have been under discussion in the CubeSat community for several years but so far, no university, institution or space agency has taken the initiative to set up and coordinate such a powerful network.

Space agencies are not pursuing a multi-spacecraft network for in-situ measurements in the thermosphere at 100 - 400 km altitude because the cost of a network of 30 - 50 satellites built to the usual industrial standards would be extremely high (over a billion Euros) and not justifiable in view of the limited orbital lifetime. A network of satellites for in-situ measurements in the thermosphere can only be realized by using very low-cost satellites, and for this purpose, CubeSats are by far the best (if not the only) candidates. The following networks have been suggested as the most interesting (in the order of increasing distance from Earth):

- Upper atmosphere and re-entry research at the lowest possible orbital altitude with the aim to assure a CubeSat nominal lifetime of three months minimum.
- Continuous Earth observation at lower altitudes for homeland security and early warning purposes
- Alternative communication networks or technology demonstration.
- Continuous environmental monitoring (e.g. wildfires, oil spills) by a network of about 30 CubeSats in low-Earth orbits.
- Plasma physics in the magnetosphere (next generation Cluster), a network of about 30 CubeSats with a mother spacecraft for communication purposes.

### 4.2.1 WAPOSAT network

Water is one of the most important natural resource that has to be preserved for future generations. Considering the risk of scarcity of clean waters in the near future, international organizations such as UNESCO [37], WHO [38], UNICEF [39], UN [40], are working focusing attention on the importance of fresh water through different programs that develop international legislation and standards that should be adopted by the state members. Indeed, one of the targets of the United Nations – Water is to achieve a world program for evaluating water resources.

At present, compared with global monitoring systems for tracking earthquakes [41], volcanic activity [42], data traffic [43], CO2 [44], etc., there is a lack of any global monitoring system for hydric resources.

In some places, like river Lee in Ireland [45] and some countries like the USA [46], real time monitoring systems have been designed but isolated. Only, for local use. The water problem is not a country problem. It is a world global problem considering that there are more than 250 rivers running along international borders.

WAPOSAT aims to provide information initially from 50 GMS located at the most polluted streams worldwide through a dynamic web site with the chance to establish a network with other monitoring nets, up to technical considerations concerning data transmission and country cooperation programs referred to water monitoring.

#### 4.2.1.1 Mission Objectives

- To place 50 Ground Monitoring Stations (GMS) worldwide and establish at least one Central ground station (CGS).

- To use a constellation of 40 nanosatellites for WAPOSAT data transmission.

- To reach at least 95% of confidence in the measurement of the physical –chemical water variables.

- To receive data from the GMS each 30 minutes. The size of the data is less to 0.5 KB. Data will be retransmitted to the CGS and storage in a database. The data values will be

compared to the maximum acceptable limits established by the country legislation. If data value exceeds the local legislation, an alarm will be activated. The database could be used also for identifying changes on the aquatic ecosystems through the time.

#### 4.2.1.2 Concept of Operations

##### *4.2.1.2.1 Ground monitoring station (GMS)*

Each GMS is composed by a flow tuning-sampling system, an automated multi-sensor system and an UHF radio system; all housed in a 6m2 booth and powered by a photovoltaic system.

###### *4.2.1.2.1.1 Water Tuning-sampling system (WTSS)*

Pipes for inlet and outlet the flow are used to collect samples from the stream in the most adequate way. The sample follows the route described at Figure 7.

The first storage pit enables to reduce the flow rate down to 1-5 l/s. At the second storage, pit sensors for dissolved oxygen, temperature and turbidity are placed.

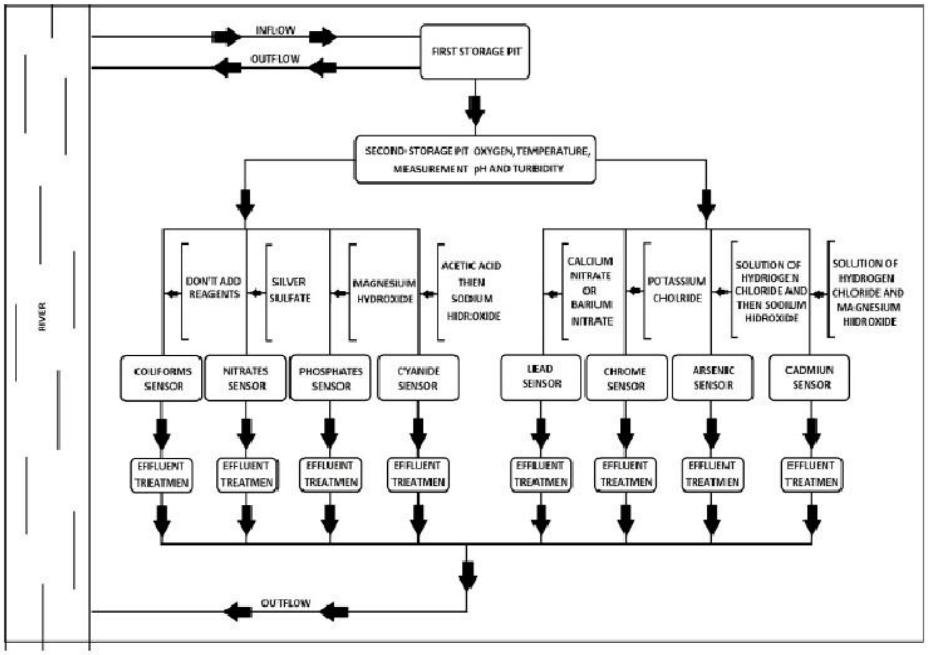


**Figure 7. Water tuning-sampling system**

These sensors are standard for all the GMS, nevertheless due to the open and modular architecture, the GMS is able to add more sensors to monitor other parameters in function of the needs of each country [47][48]. The second pit also serves to reduce the flow rate down to 0.005-0.05 l/s.

Each sensor will be calibrated periodically. Table 2 shows a list of the parameters to be measured, including extra parameters of interest. Some of them should require adding chemical reagents, so an effluent treatment module has to be considered and should be designed in function on the reagent. The tuning-sampling system outlet returns the water to the stream

**Table 2. Parameters to be measured at the GMS.**

| Parameter | Equipment /sensor | Interferents | Reagent |
|---|---|---|---|
| pH and temperature | pHC3081-8 Combined pH Electrode with Temperature Sensor, BNC plug (Radiometer Analytical) | - | - |
| Dissolved Oxygen | Dissolved Oxygen Probe (Order Code DO-BTA) | - | - |
| Turbidity | 1720E Low Range Process Turbidimeter (Turbidity) Sensor Only | - | - |
| Cadmiun | Orion ionplus Sure-Flow 9648BNWP | $Ag^{+}$, $Hg^{+2}$, $Cu^{+2}$, $Pb^{+2}$, $Fe^{+2}$ | Solution of Hydrogen Chloride and Magnesium Hidroxide |
| Arsenic | Hach Arsenic Test Kit | $Cu^{2+}$, $Hg^{+2}$ | Solution of Hydrogen Chloride, Sodium Hidroxide |
| Chrome | Aurease based biosensor | $Fe^{+2}$, $MnO_4^{-}$ | ph<4, Chloride of potassium |
| Lead | Orion ionplus Sure-Flow 9682BNWP | $Ca^{2+}$, $PO_3^{2-}$, $NO_3^{2-}$ | Nitrate of calcium, Nitrate of barium. |
| Cyanide | HI 4109 Cyanide Ion Selective Electrode | $Ag^{+}$, $S^{2-}$, Oily acids | Acetic acid, hexano, sodium Hidroxide. |
| Phosphates | PHOSPHAX(TM) sc Phosphate Analyzer | $Si^{4+}$ | Magnesium hydroxide |
| Nitrates | $NO^{3-}$BTA | $Cl^{-}$ | Silver sulfate |
| Coliforms | Electronic tongue [52] | - | - |

#### *4.2.1.2.1.2 Automated multi-sensor system*

The automated multi-sensor system (AMSS) is based on a set of electronic instrumentation designed for each sensor and includes: a USB data acquisition card (Labjack U6), a RS-232 GPS (Olimex MOD-GPS), and a data acquisition software running in a Linux powered notebook computer as is shown in Figure 8.

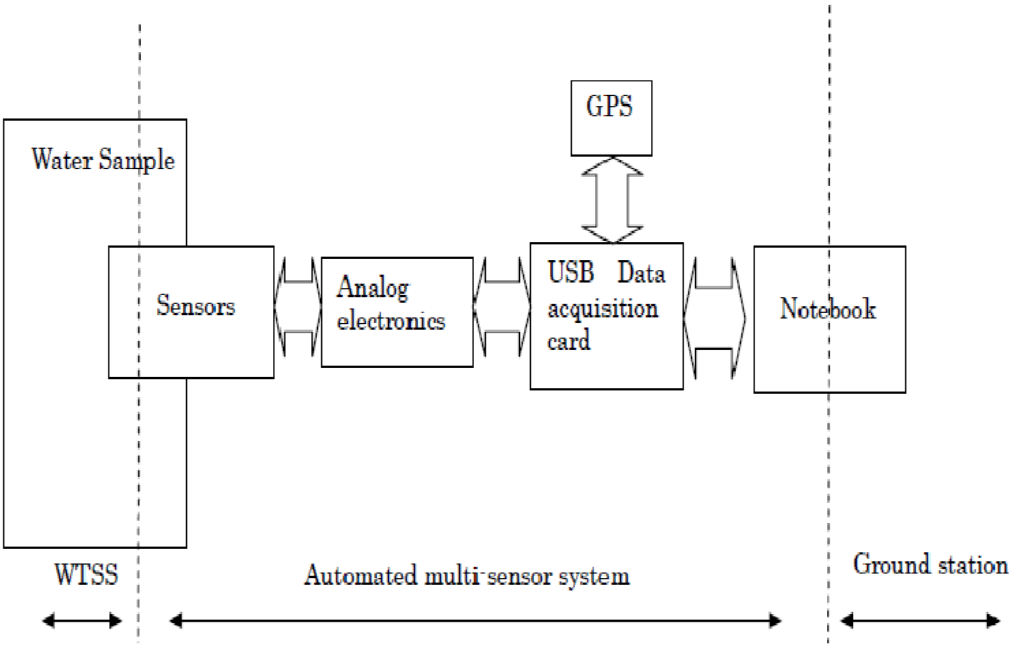


**Figure 8. AMSS schematics**

The software acquires data from the sensors as well as time and position from the GPS. The data is packed and send to the GMS´s embedded system.

#### *4.2.1.2.1.3 Ground station system for GMS (GS-GMS)*

WAPOSAT Project considers two kinds of ground stations, one kind placed in each GMS (50 in total) and called GS-GMS and the other kind is a single ground station for data gathering (GS-DGT) located in Peru. This gathering station is already operational and is placed at university campus. The GS-GMS shares the notebook with AMMS and a schematic is shown in the Figure 9.

Each sensor collects 500 bytes every 15 minutes, that is, 48000 bytes /day = 384000 bits/day. With a link of only 9600 bps, we can upload the daily data of one GS-GMS in only 40 s (daily) or less (more frequent updates). Allowing for some extra time for control, timers and ACKs, total time could grow up to 60 s in the worst case (one daily update). Using a fixed antenna with 13 dBi of gain and beam-width at least 42º we can download the data without rotors for moving the antennas. Two Quad antennas are required (one for download, one for upload) or one antenna plus a switch (TX mode/RX mode) in the TNC. If the mission requires to upload more data to the constellation, instead of one antenna we suggest installing an array of 4 antennas, with beam steered by electronics instead of a mechanical rotor, because electronic beam steering consumes less energy and it is less sensitive to high operating temperatures and harsh

environments than servo-motors. The custom made TNC contains also a radio; it uses a Chipcom CC1000 modem, a PIC32 microcontroller and I2C bus. It is better to use a custom made TNC+radio board instead of TNC and separate radio because we can get less power consumption and cheaper devices. FSK modulation over UHF band and 9600 bps for both TX and RX is proposed. Total power consumption is below 500 W and it would be necessary to supply this GS with autonomous power through solar power. Twelve solar cells (for a total area of 3,6 $m^2$) and six lead-acid batteries would be needed. The transmission amplifier would be a Mini circuits ZHL-100W-52-S or similar, capable of 47 dB or more gain. The reception amplifier only needs gain of 20 dB. The attached computer should be implemented with a microcontroller as an embedded system controlling the radio and the sensors.

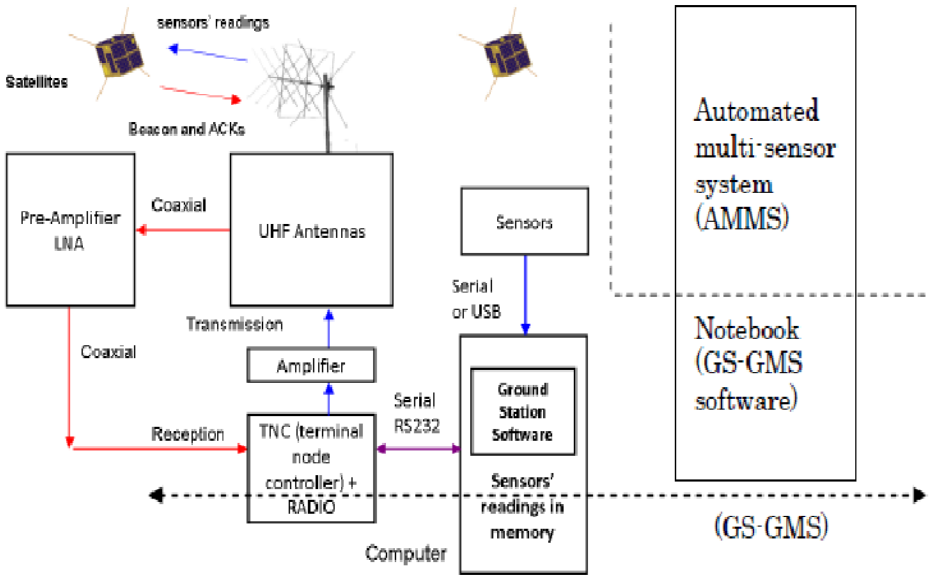


**Figure 9. Schematics for the ground station embedded in the ground monitoring station**

#### *4.2.1.2.1.4 GMS infrastructure and power system*

Each GMS is housed in a 6$m^2$ booth where all the subsystems are located. A little stream channel is planned for each GMS, so the water passes through the GMS.

A photovoltaic system composed by ten 85W solar panels, six 100Ah batteries, one 1600W power inverter and five 12A controllers. A scheme for the GMS booth is shown in the Figure 10.

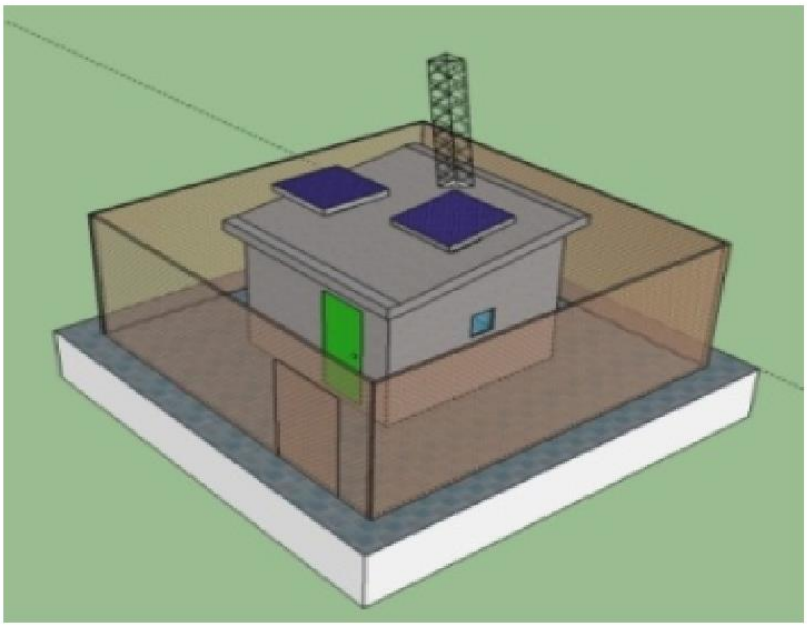

**Figure 10. Scheme of the GMS booths. The solar panels and radio antenna are shown**

#### *4.2.1.2.1.5 Location of GMS*

We identified 50 of the most polluted rivers in the world; at those locations, the GMS should to be placed (Table 3 and Figure 11).

**Table 3. Location of WAPOSAT global monitoring**

| NUMBER | COUNTRY | NAME | LATITUDE, LONGITUDE |
|---|---|---|---|
| 1 | Argentina | Reconquista river | (-34.5846, -58.6826) |
| 2 | Brazil | Xingu river | (-6.6534, -51.9848) |
| 3 | Canada | St. Lawrence river | (45.4618, -75.7190) |
| 4 | Canada | Fraser river | (49.1646, -122.9343) |
| 5 | Chile | Lluta river | (-18.4158, -70.3224) |
| 6 | Costa Rica | Virilla river | (9.9290, -84.3553) |
| 7 | Ecuador | Tenguel river | (-3.0010, -79.8347) |
| 8 | United States | Columbia river | (38.8872, -77.0576) |
| 9 | United States | Mississippi river | (32.3339, -90.9035) |
| 10 | Guatemala | Motagua river | (15.2530, -89.0956) |
| 11 | Mexico | Apatlaco river | (18.8521, -99.2208) |
| 12 | Mexico | Grande river | (23.8390, -103.0327) |
| 13 | Peru | Madre de Dios river | (-12.5045, -68.7793) |
| 14 | Peru | Mantaro river | (-11.5213, -75.9014) |
| 15 | Venezuela | Orinoco river | (5.7344, -67.5581) |
| 16 | Congo | Congo river | (-3.1224, 16.1767) |
| 17 | Egypt | Nile river 1 | (31.4561, 30.3704) |
| 18 | Egypt | Nile river 2 | (30.1481, 31.1581) |
| 19 | Senegal and Mauritania Border | Senegal river 1 | (16.5030, -15.8327) |
| 20 | Malawi | Zambezi river | (-16.1398, 33.5398) |
| 21 | Mali | Senegal river 2 | (14.4772, -11.5005) |
| 22 | Nigeria | Niger river | (5.1934, 6.3188) |
| 23 | South Africa | Orange river | (-30.6152, 25.4570) |
| 24 | Sudan | Nile river 3 | (15.7543, 32.5350) |
| 25 | Zambia | Limpopo river | (-22.2731, 30.0759) |
| 26 | Germany | Rhine river | (48.5129, 7.8046) |
| 27 | Spain | Nalon river | (43.2349, -5.5040) |

| | | | |
|---|---|---|---|
| 28 | Estonia | Kasari river | (58.7546, 23.8434) |
| 29 | France | Sena river | (48.8580, 2.3416) |
| 30 | Italy | Sarno river | (40.7288, 14.4725) |
| 31 | Poland | Oder river | (52.8238, 14.1863) |
| 32 | Romania | Danubio river | (45.3342, 28.9695) |
| 33 | Russia | Pechora river | (65.3983, 52.5973) |
| 34 | Russia | Volga river | (46.2972, 46.2972) |
| 35 | Ukraine | Dnieper river | (46.6684, 32.7183) |
| 36 | Australia | King river | (-14.6143, 132.3827) |
| 37 | Australia | Brisbane river | (-27.4989, 152.9162) |
| 38 | Australia | Murrumbidgee river | (-35.3933, 149.0338) |
| 39 | New Zealand | Wairau river | (-41.7974, 173.4505) |
| 40 | New Zealand | Mahurangi river | (-36.4010, 174.6732) |
| 41 | China | Yellow river | (34.9220, 97.5119) |
| 42 | China | Yangtze river | (33.4681, 91.1958) |
| 43 | China | Salween river | (24.8745, 98.8938) |
| 44 | China | Songhua river | (46.8625, 130.4626) |
| 45 | India | Ganges river | (27.6248, 81.6050) |
| 46 | India | Tawi river | (32.7361, 74.8172) |
| 47 | India | Brahmani river | (20.9181, 85.8222) |
| 48 | Indonesia | Citarum river | (6.2178, 107.2656) |
| 49 | Israel | Kishon river | (32.8015, 35.0344) |
| 50 | Pakistan | Indus river | (24.5382, 67.9616) |

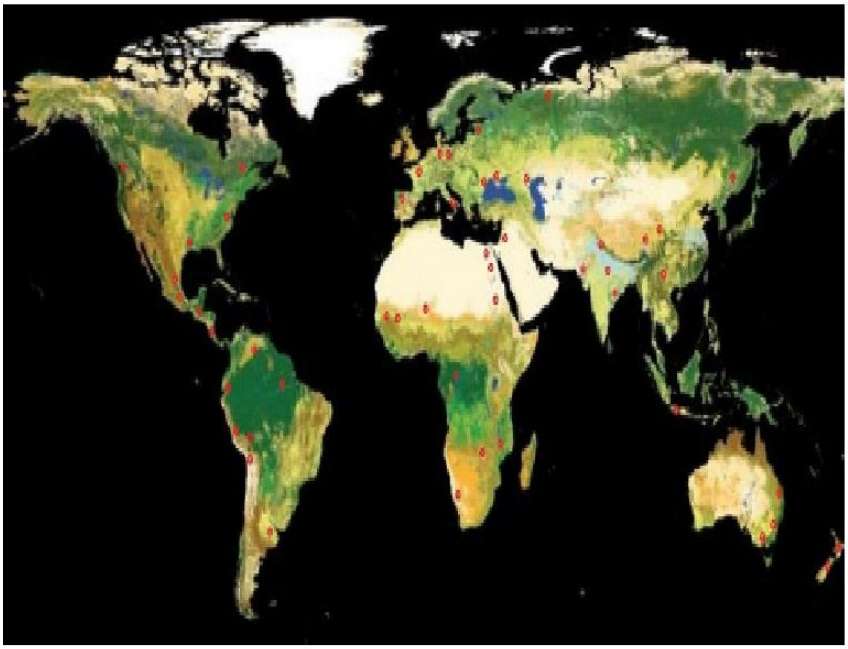

**Figure 11. Location of the 50 most polluted rivers in the world**

#### *4.2.1.2.2 Ground station for data gathering (GS-DGT)*

The GS-DGT structure (Figure 12) is similar to the GS-GMS but has three extra elements, an azimuth-elevation rotor for tracking, a separate radio and an internet connection. We suggest using Yaesu G5500 or similar rotor, and radio ICOM 9100 or similar. The software in the gathering GS is more complex, because it must manage all connections with the 40 nanosatellites in the constellation, the database of readings, security of access, etc.

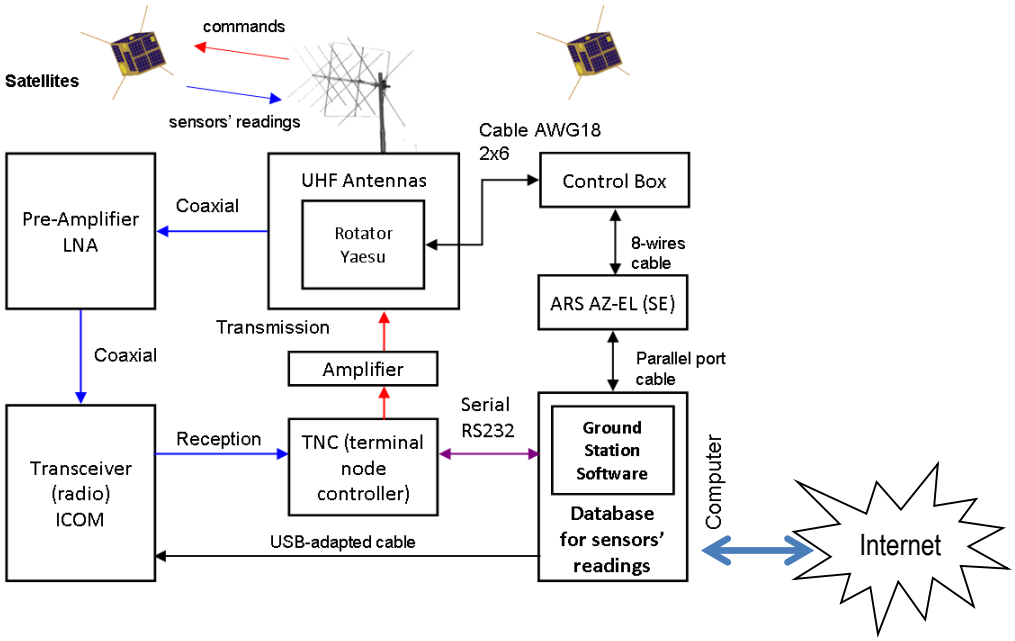


**Figure 12. Schematics for the GS-DGT**

Once we have the data processed by the GS-DGT, the result is flat information. We will use the client-server architecture (Figure 13); this information may be accessible to all users worldwide through a dynamic Web page (Web Interface). We need a server, a web application service, access to the web (internet), disk space. Client: Is the one who initiates and requests, are therefore it has an active role in communication. Server: Receives request, process it and then send the client response. Application Server varies depending on the programming language used (Table 4).

**Table 4. Architecture Client/Server**

| CLIENT | |
|---|---|
| Programming Language | Server |
| JAVA | APACHE TOMCAT, JBOSS, GLASSFISH |
| PHP | APACHE |
| .NET | IIS |

Internally in the architecture of Client / Server the following procedures will be developed:

1. Files are copied to a folder or directory (from the database.)
2. A half-hourly application reads the contents of the folder.
3. The application updates the database and move the files to be read by the web server (pollutant, date, comment, size, etc.)

4. The application clears the original folder so when the file is uploaded the user will not have problems space.

5. The web application communicates with the database and detects new uploads.

6. When an Internet user requests information about pollutants, it is automatically generated providing the information requested as available in the database.

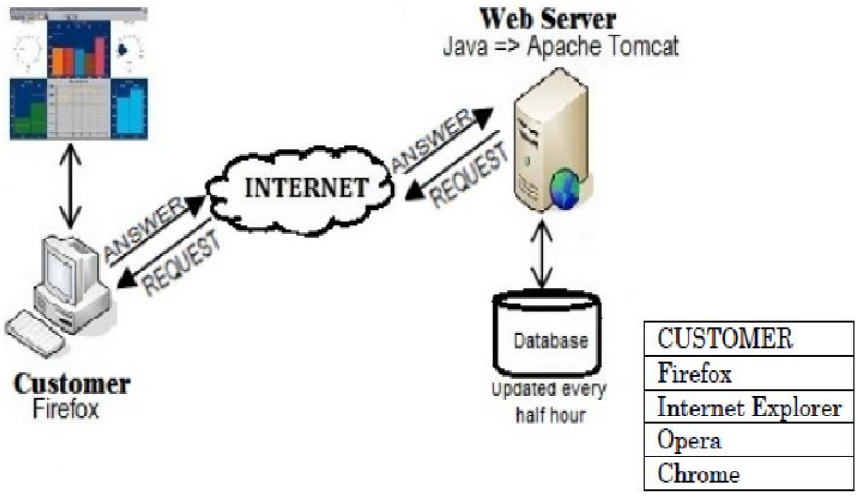


**Figure 13. Client-server architecture.**

#### 4.2.1.3 Key Performance Parameters

-Ion-selective sensors, only give accurate readings when in the sample are present other dissolved solutes, should be calibrated every week to ensure smooth operation

-Take a representative sample of river water as the concentration of dissolved solids in the river varies with depth, etc.

-Make a good preparation of the samples as selective ion sensors could give an error if there are other components that interfere with the measurement.

-Keep in mind that the river flow is variable, there is a greater flow in the rainy season, higher river flows makes more dilute pollutants, which does not mean that this polluting is less.

- Effective transmission rate: 1200 baud, proposing a NanoCom UHF Half-Duplex Transceiver for each satellite. Frequencies: 432 – 438 MHz, Output Power: 200mW – 600mW. Modulation: FM + MSK.

- Power System: a NanoPower P30U Power Supply is proposed, together with two quad-battery pack for extra energy capacity. Up to 30 W supplies.

#### 4.2.1.4 Space Segment Description

##### *4.2.1.4.1 Nanosatellite description*

We propose to use 40 similar nanosatellites based on CubeSat technology [49] each one is a 2U Double CubeSat (10cm x 10cm x 20cm). The nanosatellite mass is less than 2 Kg. The communication is based on UHF band. The WAPOSAT idea is just to use a little part of the processing time and transmission facilities of each nanosatellite in the constellation. So, when a CubeSat passes above any of the ground monitoring stations, the GS-GMS links to the satellite and sends the identification GMS number, the time, position and acquired sensor data. When the nanosatellite containing the water pollution data passes above the ground station for data gathering, sends the data to the station. At the station, the results are computed and served to the final users. An algorithm for GMS´s connection and data interchange has to be developed.

The following considerations have to be taken into account by each CubeSat in the constellation in order to meet the ends of WAPOSAT.

##### *4.2.1.4.2 Communication*

The estimate link margin is 0.7 dB for the downlink (worst case) and 9.5 dB for the uplink. The data rate is 1200 bps with a BER=10-5. Effective transmission rate: 1200 baud, proposing a NanoCom UHF Half-Duplex Transceiver for each satellite. Frequencies: 432 – 438 MHz, Output Power: 200mW – 600mW. Modulation: FM + MSK.

##### *4.2.1.4.3 On Board Computer:*

It is planned to use 32-bit ARM7 RISC CPU [49]. The real time operating systems is eCOS with a 2MB Static RAM , 4MB Data Storage (Flash Memory) and 4MB Code Storage (Flash Memory).

The scalability for the project is assured since any nanosatellite mission could be part of WAPOSAT initiative just considering the previous consideration.

#### 4.2.1.5 Orbit/Constellation Description

The election of the number of satellites and the number of planes aimed to minimize costs as much as possible [36]. First, more satellites will imply the need for a bigger budget. The aforementioned altitude was chosen to be 1000 km in order to have the maximum coverage per satellite, and thus reduce the number of them. Ground stations will be able to establish communication with satellites at this height, at 1200 bps and BER=$10^{-5}$.

In addition, it is worth performing a trade between the number of satellites per plane and the number of planes in the satellite constellation. A Walker Delta Pattern constellation was encouraged for this mission.

Thus, the choice selected is to have a constellation of 40 satellites, 4 satellite planes (45 degree separation between each plane), and inclination 98.5º. Each plane will have 10

equally spaced satellites. The number of satellites suffices for the intended Earth coverage (which yields approximately 85% of the time), as shown in Figure 14, as 10 degree ground station elevation mask angle is considered (worst case). Using better reception conditions, i.e. less than 10 degree angle can improve that 85% minimum.

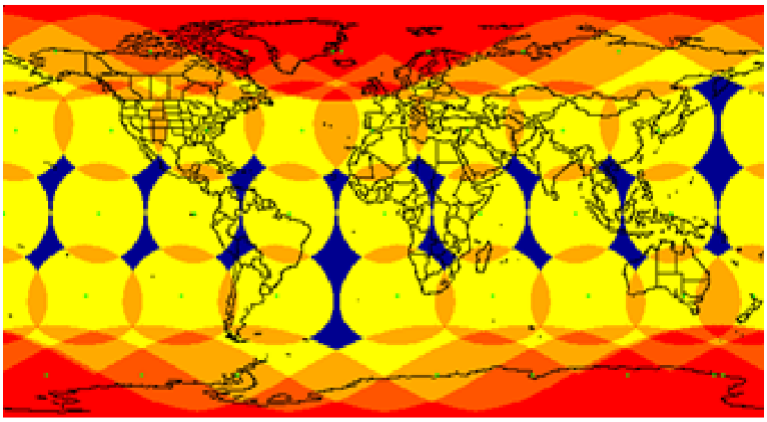

**Figure 14. Mission coverage with SaVi software.**

## 4.3 Nanosatellite Internetworking

The use of communication mechanisms similar to those used by the Internet has been experimenting in space through some successful projects such as the CLEO project [50]. Within the efficient transport mechanisms are being evaluated include those based on Delay Tolerant Networks (DTN) [51] one of which is Saratoga [52] which is based on User Datagram Protocol (UDP / IP) and those seeking improvements to the transport protocol TCP [53], but all of these transmission mechanisms are oriented to commercial satellites (commercial broadband satellites) but are not designed for satellite communication with few limitations such as CubeSats. Hence, our objective in this chapter is to evaluate the communication mechanisms that exist on the Internet for a constellation of satellites that have reduced communication capabilities such as the constellation of satellites QB50. Our contribution is focused on generating and simulating two scenarios of this constellation to assess throughput and delay parameters as a function of inter-satellite link (ISL) and thus provide a better understanding on the communication aspects of the constellation referred.

### 4.3.1 TCP/UDP over constellations

Small satellites communications for the QB50 constellation face several problems due to the intrinsic characteristics of satellite links, like the low ISL and GSL transmission bitrate, the high and variable value of the RTT (Round-Trip Time) and the significant error introduced in the link. The error rate will depend on the communication system

features (e.g. the link distance, coding and modulation) and the operational conditions (like rain or humidity). These aspects greatly limit the performance of the data transport (transport layer).

In the standard versions of the TCP protocols, the RTT allows to measure the satellite channel, evaluating the congestion and influencing in the variation of the congestion window. Packet loss due to congestion or channel errors would imply packet retransmission. The increment of the congestion window size is rather slow, because ACK's should arrive first for this to be possible. First, that increment performs in an exponential way depending of the number of received ACK's (this behavior is called "Slow Start") until reaching a certain threshold level, when it begins a linear and more quiet increment (called "Fast Recovery"), thus avoiding congestion.

TCP Westwood [54] was introduced with the purpose of limiting the consequences of the losses introduced by a wireless channel. It establishes the threshold level (sstresh) as a measurement of the available bandwidth, using the arrival rate of the ACK's, this way optimizing the variation of the Slow Start and Fast Recovery (called "Faster Recovery" for Westwood version), resulting in a better efficiency. There is a performance modification for all TCP standards, called "NewReno" Modification, which optimizes even more the Faster Recovery. TCP Westwood with New Reno features exists and is analyzed in this document.

In contrast to TCP (which is always requesting receipt acknowledgements), UDP is a connectionless protocol and does not guarantee any reliability for the packets delivery. In addition, the lack of use of ACK's does not allow the protocol to sense the efficiency, so the data transmission rate is never modified.

UDP and TCP Westwood with New Reno features are compared in this document.

### 4.3.2 Simulation Environment and Topology

QB50 is the first project that considers a network of CubeSats to be launched to the upper atmosphere. QB50 has the scientific objective to study in-situ the temporal and spatial variations of a number of key parameters in the lower. Two different network topologies for the QB50 constellation are evaluated in this document. The first scenario is a ring of 50 equally spaced CubeSats. In the second scenario, we analyze a 10000 km long CubeSat string.

For the preparation of this thesis the TCL-based ns-2 network simulator [55] (with an add-on called NS-Sat-Plot and created by Lloyd Wood) and SaVi (Satellite Visualization software, based on Linux OS and Geomview) were used. The first allowed for the simulation of the proposed environments. The latter helped for the visualization and animation of the proposed satellite constellations. For the simulation of the aforementioned environments, the design of TCL scripts for ns-2 was needed. These scripts were based on the following facts:

- The constellation is composed of only one polar plane. The orbit height will be of 300 km and the inclination of 79 degrees.

- Nine ground stations distributed over the Earth. Most of them are from GENSO Project [56], one of them was implemented at UNI, and it is part of the Peruvian Satellite Network (PSN) [57].
- Both uplink and downlink bitrates are of 9600 bps.
- The ISL (inter-satellite links) bitrate will take the following different values in the simulations: 0.5 kbps, 1 kbps, 3 kbps, 6 kbps, 8 kbps and 10 kbps.
- Two transport protocols will be evaluated: First, UDP; then, TCP Westwood with New Reno features (Westwood-NR).
- The traffic will be "CBR" (Constant Bit Rate), composed of packets of 210 bytes sent at one-second intervals. When inserted in a transport protocol, these packets are still of 210 bytes at UDP. When TCP, the length is 1040 bytes.
- Link Layer Protocol used is a basic one for NS, with no special features and neither FEC nor ARQ models implemented. A random error model is introduced too. The error probability for each interface is 10 -3; i.e. 0.1%. This means that in each interface, there is a probability of 0.1% in receiving a corrupted packet (this, in our analysis, would become a loss packet because there are no error recovery mechanisms after the packet is received).
- The queue has a limit of 50 packets and the queuing policy is TailDrop (if the queue is full, packets arriving are discarded).
- The traffic consists in five CBR flows originating in satellites numbered 1, 10, 20, 30 and 40, and destined to Lima. For TCP, Lima sends standard acknowledgements (ACK's). A TCP Westwood-NR ns-2 package of algorithms created and edited by University of California, L.A. (UCLA) is used in the simulation [58]. The instants of beginning of the flows are shown in Table 5, and are different for both scenarios.

**Table 5. Beginning Moments for Traffic Flows**

| Source | Satellite Constellation | |
|---|---|---|
| | ***First scenario*** | ***Second scenario*** |
| Satellite 1 | 1 | 1 |
| Satellite 2 | 200 | 100 |
| Satellite 3 | 400 | 200 |
| Satellite 4 | 800 | 400 |
| Satellite 5 | 1000 | 500 |

Satellite 1 is placed in the middle of the topology always, and it is near Lima at the beginning of the simulation. In those seconds, satellites 10 and 20 are northwards; and 30 a 40 are southwards. It will happen that packets will travel across the ISL until they find a satellite as close to Lima as possible and this will strongly influence in the results. The different topologies can be observed in Figure 15 and Figure 16, generated with SaVi.

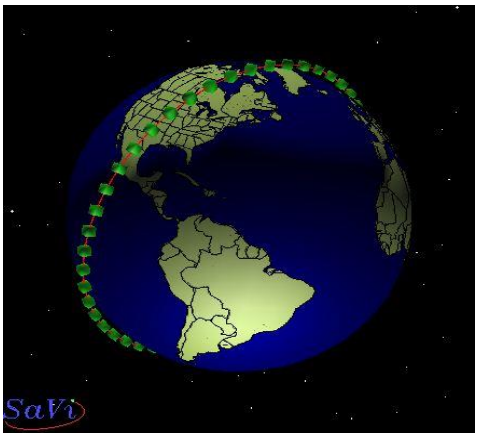


**Figure 15. First satellite topology to be analyzed**


**Figure 16. Second satellite topology to be analyzed, a 10000 km long satellite string**

In this document, three parameters are measured: a) Throughput arriving to Lima ground station (total number of bytes received by Lima for a time). b) Delay of the packets for the flow from Satellite 1 until they are received in Lima. c) Packet Loss rate (due to channel errors or congestion only), showing also the total analyzed packets, received packets and lost packets. For UDP protocol case Throughput is measured with an algorithm that measures the total bytes received with a time basis of every 40 seconds for UDP and 200 (for Topology 1) and 140 (for Topology 2) seconds for TCP. The total simulation time will be of 1500 seconds for the first topology and 700 seconds for the latter (this is because after 700 seconds the satellites lose line of sight with any ground station for several seconds). Losses due to lack of line of sight for Topology 2 are not considered in the packet loss rate.

### 4.3.3 Simulation Results

*1) First scenario (50 CubeSats equally spaced around the Earth):* First, let us analyze the results for UDP in this first network topology. When varying the ISL bitrate, it results in different throughput curves, being shown in Figure 17. Some remarks should be done here.

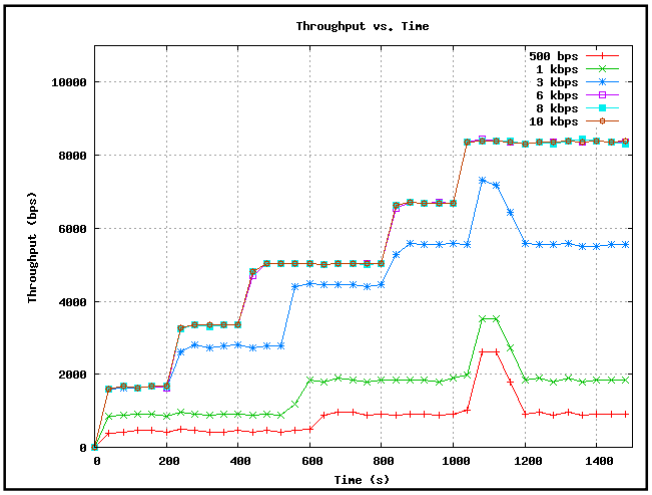


**Figure 17. Throughput vs. Time for UDP in Topology 1**

It can be observed that new traffic flows (first at 200, then 400, 800, and finally 1000 seconds) give staggered rises to each throughput curve in the graph. It must also be commented that, when observing the ns-2 trace files, as soon as packets are produced by the CBR sources, they are sent. In addition, the throughput does not make any significant change when incrementing the ISL bitrate capacity from 6 kbps to 10 kbps because the 6 kbps capacity is large enough to carry the traffic. The average traffic flow per source will be a bitrate of 1.68 kbps. Given that there are five flows, the total downlink rate should be 8.4 kbps. A capacity of 6 kbps in the ISL bitrate, as commented, is large enough to achieve this, because it should carry as much as twice the value of 1.68 kbps (3.36 kbps). Finally, let us focus just on the first ISL bitrate values (0.5, 1 and 3 kbps). For these values, there are peaks observed between 1000 and 1200 seconds in the simulation. This is because the current downlink satellite is a traffic source satellite. Thus, the ISL maximum rate cannot limit the additional 1.68 kbps originated by the downlink satellite. Thus, the throughput is added 1.68 kbps for this period.

When analyzing the Delay from Satellite 1 to Lima vs. Packet ID, the result is shown in Figure 18. When observing the graphs it can be commented. For the latter three values, the graph shows a subtle variation in the delay. Also, The increase in the delay becomes more subtle as time goes by, and it relies on the fact that first, the satellite 1 (which is evaluated in this graph and according to the ns-2 trace files), sends its packets to its neighbor, satellite 50, which is the first downlink satellite (one hop). After some seconds, the downlink satellite is 49 (two hops), then satellite 48 and so on. For the total simulation time considered, it should finally be remarked that 10 kbps is the best ISL rate for addressing delay issues.

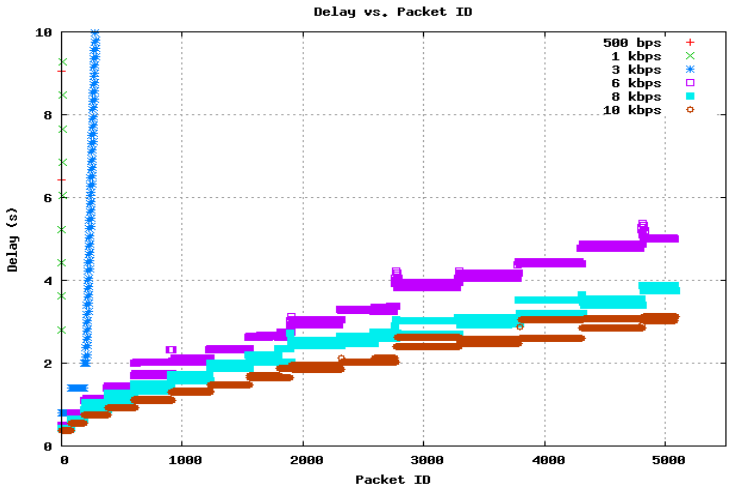


**Figure 18. Delay from Satellite 1 to Lima vs. Time for UDP in Topology 1**

Finally, the results for the packet loss are stated below (Table 6). Due to the lack of retransmissions and congestion mechanisms when using UDP, error channels and congestion can seriously affect the communications. In addition, for a satellite being a source of traffic, it may discard some packets from its queue depending on the amount of bits incoming from the ISL links. It can be seen that the packet loss is greatly reduced since ISL bitrate limit is 6 kbps, because it does not limit the traffic between satellites anymore. Thus, 6, 8 or 10 kbps are enough for an adequate performance of UDP in this first scenario.

**Table 6. Packet Statistics for UDP on Topology 1**

| ISL bitrate limit (kbps) | Packet Statistics | | | |
|---|---|---|---|---|
| | *Total Packets* | *Received* | *Lost* | *Packet Loss (%)* |
| 0.5 | 4770 | 754 | 4016 | 84.1929 |
| 1 | 4771 | 1444 | 3327 | 69.7338 |
| 3 | 4875 | 3868 | 1007 | 20.6564 |
| 6 | 5077 | 5069 | 8 | 0.1576 |
| 8 | 5081 | 5073 | 8 | 0.1574 |
| 10 | 5084 | 5076 | 8 | 0.1574 |

When performing the TCP analysis, the throughput graph, shown in Figure 19, looks a bit odder than the one for UDP.

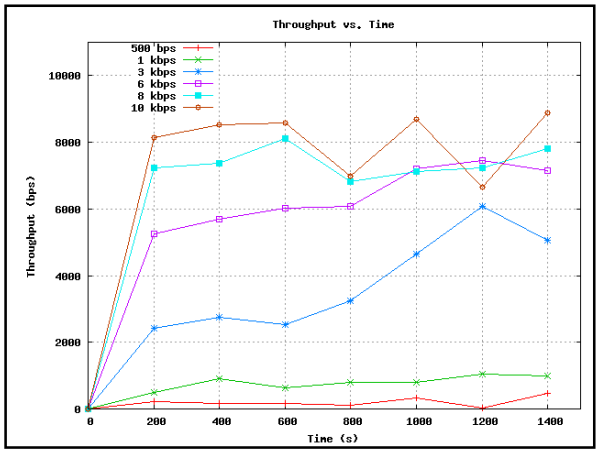


**Figure 19. Throughput vs. Time for TCP in Topology 1.**

In TCP, there are some peaks in the graph because of the congestion window mechanism, which varies the time and amount of sent packets depending on the traffic it perceives from measuring the acknowledgements return rate. It can be seen that the throughput increases to 8 kbps since the beginning, this is because the packets sent are much bigger and the TCP mechanisms try to optimize the use of the available bandwidth. In the beginning, according to the ns-2 trace files, TCP send packets of 40 bytes, in order to set up a connection with Lima. This way, first CBR data is buffered by TCP mechanisms and, as soon as the connection is established, it begins sending the data in the 1040 bytes long information packets.

The TCP delay results are shown in Figure 20. Here, the delay for ISL values of 500 bps and 1 kbps is not entirely shown in order to emphasize the results for 3 kbps, 6 kbps and so on. The delay is remarkably different to the one in UDP. It is much bigger for many of the sent packets, because the congestion mechanisms buffer the delayed 1040 bytes long packets. The TCP thus demonstrates to give a huge packets delay due to the length of its packets and bits overhead. Nevertheless, the packet loss is always greatly reduced, this being a TCP intrinsic feature.

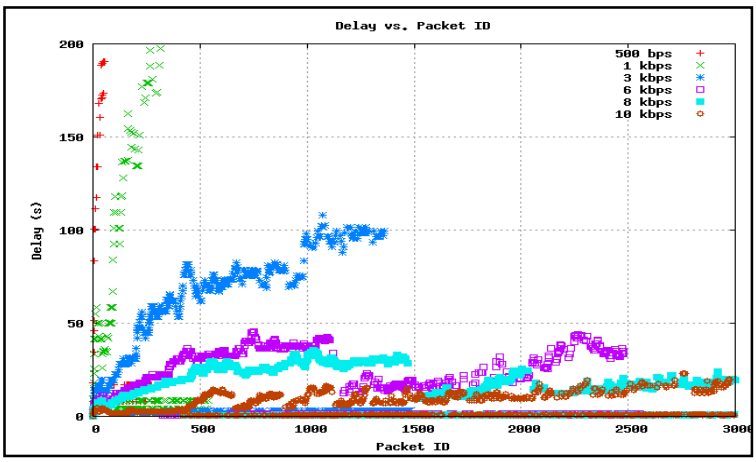


**Figure 20. Delay from Satellite 1 to Lima vs. Time for TCP in Topology 1.**

*2) Second scenario (A CubeSat string 10000 km long):* As a first glance for this topology, the variation in UDP throughput because of changing the ISL bitrate limit is shown in

Figure 21. As for the first scenario, the throughput increases in a staggered way, due to new traffic flows in other satellites. Each step in the graph relies in an increment of the traffic amount increase of 1.68 kbps. In addition, the augment in the ISL value greatly raises the throughput, until 6 kbps. From this value on, the throughput does not show any significant variation anymore, for the same reasons than the first topology. Nevertheless, the performance begins to fall at approximately 540 seconds, given that the topology is a string and the information is sent towards one of the ends, being this end the only part of the constellation to be in the ground station's line of sight. This reduction causes saturation in the ISL links if these do not have enough capacity. Only the 10 kbps ISL link is able to cope with this fact.

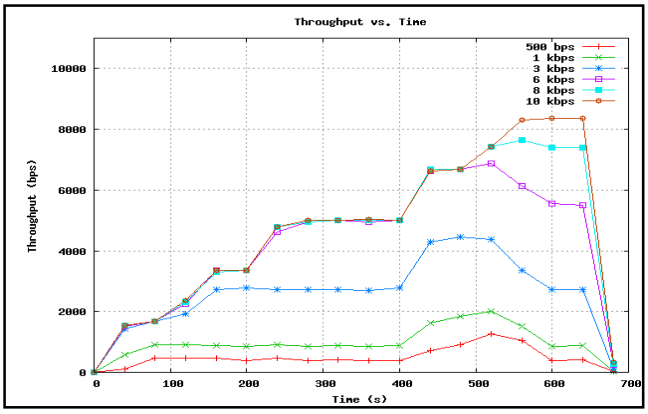


**Figure 21. Throughput vs. Time for UDP in Topology 2.**

The delay results are displayed in Figure 22. The gradual increment in the ISL bitrate value provokes a significant reduction in the delay for 500 bps to 3 kbps, which is not shown in the graph for the same reasons as topology 1. For the greater ISL values, the delay is even more reduced, reaching 5 seconds as the maximum delay. It can be observed too that the delay for lower ISL values is considerably great, which coincide with the throughput graph, where these ISL values don't exceed the total traffic produced when all this traffic is sent, in one direction, towards the downlink satellite.

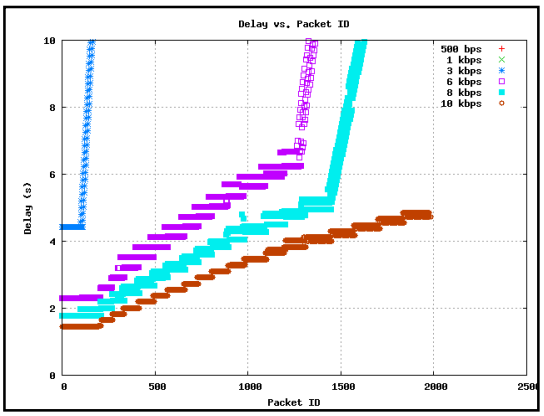


**Figure 22. Delay from Satellite 1 to Lima vs. Time for UDP in Topology 2.**

By the way, as stated in Table 7, it is worth remarking again that a large ISL rate causes less packet losses, just as in the first topology. For low ISL values, many packets are lost, especially for 500 bps and 1 kbps. In addition, when a satellite is a traffic source, it may

drop packets due to its saturated queue, because it receives packets from ISL links apart from producing them, as for the first scenario. Finally, channel loss influences in the packet loss rate too.

**Table 7. Packet Statistics for UDP on Topology 2**

| ISL bitrate limit (kbps) | Packet Statistics | | | |
|---|---|---|---|---|
| | *Total Packets* | *Received* | *Lost* | *Packet Loss (%)* |
| 0.5 | 1943 | 207 | 1736 | 89.3464 |
| 1 | 1928 | 412 | 1516 | 78.6307 |
| 3 | 1966 | 1101 | 865 | 43.998 |
| 6 | 1976 | 1770 | 206 | 10.4251 |
| 8 | 1965 | 1916 | 49 | 2.49364 |
| 10 | 1984 | 1982 | 2 | 0.100806 |

In order to prove reliability for data transmission, now a TCP analysis for this topology is done. Results for throughput are shown in Figure 23. Here, each curve tries to keep a constant and great bitrate. The same way, when observing the ns-2 trace files, the same for the other topology, many packets are not sent automatically, but they are buffered instead in order to send them later. Also, the network performance is affected, reducing the throughput, because of the topology being a string, as for UDP.

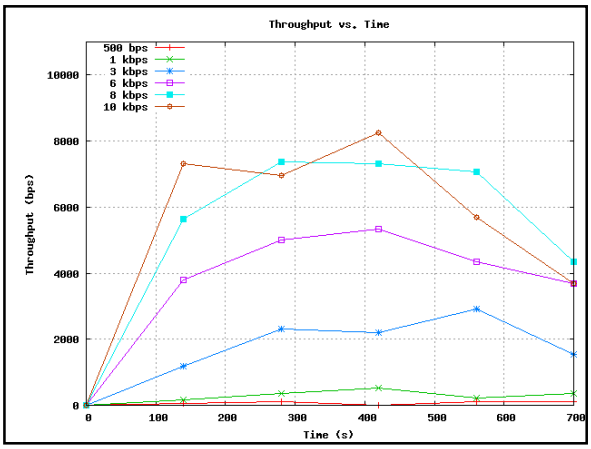


**Figure 23. Throughput vs. Time for TCP in Topology 2.**

Finally, the delay results are shown in Figure 24. The delay rises throughout the packet ID (thus, throughout time). This is a result of new traffic flows, as for aforementioned cases, which increase the amount of sent data (this brings more acknowledgements for each traffic flow to be delayed). In contrast, the increment in the ISL again reduces the delay, greatly at first, and slightly for the greater ISL values. As for topology 1, delay for TCP is greater than for UDP, thus making this aspect a disadvantage. Nevertheless, the insignificant packet loss makes up for this issue.

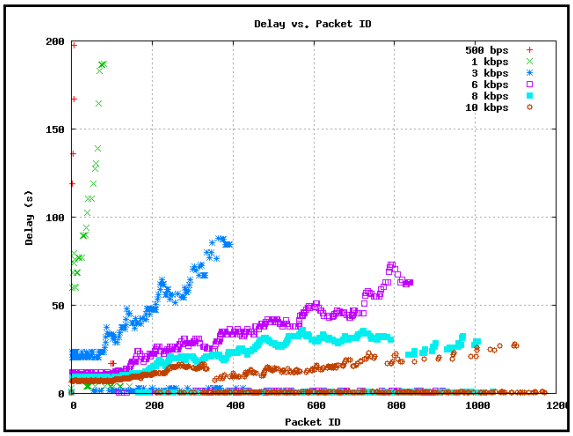


**Figure 24. Delay from Satellite 1 to Lima vs. Time for TCP in Topology 2**

## 4.4 Summary

In this section, I showed the basic characteristics of a satellite using the example of the satellite Chasqui I, currently in space. Among the advantages of this new technology, I can see that these nanosatellites contain much of the functionality of larger satellites and it is a great academic experience to participate in this kind of projects because it allows real access to space in less time than commercial satellites. In addition, nanosatellites modules are based on COTS components making them viable to be implemented due to their relative low cost. Among the limitations, I can consider low power batteries, which restricts the operation time and power in attitude control, payload and communications module. In the case of communication modules, it is quite common to work with data transmission speeds of 1200 bps. Another important limitation is the time of contact with the ground segment. When placed in LEO orbits either as part of a secondary load or launched from the ISS, these satellites have different times of contact with the ground station, which greatly limits the amount of data sent to Earth. Also, I have proposed an innovative application using nanosatellite networks for water quality monitoring, which has allowed me to estimate if the requirements should address communication mechanisms to solve these types of applications. Finally, I have been able to explore the impact of ISL links within both proposed topologies for two kinds of constellations, observing an enhancement in throughput and a reduction in the delay, as the ISL maximum rate is increased. It can also be appreciated that, when analyzing the TCP protocol in both topologies, the throughput saturation level is limited by the downlink bandwidth. It has been demonstrated that TCP performs an optimum throughput management throughout the simulation time (unlike UDP). Nevertheless, the delay is greater than for UDP; although the low packet loss, characteristic of TCP, compensates that issue. Finally, it was observed that the topology proposed for the first scenario offers a better traffic distribution due to the great symmetry level of that 50 CubeSat ring, in contrast to the second scenario. As to which protocol performs better,

we can state that TCP should be the choice when looking for reliability in data error free communication and throughput optimization; and UDP would be the ideal election for quick data transmission, together with a proper error correction mechanism.

In the next chapter, I will propose a communications architecture that is linked to the application scenario presented in this chapter and that includes the disruptive nature of communications satellites in LEO orbits.

# 5 Definition of Delay/Disruption Tolerant Network Architecture

In this chapter I will consider a scenario (Figure 25) similar to the HUMSAT [7] or WAPOSAT [8] proposals described in Chapter 4, where a network of sensors or sensor hubs such as unmanned aerial vehicles (UAV), hereinafter sensors (S), located within the coverage area of the nanosatellite send their data to it during service time (approx. 480 s). A nanosatellite that has received the data uses a store&forward mechanism and then transmits the data to the first available ground station of the gateways network, similar to the GENSO [56] network. If the service time is not sufficient to transmit the information from terrestrial nodes (Sensor, Gateway) to nanosatellite or vice versa, both sensor and nanosatellite will wait for another contact opportunity to complete the submission. The Gateway (GW) has an Internet connection through which data is transmitted to the central server located in the Mission Control Center.

Given the disruptive nature of this type of scenario, I propose a solution in [59], based on Delay Tolerant Networks (DTN) architecture, which provides end-to-end communications in such environments. In this context, it is proposed that each node in the system (Sensor, Gateway, Nanosatellite and Server) supports the DTN Bundle Protocol (BP) of the DTN architecture. The overlay feature of DTN allows the integration of different kinds of networks, in our case the nanosatellite network, the gateway network and Internet.

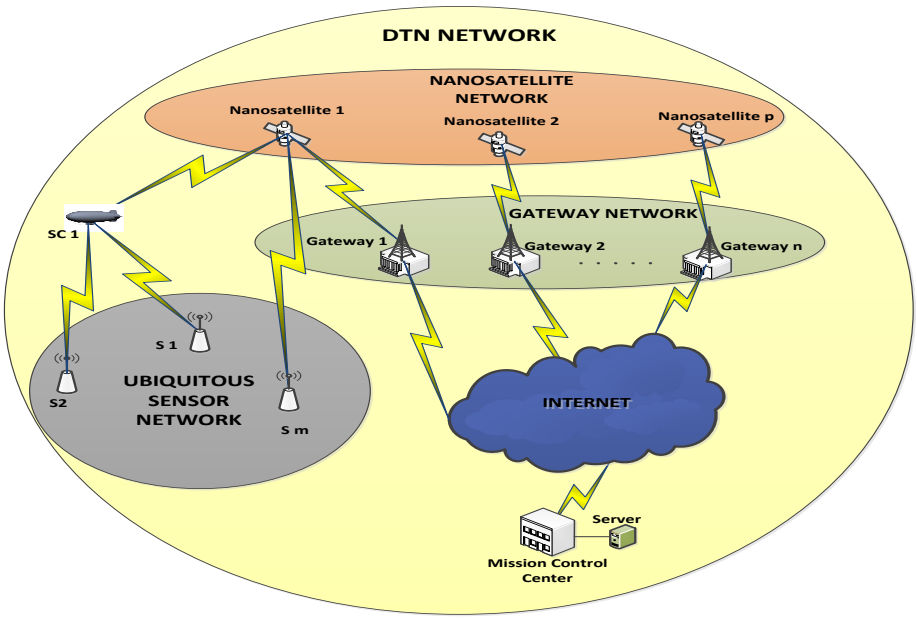


Figure 25. DTN System Overview

## 5.1 DTN System Architecture

In order to support DTN communication in sensors, nanosatellites and gateways, I propose a simple link layer, which uses an extension of unslotted Aloha Multiple Access (ALOHAGP, Aloha with Gateway Priority) and a convergence layer adapter ALOHAGP-CL (ALOHAGP- Convergence Layer) similar to that proposed for TCP [60], which sends and receives bundles using ALOHAGP service.

The architecture and protocol stack for the system proposed can be seen in Figure 26. Taking into account the proposed architecture, we have considered the following layers:

Application: This segment includes information of all sensors under its control.

DTN Bundle layer: A bundle is a protocol data unit of the DTN bundle protocol used in this layer.

ALOHAGP-CL: A convergence layer adapter sends and receives bundles on behalf of the Bundle layer, using the service of ALOHAGP protocol.

ALOHAGP: A reliable contact-oriented protocol that supports multiple access priority.

Satellite: Represents the physical layer of the nanosatellite.

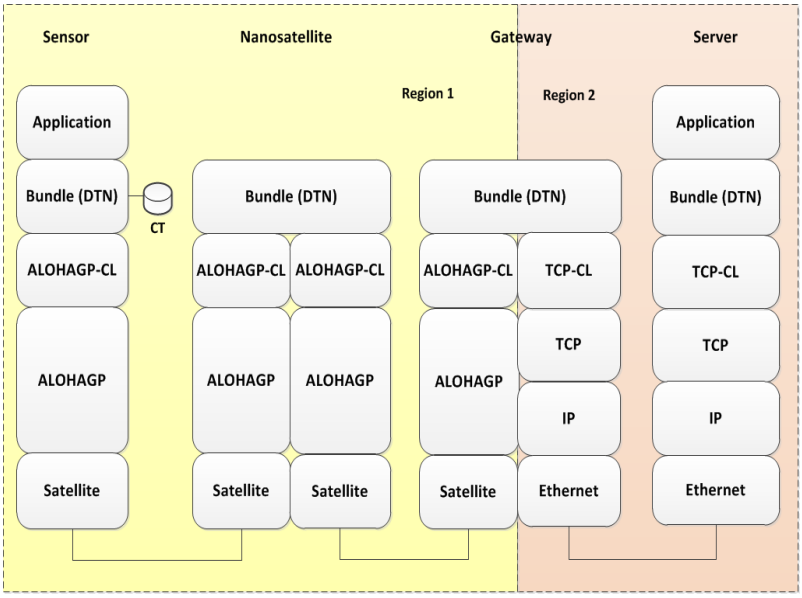


**Figure 26. DTN Architecture Network and protocol stack with two regions**

In order to understand the overall behavior of the proposed architecture we briefly describe the data flow in each layer and optimization crosslayer proposed in the system. First, we will start with the description of how the system works (Figure 27) in a disruptive environment shown in Figure 25. We will consider an example with a sensor node that generates a data bundle B; two nanosatellites support the store&forward mechanism and act as a DTN node, a gateway receives information from the nanosatellite and a server is the destination of the information.

When nanosatellite 1 appears within the coverage of the sensor and the service contact is started, a bundle, B, is sent to the nanosatellite. Supposing that contact is lost with the nanosatellite and only a fraction of bundle B is sent, the fraction that was not sent in the sensor forms a new bundle, B2, waiting for a new contact opportunity to be sent. The bundle fraction that reached nanosatellite 1 forms a new bundle, B1. When a gateway appears into nanosatellite 1's coverage and service contact starts, it sends bundle B1. If contact is lost again, only a fraction of bundle B1, called B11, is sent to the gateway. The remaining fraction, B12, will be sent in the next contact between nanosatellite 1 and the gateway. B11 and B12 received at the gateway are sent to the server via Internet. Similarly, when nanosatellite 2 appears within the coverage of the sensor and contact service is started, the remaining fraction, B2, is sent to nanosatellite 2. Bundle B2 is sent to the gateway and hence to the server located in the Mission Control Center. In the server, bundles B11, B12 and B2 are reassembled to form bundle B. Once it has verified that the bundle was correctly received a DTN ACK bundle may be sent.

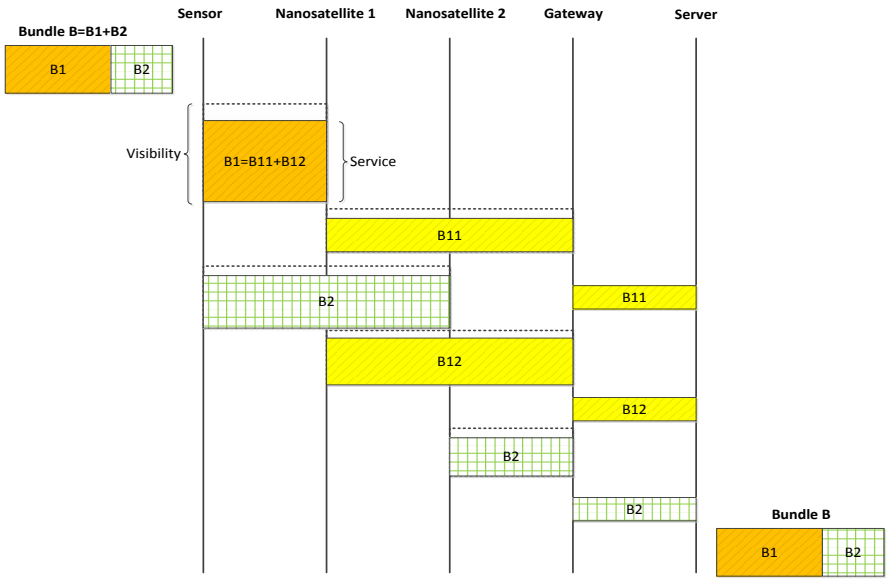


**Figure 27. DTN bundles in forward direction with reactive fragmentation**

It should be noted that our proposal uses DTN reactive fragmentation in order to cope with the variable service time and variable channel capacity in each contact. The usage of the DTN ACK (status report or custody signal) bundle is an optional feature in the DTN system. This ACK bundle is sent from the server to the gateway as Figure 28 shows. The gateway, being within the nanosatellite 2 coverage area, sends the ACK bundle to it. Finally, when the sensor is within the nanosatellite coverage, the ACK bundle will be sent to the sensor. The sensor receiving this agreement may perform a custody (CT) removal for this bundle B and frees up resources assigned to this. The process described above can also occur when, for example, the server has to send a bundle "Bn" to a sensor to configure some sensor parameters.

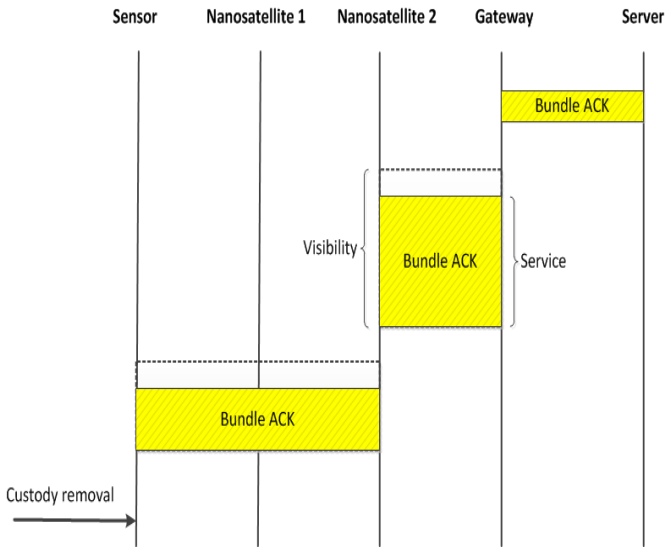

**Figure 28. DTN ACK bundles in return direction**

"Visibility time" is the time period the sensor is within range of the nanosatellite (contact), and "service time" is the time that starts when the sensor bundle layer generates a bundle sending request and ends when the bundle layer receives a report or is disconnected (no contact). Nanosatellite visibility starts before the sensor can detect its existence and ends before the sensor detects that the nanosatellite is no longer in its coverage.

ALOHAGP-CL is the convergence layer used in our architecture that supports higher level protocols such as DTN. It is fully compliant with the already defined TCP-CL standard [60]. This layer uses the services provided by the link layer ALOHAGP shown in Figure 26. ALOHAGP-CL builds and sends the local EID (e.g. <scheme>: G/S<radioID>) to the DTN layer, based on the radio ID information, provided by the ALOHAGP layer. When a sensor, a gateway or nanosatellite has something to send to another node, it first has to send a Contact Header [60] to that node. The node will also respond with a Contact Header that defines the initial contact parameters and allows the exchange of a singleton endpoint identifier (EID Singleton) to identify each node in the DTN bundle layer. Once the contact is defined and configured in this way, the bundles can be transmitted in both directions. Each bundle is sent in one or more data segments in bundle format. The maximum segment length of ALOHAGP-CL has been set to 128 Bytes, a value which is the size of the payload of the ALOHAGP data frame.

ALOHAGP-CL protocol states that the receiving node optionally sends acknowledgments after the arrival of the data bundle (ACK_SEGMENT). The idea is to allow the transmitting node to determine how much of the bundle has been received, so that if contact is interrupted, the transmitting node can perform a reactive fragmentation and avoid forwarding parts of the bundle that have already been transmitted. To make a cross-layer optimization of satellite resources this ACK_SEGMENT will be piggybacked onto the SIGNALING_FRAME (ACK) of the ALOHAGP protocol. Optional features established in [60] such as REFUSE_BUNDLE and SHOUTDOWN message are implementation dependent.

In order to clarify the DTN bundle transport from sensor to nanosatellite 1 through the exchange of segments, we will describe what happens in the ALOHAGP-CL convergence layer during service time (Figure 29). After a request to send a bundle a Contact Header message is sent to nanosatellite 1, nanosatellite 1 responds with another Contact Header to the sensor. Once the connection is established a DATA_SEGMENT 1 segment is sent from the sensor and ACK_SEGMENT 1 is received. After receiving ACK_SEGMENT 1, the sensor proceeds to send DATA_SEGMENT 2 and so on.

After receiving the ACK_SEGMENT 2, we assume that at this point a report is received from ALOHAGP layer, indicating that the sensor is no longer within the coverage area of nanosatellite 1 ("disconnect"). The ALOHAGP-CL layer generates a

report to the Bundle layer, reporting how many bytes have been sent successfully. With this information, the Bundle layer, using reactive fragmentation, generates a new bundle B2 (Figure 27). In the event that "disconnect" had occurred before the arrival of ACK_SEGMENT 2, then the DATA_SEGMENT 2 should be resent later.

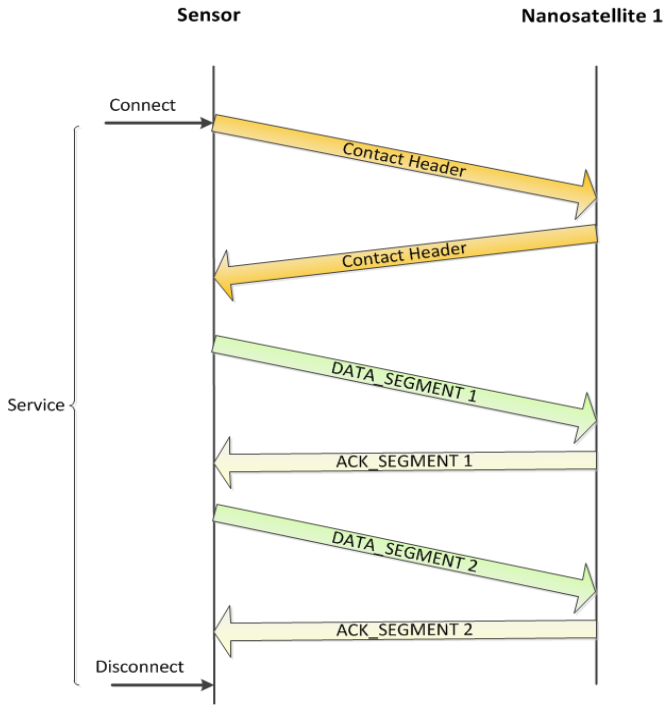


**Figure 29. ALOHAGP-CL segments exchange in uplink direction**

Finally, we also discuss what happens at ALOHAGP layer level during the data frame exchanges in the uplink direction considered above (Figure 30). Upon receiving the connection request ("Connect") of the top layer, ALOHAGP first sends DATA_FRAME 1, where the Contact Header is sent as payload. Nanosatellite 1 responds with a SIGNALING_FRAME (ACK) and then sends DATA_FRAME 11 to a sensor. The sensor responds with a SIGNALING_FRAME (ACK) and sends DATA_FRAME 2. If this frame is lost due to error or collision, then the sensor will resend it until it receives a SIGNALING_FRAME (ACK) that it has been received correctly. In the same way DATA_FRAME 3 is sent and a SIGNALING_FRAME (ACK) is received. Also, in each SIGNALING_FRAME the number of existing terrestrial nodes is indicated. In the future this information could allow a sensor to control its data rate depending on the number of ground sensors currently connected to the nanosatellite. After this point let us assume that it reaches a disconnect signal ("Disconnect") at the bottom layer and the sensor stops sending frames; after a while it will start sending DISCOVERY_FRAMEs.

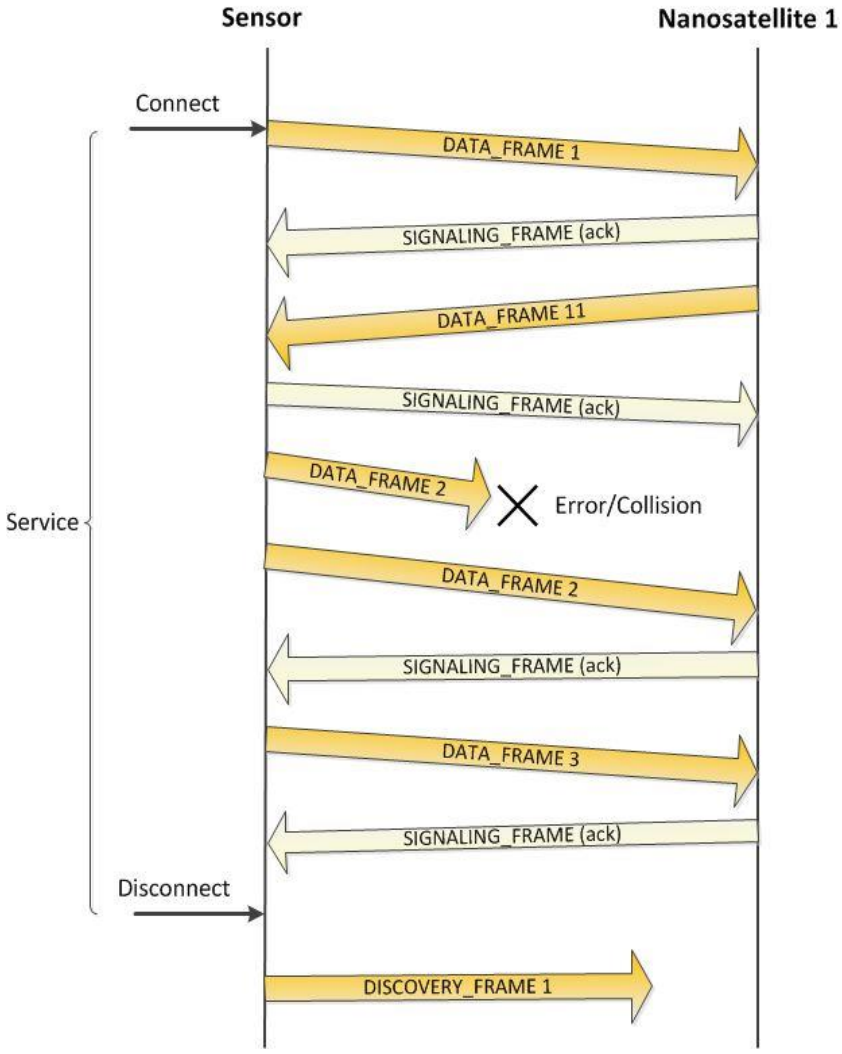


**Figure 30. ALOHAGP frames exchange in uplink direction**

## 5.2 ALOHAGP Protocol

### 5.2.1 ALOHAGP Features

In order to improve performance in nanosatellite networks, where Pure Aloha mechanism is typically used to service a sensor network [7], we propose an extension of unslotted Aloha. The basic features of the ALOHAGP protocol include:

Reliability: ALOHAGP protocol provides reliable data transfer. An exponential backoff mechanism is used to manage retransmission of frames, which prevents contention channel congestion.

Fairness: The fair use of satellite channel by all sensors is a very important requirement in the proposed service scenario. Fairness can be measured as the dispersion in the number of packets that each sensor transmits successfully (pi) with respect to the number of packets (m) that a sensor would transmit successfully if the channel capacity is used equally. If N is the number of sensors, m can be calculated as follows:

$$m = \frac{\sum_{1}^{N} p_i}{N} \quad (1)$$

We implemented a fair mechanism when a collision occurs; giving more chances to the node that was not currently using the channel. This was achieved by setting a very short retransmission time to the newly transmitting node and a long retransmission time to the currently transmitting node. These parameters will be shown later in Table 8.

Saturated traffic support: ALOHAGP is oriented to supporting saturated traffic patterns, where congestion decreases by reducing the probability of collision. The probability of collision is reduced when retransmission times differ for each node when a collision occurs (fair use mechanism).

Gateway Priority: When a node detects communication between a nanosatellite and a gateway, the node releases the channel. This allows the nanosatellite to download all content stored in memory and avoid saturation as a result of low storage capacity. When this occurs, the node considers all communications disconnected. This mechanism has been proposed because sensors located within the coverage of the nanosatellite degrade significantly the communication between the nanosatellite and the gateway. Once the nanosatellite has finished downloading and / or uploading data to/from gateway, other nodes can use the satellite channel. In principle this is subject to the implementation policies which may allocate only a fraction of the contact time to this priority connection.

### 5.2.2 ALOHAGP Protocol Definition

ALOHAGP (Aloha Gateway Priority) is a protocol that uses the unslotted ALOHA multiple access mechanism based on a strategy with Gateway priority access. Given the characteristics of the scenario, the nodes do not have synchronization mechanisms.

The protocol is intended to provide communication services to a network of ground sensors through a nanosatellite network and reliable service to upper layers in highly disruptive scenarios such as space segment. The frame structure of ALOHAGP protocol is shown in Figure 31. This consists of a header and a data payload of 14 and 128 bytes, respectively. Each frame has a preamble of 30 bytes and a Cyclic Redundancy Check (CRC) of 2 bytes.

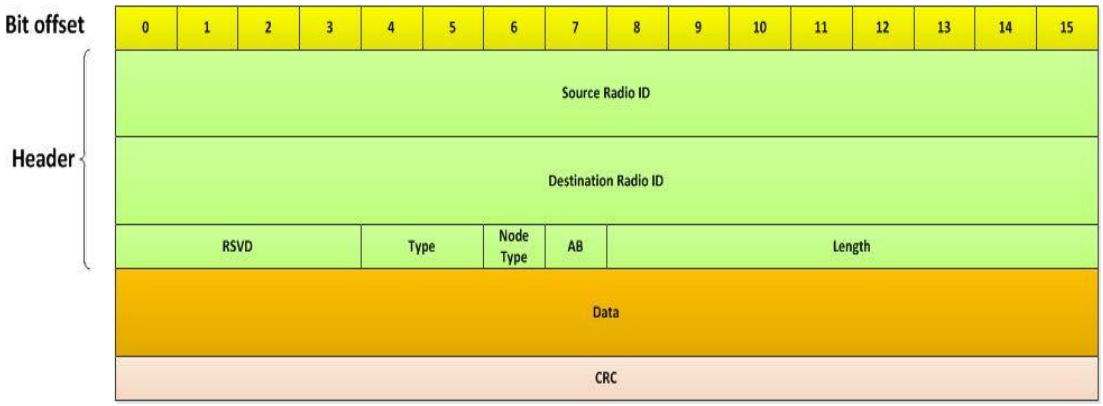


**Figure 31. ALOHAGP frame**

The ALOHAGP frame consist of a header and data field. The SIGNALING frame is the acknowledgment frame in ALOHAGP and its data field is empty. The DISCOVERY frame carries no data field and the destination ID is a broadcast Radio ID; it is used to indicate the presence of a node. DISCOVERY frames are generated periodically when a node has no data to send.

Proposed fields for ALOHAGP frame (Figure 31) are described below:

- Source Radio ID identifies the source radio interface, which is either sensor, gateway or nanosatellite.
- Destination Radio ID identifies whether the destination radio interface is sensor, gateway or nanosatellite. The radio ID of the DISCOVERY frame is broadcast type and implementation dependent.
- AB Flag is used to implement the "alternating bit protocol" [61] to manage the loss or damage of frames and can be "0" or "1".
- Type this is a 2-bit flag that identifies frame types: if it is a DATA frame, it is "01"; if SIGNALING, it is "10"; and if DISCOVERY, it is "00".
- NodeType Sets the type of the node from which the frame comes (uplink) or the type to be targeted (downlink): if it is a gateway node, it is 0; and if sensor, it is 1.
- RSVD 4-bits reserved for future use.
- Length indicates the size of the payload in bytes.
- Data Data field. This field exists only for the data frame and signaling.
- 16-bit CRC on the whole ALOHAGP frame without the preamble field.

### 5.2.3 ALOHAGP States

A node starts in the NO CONTACT state (Figure 32). When contact between the node and the satellite is established, the node goes into IDLE. When a data frame is transmitted, the node goes into WAIT ACK state. In this state, after a retransmission time-out "To" it retransmits the data, based on the backoff mechanism described above (to provide fairness and congestion control). If it receives acknowledgment (ACK), the

data has been correctly received, and confirmation is generated to the upper ALOHAGP-CL layer. The node then returns to IDLE, and more data waiting for transmission can be sent. Also, in WAIT ACK, the contact with the satellite may be lost ("Disconnect") and goes into NO CONTACT. In this state, DISCOVERY frames are sent every time (T1).

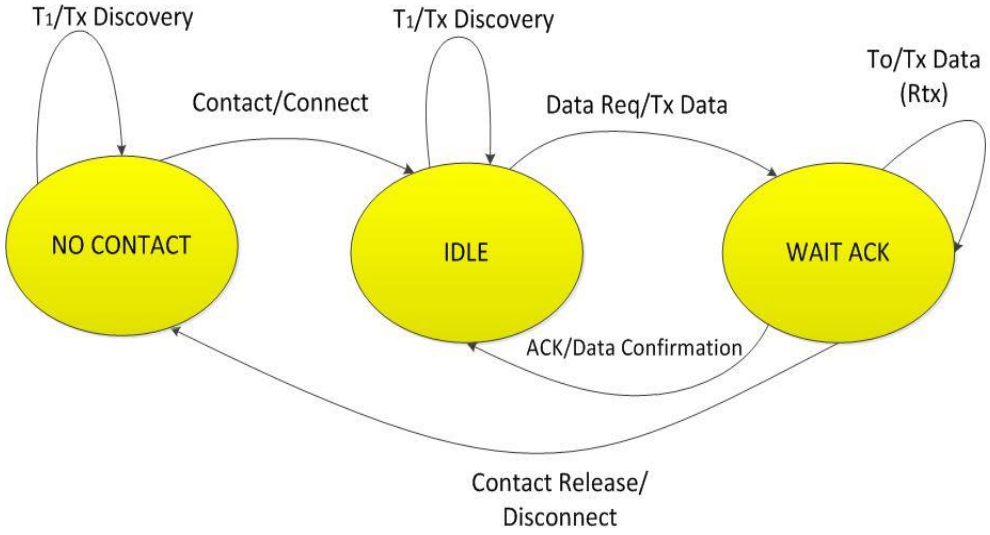


Figure 32. ALOHAGP Diagram States

### 5.2.4 Discovery mechanism

This mechanism maintains on each node a list of all the nodes with which it has contact. Figure 33 shows the Contact Table of nodes present within the coverage area of another node. Fields Source Radio ID and Type are defined in 5.2.2 and Age field gives us the time of arrival of the frame. We use this time to discard a frame after a period (T) of inactivity. Table completion is performed through the reception of SIGNALING, DISCOVERY and DATA frames that are addressed to it or to a different node. Each time a change is made to the table, either by detection of a new contact or inactivity of another contact already in the table, the information is sent to the upper ALOHAGP-CL layer (within the Connect or Disconnect indications shown in Figure 30).

| Radio ID Source | Type | Age |
|---|---|---|

Figure 33. Contact Table structure

The discovery function operation in node j is shown in Figure 34. Whenever a node receives a DISCOVERY_FRAME, SIGNALING_FRAME or DATA_FRAME, it updates the Contact Table with the Source Radio ID, the node Type targeted and the arrival time. The nanosatellites may generate as many connections (Contacts) as nodes are detected

in earth, and ground nodes (sensors, Gateway) may provide as many connections as nanosatellite are detected in space.

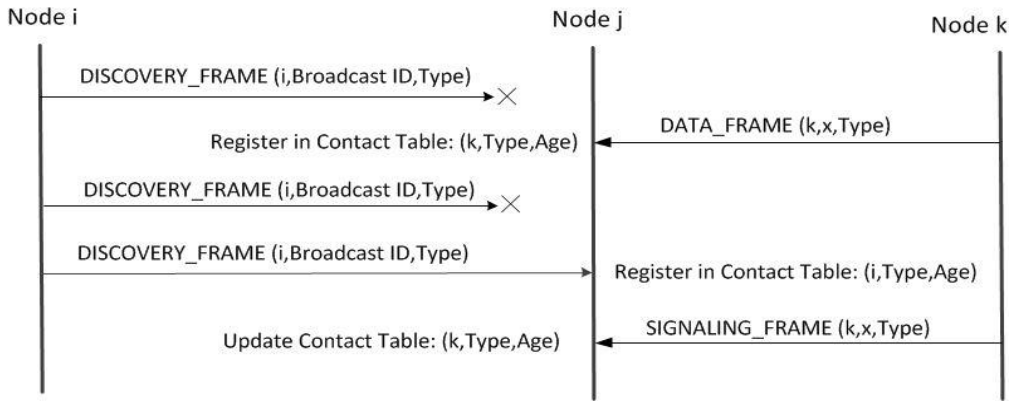


**Figure 34. Discovery Mechanism for Node j**

### 5.2.5 Contact Establishment

A sensor considers that a contact is established ("Connect" indication to ALOHAGP-CL) with a nanosatellite at ALOHAGP when the nanosatellite is in the Contact Table and there is no communication between the nanosatellite and a gateway (Type different from GW).

### 5.2.6 Contact Release

A node releases a contact ("Disconnect" indication to ALOHAGP-CL) with another node at ALOHAGP when:

- That node disappears from the Contact Table or
- Communication is detected between a nanosatellite and a gateway. In this case, all the nodes in the Contact Table are disconnected.

## 5.3 DTN System Performance

### 5.3.1 Simulation environment

The evaluation of the proposed DTN system with ALOHAGP was carried out using the ns-2 simulator. Backoff algorithms and the unslotted ALOHA retransmission policies were modified for the LEO satellite link. If a collision occurs between two sensors as we have described earlier, we set a very short retransmission time to the newly transmitting node and a long retransmission time to the currently transmitting node.

We have considered a scenario of terrestrial sensor monitoring where they communicate directly with a nanosatellite in saturated traffic condition. For our evaluation we have considered a nanosatellite in LEO orbit at an altitude of 700 km with an orbital inclination of 98 °. The sensors are visible, with elevation angles greater than 10 °, and the time of service is approximately 480 s [62]. Let us consider a maximum of 50 sensors within the satellite coverage. Given the number of sensors to be evaluated, it

is considered that the sensors enter incrementally within nanosatellite coverage. The configuration of simulation parameters can be found in Table 8. The data rate is fixed at 9600 bps, characteristic of such nanosatellites. The metrics used to evaluate the performance of our DTN system are: the goodput defined as the effective throughput for DTN layers, the average delay and fairness.

**Table 8. Configuration of simulation parameters**

| Parameter | Value |
|---|---|
| Bandwidth Uplink/Downlink | 9600 bps |
| Channel | 1 |
| Nanosatellite altitude | 700 km |
| Nanosatellite average visibility | 480 s |
| Maximum sensors in coverage area | 50 |
| Frame size | 174 B |
| Aloha retransmission policy<br>-Short retransmission time<br>-Long retransmission time | <br>0.145 s<br>75 s |

### 5.3.2 Goodput, Delay and Fairness

We carried out the goodput analysis considering two situations: environments with and without the presence of gateways.

In the scenario without the presence of a gateway, Figure 35 shows the goodput at the nanosatellite, which acts as a sink node as a function of the number of sensors that are within its coverage area. For the purpose of comparison, we also show the maximum efficiency obtained if we use a Pure Aloha. We can observe that system performance drops and the number of collisions increase due to the increase in the number of sensors simultaneously accessing the nanosatellite. Even in the case of a highly congested system, the performance falls to 44%, much greater than the 18% obtained by the Pure Aloha.

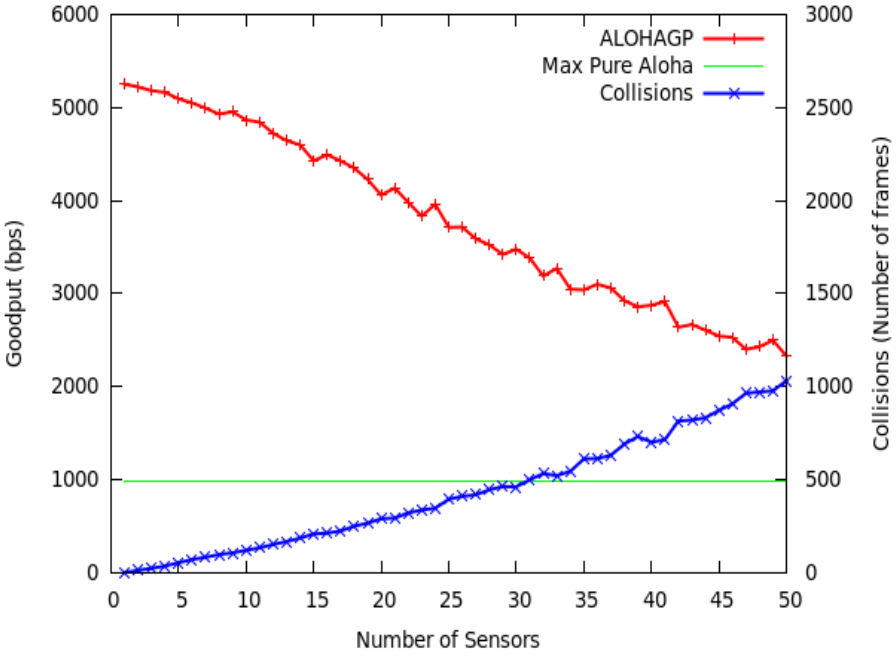


**Figure 35. Goodput at sink nanosatellite versus number of sensors without gateway presence**

In a situation with gateway presence, we can see a big improvement in the gateway goodput using our proposal. Without the ALOHAGP protocol implementation, the goodput of a gateway in a scenario of high congestion may be only 1% of the goodput obtained using ALOHAGP implementation as seen in Figure 36. This gain on ALOHAGP implementation is key in this type of limited contact system where download data from the nanosatellite is a priority.

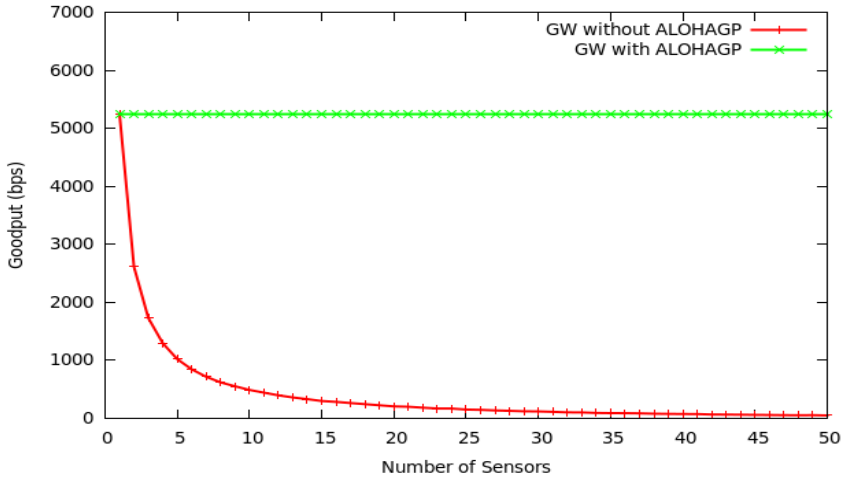


**Figure 36. Goodput at GW versus number of sensors with gateway presence**

Increasing the number of sensors simultaneously accessing the satellite channel without the presence of a gateway causes an increase in mean frame delay as shown in Figure 37. This is because the probability of collision increases with the number of sensors. Note that the delay obtained is close to the delay that we would achieve if each

node uses a homogeneous portion of the channel capacity "goodput (bps)/N (Sensors)"; this means that the mean number of retransmissions is low and the contention mechanism is stable.

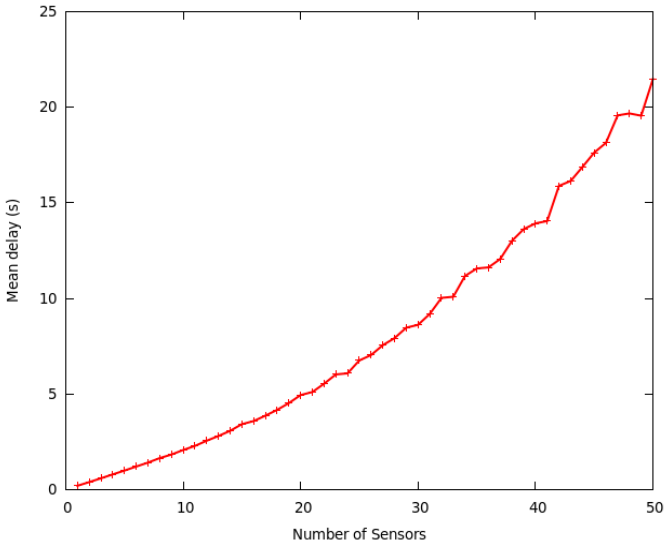


**Figure 37. Average transmission delay versus sensor ID**

The fair use of the satellite channel can be seen in Figure 38. This shows that the multiple access mechanism implemented in ALOHAGP distributes satellite channel well between the sensors, considering the number of frames a nanosatellite receives successfully. These can be compared to the value they would have if the channel was equally distributed (m = 22 frames). This value is obtained by using the Equation 1 for our system. We can easily see that all the sensors have access to the satellite channel.

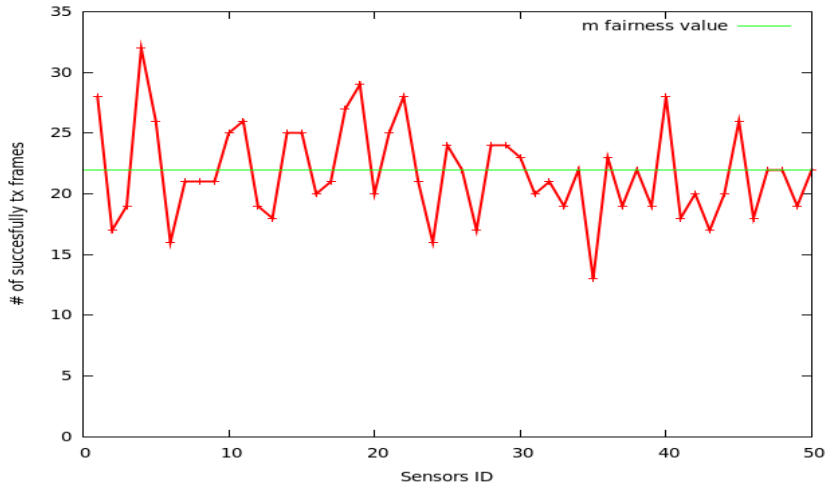


**Figure 38. Successful tx frames versus sensor ID in a nanosatellite contact of 480s**

### 5.3.3 DTN Bundle performance

Given that each transmission of a DTN bundle needs at least two frames that are properly acknowledged, we can estimate the size of the DTN bundle transmitted during service time with the nanosatellite, as shown in Figure 39. It can be seen that the size of

the DTN Bundle in our system is variable, which leads us to think that we have to implement a reactive fragmentation mechanism in our DTN system. We can also observe that in our scenario, DTN bundles of less than 1500 bytes are very likely to pass without fragmentation. Given that a nanosatellite has at least two contacts per day with the same sensor, the transferred bundle amount doubles every day. If we increased the number of nanosatellites forming a nanosatellite network, this would also increase the amount of contacts with the sensor and therefore the amount of transmitted bundles. Finally, we can infer that increasing the number of globally distributed gateways will reduce the data download time from nanosatellites in this disruptive scenario.

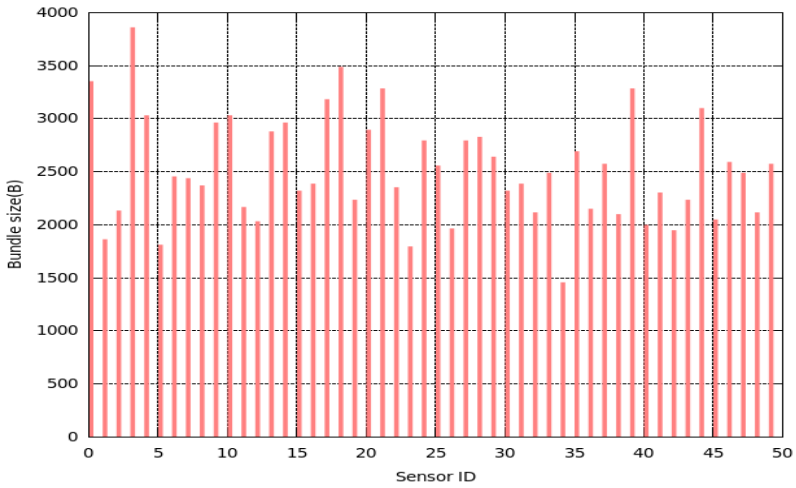


**Figure 39. Bundle size successfully received at sink nanosatellite per sensor ID in a nanosatellite contact of 480 s**

## 5.4 Summary

In this chapter, I propose and evaluate a new communications architecture based on DTN to provide data service to a network of ground sensors, using satellite communications based on nanosatellites. In addition, I propose and evaluate a new ALOHAGP multiple access mechanism in our system based on goodput, delay and fairness, and it assumes a finite population and saturated traffic condition. I conclude that the proposed architecture provides simple, optimal and fair distribution performance in terms of transmission of DTN bundles. In the next chapter, I will deepen the study of multiple access mechanisms herein proposed for this type of satellite networks.

# 6 Multiple Access Design and Analysis

In this chapter I analyze, evaluate and optimize a new multiple access protocol (ALOHADP) based on a deeper study of ALOHAGP protocol described before in the last chapter, to provide services to terrestrial wireless sensor network, using a space Disruptive/Delay Tolerant Networking (DTN) based solution. This new multiple access protocol is based on unslotted ALOHA extended with an adaptive contention mechanism. It uses satellite feedback to implement the congestion control, and to dynamically adapt the channel effective throughput in an optimal way. The effective throughput has been optimized by adapting the protocol parameters as a function of the current number of active sensors received from satellite. The proposed protocol also takes into account the priority of the satellite downlink traffic. We assume a finite sensor population model and a saturated traffic condition. The system model proposed has been analyzed and the performance has been evaluated in terms of effective throughput, delay and system fairness among sensors. A good matching has been obtained between the analytical model and the simulation results.

## 6.1 ALOHADP Protocol

ALOHADP is a reliable protocol that uses the unslotted ALOHA multiple access mechanism based on a strategy with downlink priority access. Given the characteristics of the scenario, the terrestrial nodes and nanosatellite do not require synchronization mechanisms.

The protocol is intended to provide communication services to a network of ground wireless sensors through a nanosatellite network and aims to provide reliable service to upper layers in this highly disruptive scenario. The frame structure of ALOHADP protocol consists of a header of 14 bytes and variable data payload. Each frame [59] has a preamble of 30 bytes and cyclic redundancy check (CRC) of 2 bytes.

I propose a simple fair mechanism when a collision occurs as shown in Figure 40, giving more chances to the node that was not currently using the channel. This is achieved by setting a very short retransmission time to the new transmitting node and setting a long random retransmission time ($T_{rtl}$) to the currently transmitting node. This $T_{rtl}$ time is always much lower than visibility time. These parameters are shown in **Table 9**.

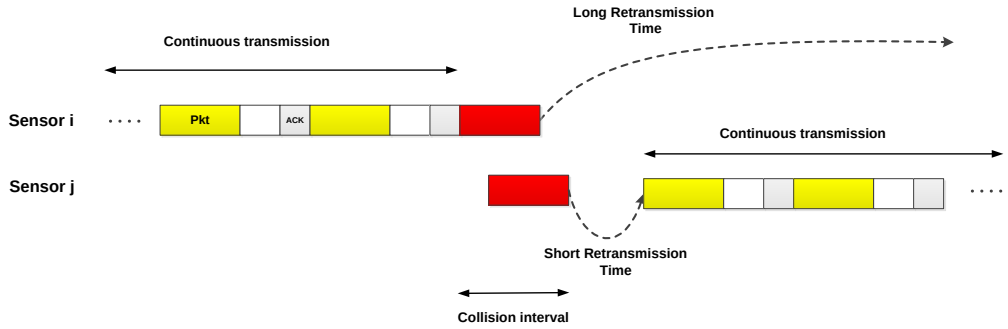


Figure 40. Fair mechanism in ALOHADP

- Saturated traffic support with congestion control: ALOHADP is oriented to supporting a saturated traffic pattern generated by each sensor, where the congestion is reduced by reducing the probability of collision. The probability of collision is reduced when retransmission times differ for each sensor when a collision occurs (fair use mechanism). The acknowledgment (ACK) received from the nanosatellite contains the number of terrestrial nodes present within the nanosatellite coverage area. This information is used to control the ALOHA congestion, adapting the Long Retransmission time and packet size in an efficient way as we will analyze below.
- Downlink Priority: When a nanosatellite detects the existence of a gateway, all the downlink traffic is priority. This mechanism allows the nanosatellite to download all the information as soon as possible to the gateway. This is also useful in the case of a satellite's low storage capacity. Once the nanosatellite has finished downloading its data to the gateway, the satellite channel can be used to upload data from sensors to nanosatellite. In principle, this is subject to the implementation policies which could allocate only a fraction of the contact time to this downlink priority connection. When sensors detect this priority traffic (It receives some Frame/ACK addressed to the gateway), they stop frame transmission.

## 6.2 ALOHADP States

ALOHADP Data Transmission State Diagram of a terrestrial node is shown in Figure 41. It uses satellite layer services primitives (Contact.ind, ContactReleased.ind, Rx.ind

and TxData.req) and provides services primitives to the ALOHADP-CL layer (Connect.ind, Disconnect.ind, DataConf.ind and Data.req).

ALOHADP starts in the NO CONTACT state. When the Contact.ind indication is received from the satellite layer a Connect.ind indication is sent to the ALOHADP-CL layer and the node goes into the IDLE state. When a Data.req request is received from the ALOHADP-CL layer a TxData.req request is transmitted to the satellite layer and the terrestrial node goes into the WAIT ACK state. When an Rx.ind indication is received, indicating that an ACK has arrived from satellite layer, a DataConfirmation.ind indication is sent to the ALOHADP-CL layer and the nanosatellite returns to the IDLE state, where more data waiting for transmission can be sent. If no Rx.ind indication is received before the expiration of the retransmission time-out "To", then it retransmits using the TxData.req request, based on the retransmission mechanism described above (to provide fairness and congestion control). Also, being in WAIT ACK, the contact with the nanosatellite may be lost. In this case a ContactReleased.ind indication is received from the satellite layer and a Disconnect.ind indication is sent to ALOHADP-CL layer and the terrestrial node transmitter passes to the NO CONTACT state.

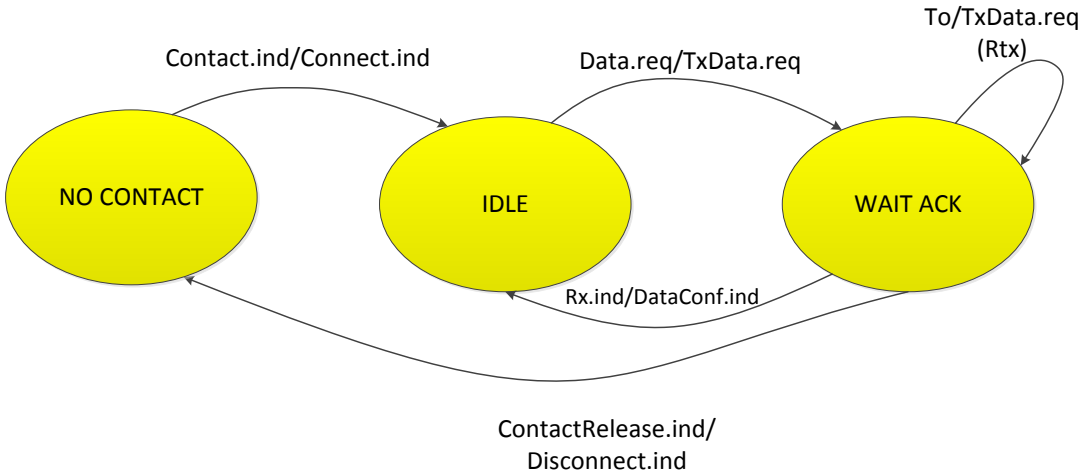


**Figure 41. ALOHADP Data Transmission State Diagram of a terrestrial node.**

## 6.3 Optimal frame size determination

In this thesis, we analyze the Aloha system, defined above, with finite user population N (sensors) and saturated traffic condition, i.e. on average each sensor queue is not empty. The validation of the analytical model proposal of the ALOHADP system was carried out using the ns-2 simulator [55].

We have considered a scenario of terrestrial sensor monitoring, where sensors communicate directly with a nanosatellite. For our evaluation we have considered a nanosatellite in LEO orbit at an altitude of 700 km with an orbital inclination of 98°. The sensors are visible, with elevation angles greater than 10° and the time of service is approximately 480 s [62]. Let us consider a maximum of 100 sensors within the satellite coverage. It is considered that the sensors enter incrementally within nanosatellite

coverage. The channel data rate is fixed at 9600 bps, which is typical in such nanosatellites.

The metrics used to evaluate the performance of our DTN system have been: throughput, average delay and fairness. **Table 9** shows the system parameters used in our study.

**Table 9. Configuration of system parameters**

| Symbol | Parameter | Value |
|---|---|---|
| R | Bandwidth Uplink and Downlink (Duplex) | 9600 bps |
| $t_v$ | Nanosatellite visibility | 480 s |
| h | Nanosatellite altitude | 700 Km |
| o | Orbital inclination | 98º |
| e | Elevation angles | > 10º |
| $t_f$ | Data frame duration ($t_{pa}$ + $t_h$) | 0.05 s … 0.3 s |
| $t_d$ | Round trip propagation delay | 0.007 s |
| $t_{ACK}$ | ACK transmission time | 0.043 s |
| $t_a$ | Time to ACK reception ($t_{ack}$ + $t_d$) | 0.05 s |
| $t_w$ | Retransmission waiting time | 0.051 s |
| $t_h$ | Header duration | 0.038 s |
| $t_{pa}$ | Payload duration | 0.012 s … 0.262 s |
| $\bar{T}_{rl}$ | Long retransmission mean time | 2…75 s |
| BER | Bit error rate | $10^{-5}$ |
| $L_f$ | Data frame length ($t_f$ * R) | 60 B … 360 B |
| N | Sensors in coverage area | 2…100 |

### 6.3.1 System analysis

In this section, an analytical approach is presented to derive parameters of effective throughput ($S_{ef}$) and the offered traffic ($G_{ef}$) as a function of data packet duration ($t_p$), sensor number (N) and long retransmission mean time ($\overline{T}_{rl}$). Trl is an exponential random variable that takes a mean value$\overline{T}_{rl}$. We will analyse our system model taking into consideration two scenaries related to collision effect. First, we will analyse a simple collisions scenario and then multiple collisions scenarios.

In our first scenario all sensors, except the one currently transmitting, have previously collided and they (N-1 sensors) are waiting $T_{rl}$ (exponential distribution) to start their transmission.

Because $T_{rl}$ random variables can be considered independent and follow an exponential distribution, the arrival of new transmission tries will follow a Poisson arrival process (λ) as shown in Figure 42, where we show an analysis of a single collision between two sensors i and j. We assume that the sensor i is using the satellite channel and sensor j is trying to use the satellite channel. Upon collision, the retransmission mechanism that we propose assigns a long retransmission time ($T_{rl}$) to sensor i, which has been using the channel and sensor j retransmit immediately. I establish these two restrictions in my proposed simulation. $\overline{T}_{rl}$ Must fulfill the following two conditions:

a. Retransmission mean time $\overline{T}_{rl}$ affects the fair channel distribution and the probability of collision. If $\bar{T}_{rl} \geq t_v$ the terminal will not have another opportunity of retransmission during the visibility time $t_v$. Thus, we require $\bar{T}_{rl} < t_v$, preventing a sensor from monopolizing the satellite channel all the time.
b. $\bar{T}_{rl}$/(N-1) is defined as the average time to find a frame collision in an ALOHA channel model, due to the Markovian characteristic of the system. We make this average time very superior to data frame duration to minimize the collision probability. Thus, we require $\bar{T}_{rl}$/(N-1) >> $2t_f$.

Let us analyze the proposed scenario with single collision. The arrival rate is given as:

$$\lambda = \frac{(N-1)}{\bar{T}_{rl}} \qquad (2)$$

Due to the Markovian characteristic of the system, on average, a collision will occur after $\overline{T}_{rl}/(N-1)$ . Therefore, if we adjust this time to the start of the collided frame the mean continuous transmission time is:

$$\bar{T}_x = \frac{\bar{T}_{rl}}{(N-1)} - \frac{(t_f + t_a)}{2} \qquad (3)$$

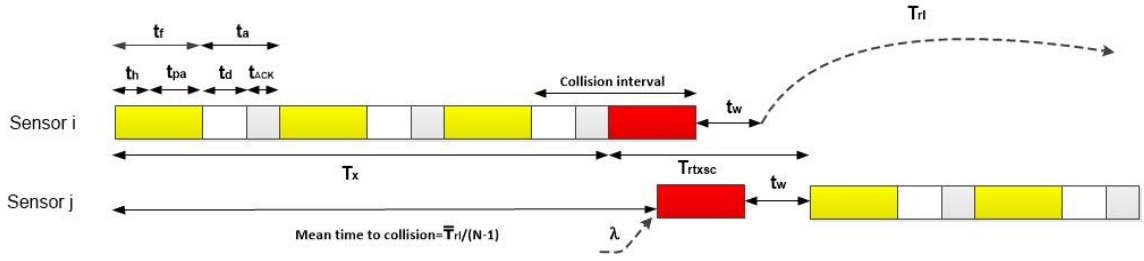


**Figure 42. Single collision mechanism for ALOHADP**

Figure 42 shows a collision between two sensors and the relation among all the variables. A collision may occur randomly at any instant from the beginning of the packet to the end of the

ACK $(t_f + t_a)$; the mean value is $(t_f + t_a)/2$. Considering that $t_f > t_a$, the simple collision resolution time for a simple collision ($\overline{T}_{rtxsc}$) is given as:

$$\overline{T}_{rtxsc} = t_f + t_w + \frac{(t_f + t_a)}{2} \qquad (4)$$

We define the retransmission waiting time ($t_w$) to be higher than the time to ACK reception $t_a$, which is the sum of ACK transmission time and the roundtrip propagation delay, which is: $t_w > (t_{ACK} + t_d)$. This condition is to ensure that the frame retransmission is needed (i.e. no ACK is received).

Now let us consider the case of a multiple collision scenario. In this case, if $\overline{T}_{rl}$ fulfills the conditions stated above, a double collision occurs with low probability, and higher collisions will be negligible. We will assume that after a first collision as described in Figure 42, a second collision will occur with a sensor k, as shown in Figure 43. Considering the interval vulnerability of this double collision, and depending on the time of arrival of sensor k to produce the double collision, we have identified two cases named case 1 and case 2. Case 1 will happen if sensor k arrives at the range of packet duration for sensor j. Case 2 will occur if the sensor k arrives at the interval included by the retransmission waiting time ($t_w$) plus the retransmitted packet for sensor j.

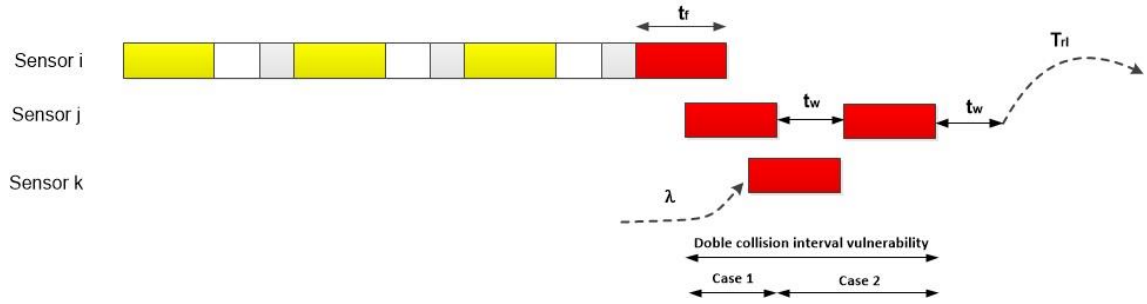


**Figure 43. Double collision mechanism for ALOHADP**

The probability of a second collision, taking into consideration the double collision vulnerability interval is given as:

$$P_{2col} = 1 - e^{-\frac{(N-2)}{\overline{T}_{rl}}(2t_f + t_w)} \qquad (5)$$

Let us analyze case 1 as shown in Figure 44.

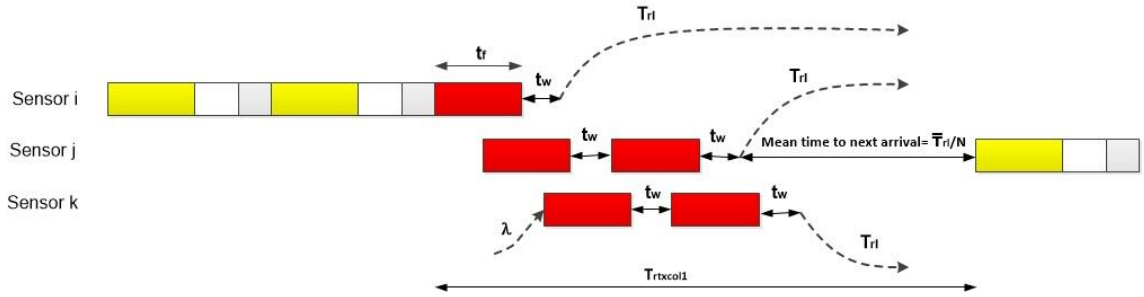


**Figure 44. Double collision mechanism for ALOHADP in case 1.**

Where double collision resolution time for case 1, $\overline{T}_{rtxcol1}$ is:

$$\overline{T}_{rtxcol1} \cong \overline{T}_{rtxsc} + t_f + t_w + \frac{\overline{T}_{rl}}{N} \quad (6)$$

And the probability that a second collision will occur in case 1, is given as:

$$P_{2col1} = 1 - e^{-\frac{(N-2)}{\overline{T}_{rl}} t_f} \quad (7)$$

In similar way, we analyze case 2 as shown in Figure 45.

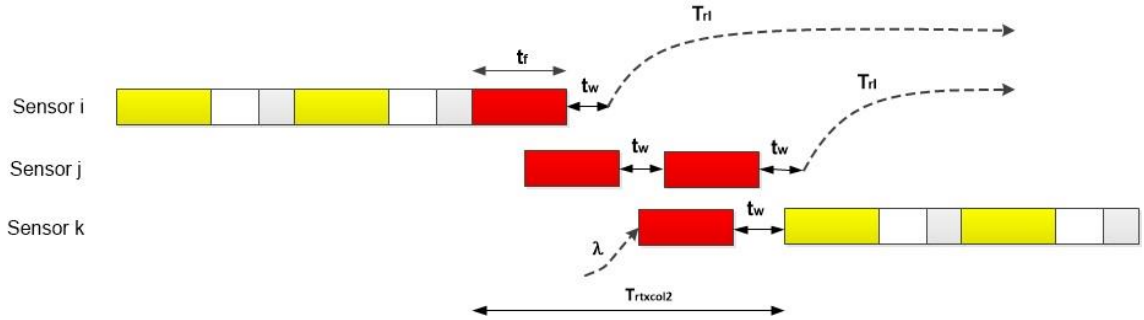


**Figure 45. Double collision mechanism for ALOHADP in case 2**

Where double collision resolution time in case 2, $T_{rtxcol2}$ is:

$$\overline{T}_{rtxcol2} = \overline{T}_{rtxsc} + \frac{3t_f + t_w}{2} \quad (8)$$

And the probability of a second collision occurring in case 2 is given as:

$$P_{2col2} = (1 - P_{2col1})\left(1 - e^{-\frac{(N-2)}{T_{rl}}(t_f + t_w)}\right) \quad (9)$$

The average total resolution time, $\overline{T}_{rtx}$ considering only single and double collisions will be expressed as follows:

$$\bar{T}_{rtx} = (1 - P_{2col})\bar{T}_{rtxsc} + P_{2col1}\bar{T}_{rtxcol1} + P_{2col2}\bar{T}_{rtxcol2} \quad (10)$$

We have considered negligible higher order collisions, and simulation results validate this assumption. Considering Eq. 10 and Eq. 3, we can obtain the normalized channel throughput (S) using the following equation:

$$S = \left(\frac{\bar{T}_x}{\bar{T}_x + \bar{T}_{rtx}}\right)\left(\frac{t_f}{t_f + t_a}\right) \quad (11)$$

And the offered traffic (G) is:

$$G \cong S + (1 - P_{2col})\left(\frac{2t_p}{\bar{T}_x + \bar{T}_{rtxsc}}\right) + P_{2col1}\left(\frac{5t_p}{\bar{T}_x + \bar{T}_{rtxcol1}}\right) + P_{2col2}\left(\frac{4t_p}{\bar{T}_x + \bar{T}_{rtxcol2}}\right) \quad (12)$$

We define the effective payload throughput ($S_{ef}$) as the normalized channel throughput (S) without considering the header overhead:

$$S_{ef} = S * \left(\frac{t_{pa}}{t_{pa} + t_h}\right) \quad (13)$$

Also, in a similar way we define the effective offered traffic ($G_{ef}$):

$$G_{ef} = G * \left(\frac{t_{pa}}{t_{pa} + t_h}\right) \quad (14)$$

Finally, we analyzed the effect of the error ratio (BER) on the satellite channel. To do so, we considered what happens when an error occurs, as shown in Figure 46. Sensor i is not aware of the error and it behaves as a single collision as described in Figure 42.

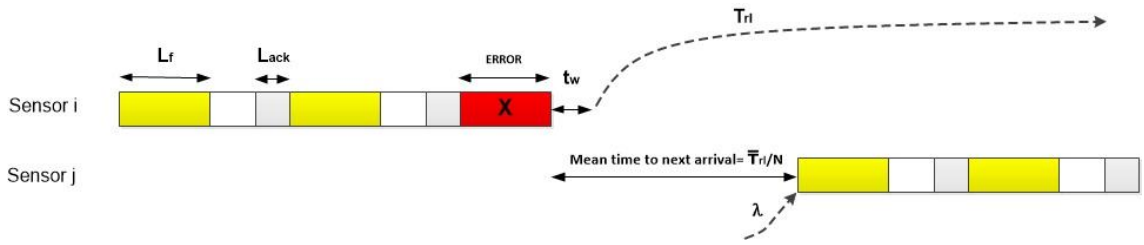


**Figure 46. BER effect for ALOHADP**

If we consider that PER ≅ BER*(Lf+Lack), where Lack is the length of the ACK frame, the average number of packets between errors is 1/PER and the mean time between errors is:

$$\bar{T}_E \cong \left(\frac{L_f}{S*R}\right) * \frac{1}{PER} \qquad (15)$$

Finally, the effective payload throughput with error ($S_{BER}$) will be:

$$S_{BER} = S_{ef} * \frac{\bar{T}_E}{\bar{T}_E + \frac{\bar{T}_{rl}}{N}} \qquad (16)$$

### 6.3.2 Throughput, Delay and Fairness

In order to validate the performance obtained from the theoretical model with BER=0 for the ALOHADP protocol given for Eq.13 and Eq.14, a simulation was performed considering ($t_p$=0.145s and $\bar{T}_{rl}$ =75 s) and the results are shown in Figure 47. A matching between the theorical and simulated results is observed. $G_{ef}$ is increased due to the collision effect analyzed above. Note that the protocol and frame overheads limit the maximum effective throughput to $\left(\frac{t_p}{t_p+t_a}\right)\left(\frac{t_{pa}}{t_{pa}+t_h}\right) = 0.55$ .

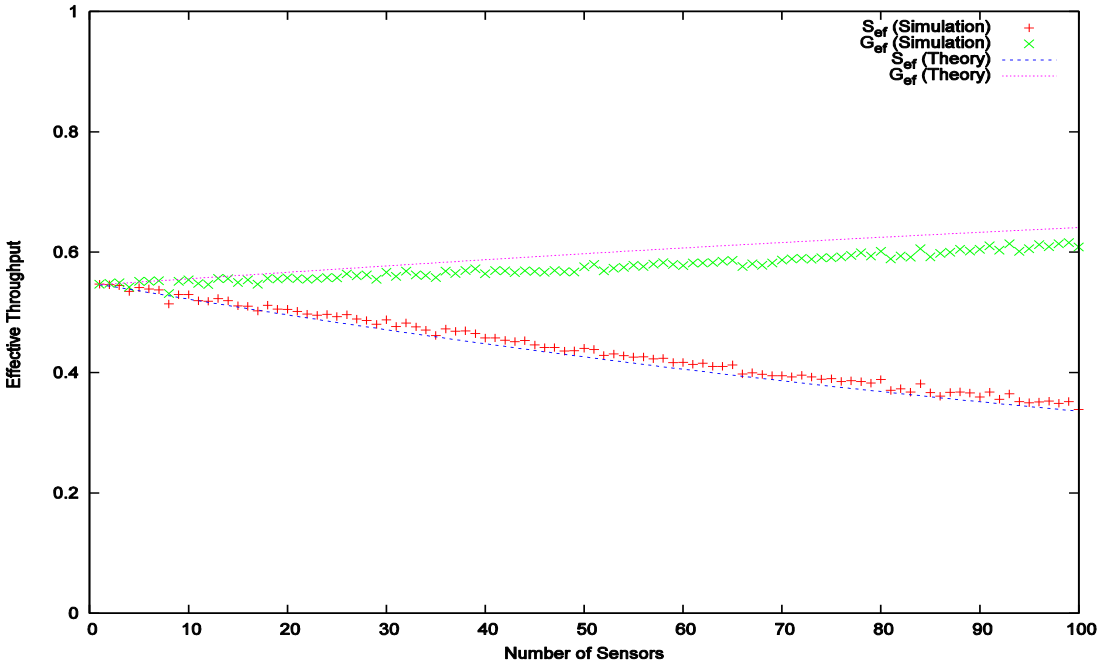


**Figure 47. Gef and Sef comparisons obtained with BER=0.**

Now, if we consider that BER=$10^{-5}$, which is an standard value used in space communications, we could compare in Figure 48 the theoretical results of $S_{BER}$ (from Eq. 16) with respect to $G_{BER}$ obtained from the simulation. It is also observed that in the worst case (N = 100 sensors) for each 10 frames sent successfully, 8 frames are resent (G/S≈1.8). If we compare Figure 47 and Figure 48, we can observe that BER affects the throughput mainly when the number of sensors is small (< 20 sensors) due to the fact that $\overline{T}_{rl}/N$ is high.

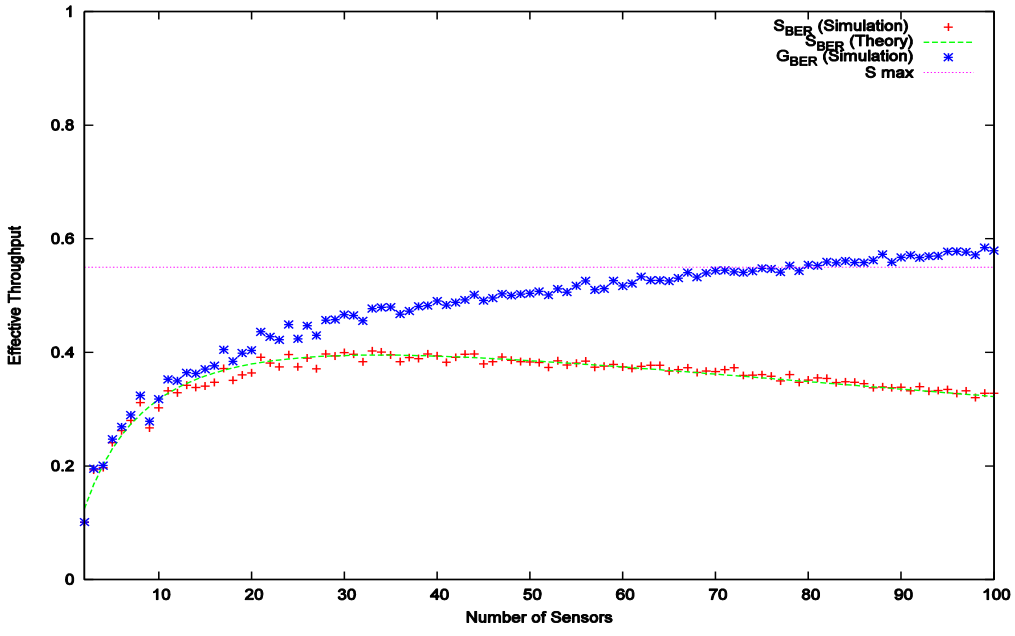


**Figure 48. $G_{BER}$ and $S_{BER}$ comparisons with BER=$10^{-5}$.**

To optimize the system performance of our model, we analyzed the $S_{ef}$ behavior with BER=$10^{-5}$ as a function of frame duration ($t_f$) and long retransmission time ($\overline{T}_{rl}$). Figure 49 shows how $S_{ef}$ changes, given a constant value of $t_f$ ($t_f$ = 0,145s) and a variable $\overline{T}_{rl}$ for different numbers of sensors. Our analysis shows that, in general, $S_{ef}$ increases with $\overline{T}_{rl}$ if the number of sensors is high, but an optimum $\overline{T}_{rl}$ exists for small N.

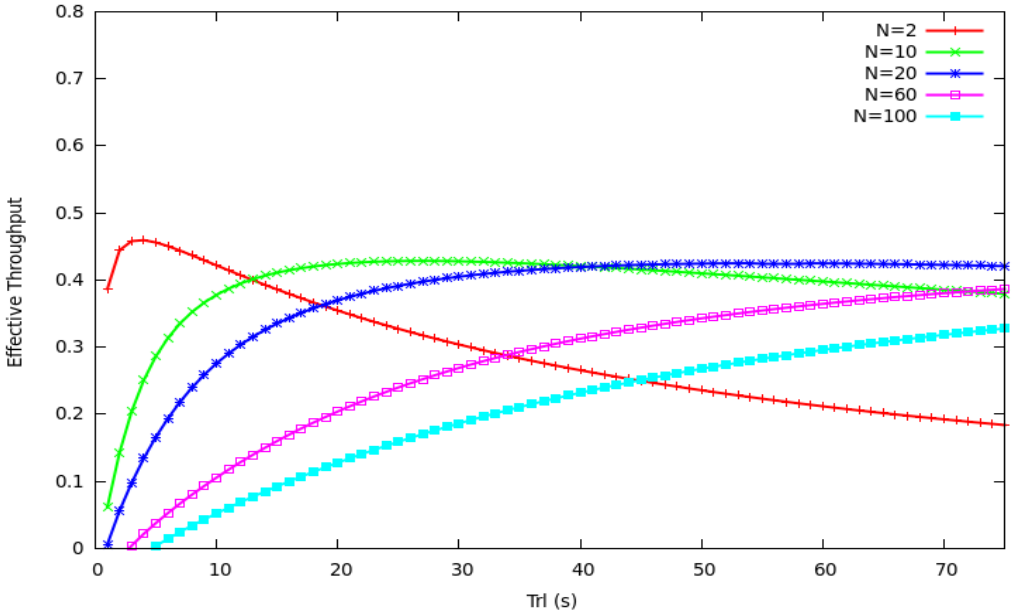


**Figure 49. Throughput behavior vs $\overline{T}_{rl}$ for different numbers of sensors in ALOHADP**

Similarly, Figure 50 shows how $S_{ef}$ changes, given a constant $\overline{T}_{rl}$=75 s with increasing $t_p$ values for different number of sensors. It also shows that $S_{ef}$ increases with $t_f$ if N is small, but an optimum $t_f$ exists for large N.

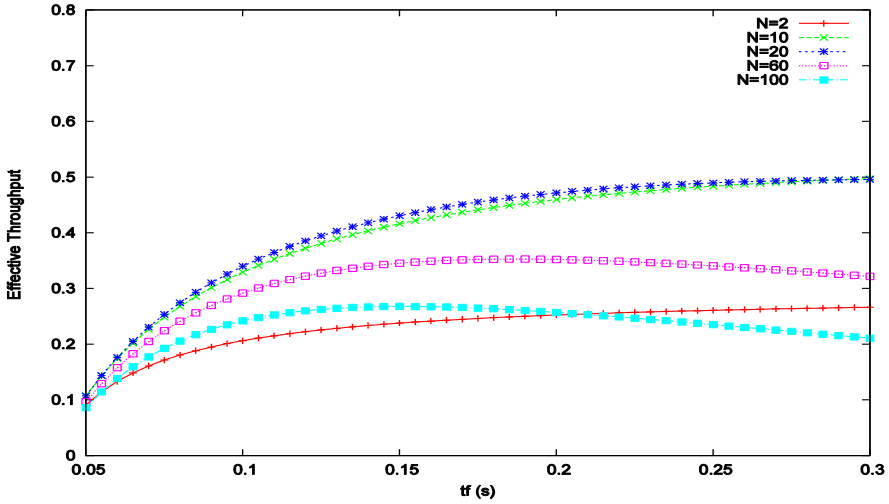


**Figure 50. Throughput behavior vs $t_f$ for different numbers of sensors in ALOHADP**

Given a fixed value sensor we observed how $S_{ef}$ changes as a function of $t_p$ and $\overline{T}_{rl}$ to obtain the maximum performance ($S_{ef\text{-}max}$). It is observed that the area of greatest performance for the two sensors (N=2) is for $t_p$> 150 ms and $\overline{T}_{rl}$ < 10 s as shown in Figure 51.

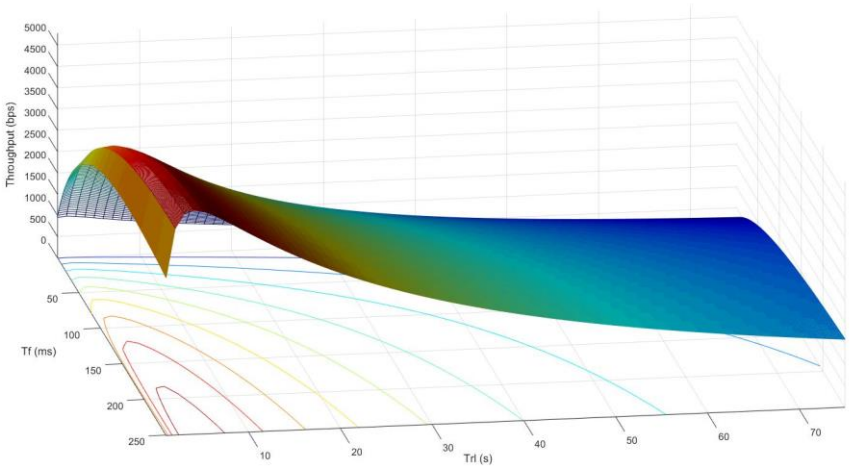


**Figure 51. Throughput behavior vs $\overline{T}_{rl}$ and $t_f$ for N=2 sensors in ALOHADP**

Figure 52 shows the maximum value of $S_{ef}$ ($S_{ef\text{-}max}$) obtained in the area of greatest performance for each number of sensors N. Each theoretical $S_{ef\text{-}max}$ point corresponds to a $t_f$ and $\overline{T}_{rl}$ that is optimal for that N, we call this "adaptive $S_{ef\text{-}max}$". Taking into account the values obtained for $\overline{T}_{rl}$ and $t_f$ to find a Sef-max, a validation has been performed in Matlab. We include Formula 16 and perform an analysis to obtain $S_{ef\text{-}max}$, by varying parameters $\overline{T}_{rl}$ and $L_f$. $\overline{T}_{rl}$ is varied from 2 to 75 seconds, $L_f$ from 60 to 360 Bytes, and N from 2 to 100 sensors, as indicated in Table 9. With this variations we obtain optimal values of $\overline{T}_{rl}$ and $L_f$ which maximizes $S_{ef}$ for an N number of sensors, obtaining the theoretical value of $S_{ef\text{-}max}$.

Optimal values of $\overline{T}_{rl}$ and $L_f$ are used in ns-2 to recreate the scenario with a satellite and two sensors, obtaining the simulated value of $S_{ef\text{-}max}$, which is compared to the theoretical value of Sef-max obtained from Matlab. It was observed that the points obtained fit quite well the theoretical results obtained for our model with a confidence interval of 95%. We can also compare the optimized $S_{ef\text{-}max}$ with an unoptimized $S_{ef}$ with values ($t_f$=0.145s and $\overline{T}_{rl}$ =75 s). A great improvement is obtained for small N values using the proposed ALOHADP adaptive mechanism, where the long retransmission time and bundle size are optimally selected.

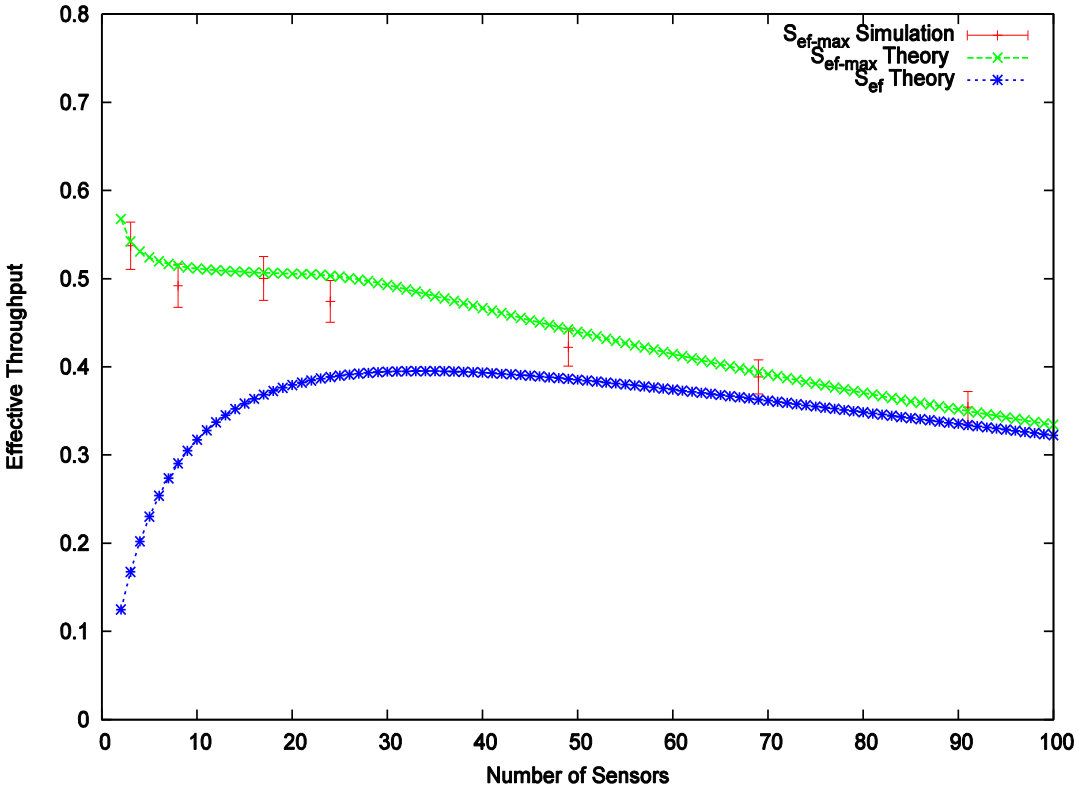


**Figure 52. Adaptive (Sef-max) vs non-adaptive (Sef) ALOHADP throughput with BER=$10^{-5}$.**

Additionally, we used simulations to obtain values for delay and fair use of the channel. Increasing the number of sensors simultaneously accessing the satellite channel causes an increase in mean frame delay as shown in Figure 53. This is because the probability of collision increases with the number of sensors, where $G_{ef}$ increases as shown in Figure 48. Note that the delay obtained is close to the delay that we would achieve if each node had used a homogeneous portion of the channel capacity "$S_{ef}/N$". This means that the mean number of retransmissions is low and the contention mechanism is stable.

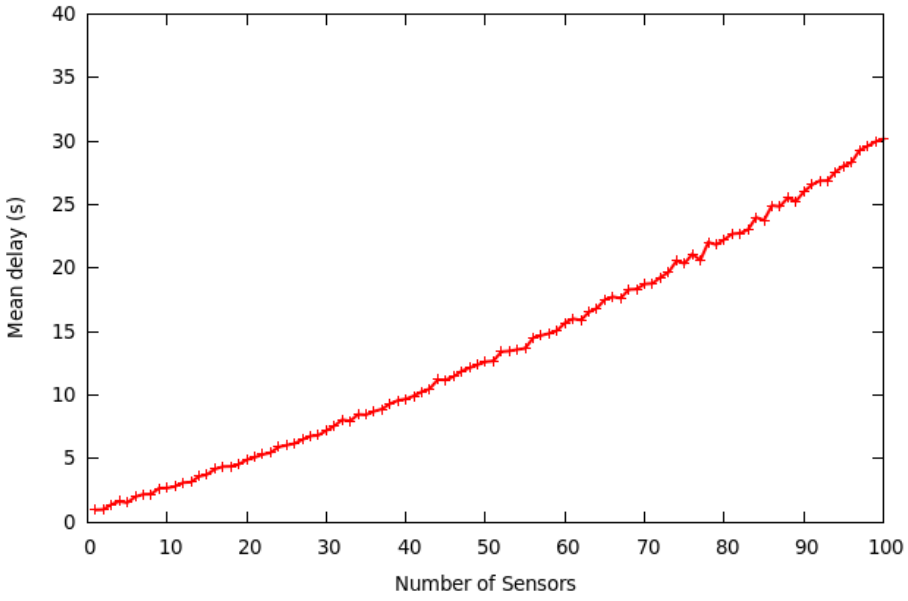


Figure 53. Average transmission delay versus sensor ID

The fair use of the satellite channel can be seen in Figure 54. This shows that the multiple access mechanism implemented in ALOHADP distributes satellite channel capacity between the sensors in a fair way. It can be compared to the value they would have if the channel was equally distributed (m = 15 frames), using Equation 1. We can easily see that all the sensors have fair access to satellite channel.

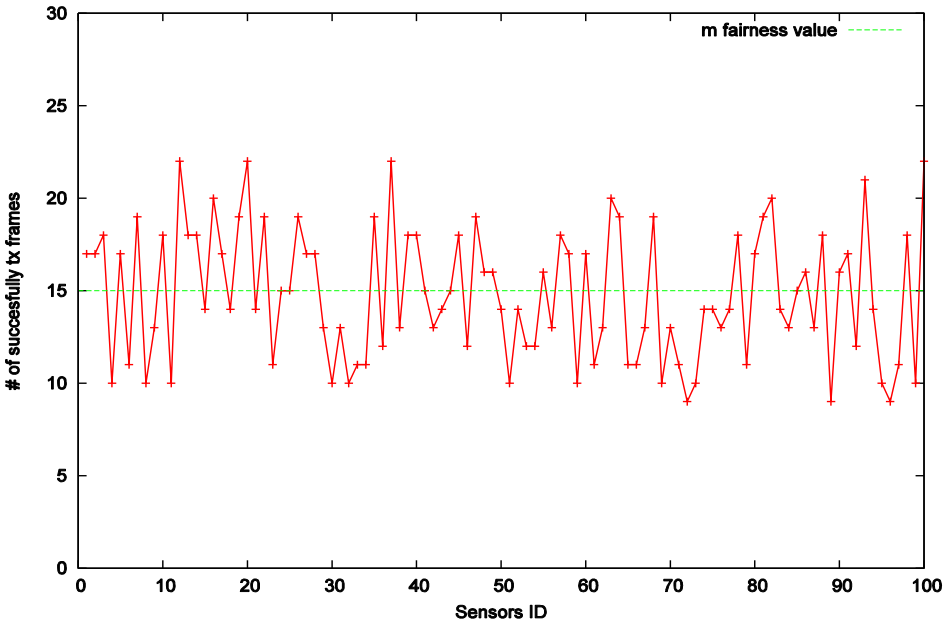


Figure 54. Successful tx frames versus sensor ID in a nanosatellite contact of 480 s.

## 6.4 Summary

In this chapter, I analyze, evaluate and optimize a new ALOHADP multiple access mechanism. I validate and optimize the main performance figures: throughput, delay and fairness. ALOHADP is a very simple protocol that is suitable to support data service for DTN nanosatellite based wireless sensor networks in a very efficient way. It assumes a finite population and saturated traffic condition. The effective throughput has been dynamically optimized by adapting the protocol parameters as a function of the current number of active sensors received from nanosatellite. I conclude that the proposed system provides a simple, optimal and fair usage of nanosatellite resources. In the next chapter, I will continue optimizing the transfer of data at the higher layers.

# 7 Delay/Disruption Tolerant Networking Optimization

In chapter 5, I propose a new architecture for a DTN nanosatellite based sensor network using a new Aloha contention based multiple access with gateway and downlink priority (ALOHAGP). In this Chapter, I investigate the reactive/proactive fragmentation of DTN bundles for this kind of scenario characterized by their small payload transmission capabilities. The optimized frame size used in our fragmented bundle is obtained through the analysis and simulations of the protocol ALOHADP fully analyzed in Chapter 6.

Nanosatellite-based sensor networks consider a low-cost small satellite (< 50 Kg) in low Earth orbit (LEO) acting as communication gateway for sensors distributed in places difficult to access. In highly disruptive environments, there are few solutions proposing a communication infrastructure to provide efficient simple data transmission with multiple access. Delay-Tolerant Networking (DTN) [51] [63] is an approach that tries to address technical issues of disruptive environments. In [59] we proposed a new architecture for a DTN nanosatellite-based sensor network using a new protocol named Aloha contention based multiple access with gateway and downlink priority (ALOHAGP).

The use of DTN for Nanosatellite-based Sensor Networks also has some challenges related to transmission optimization, delivery success and bundle fragmentation. Fragmentation techniques are classified in proactive fragmentation and reactive fragmentation. In proactive fragmentation, a node splits a bundle into fragments of a predetermined size prior to transmitting. In reactive fragmentation, the sender node starts sending the entire bundle and the bundle fragments are generated only when a link failure occurs, for example caused by a loss of visibility to the satellite. In this reactive fragmentation case both the sending node and the receiving node consider as a valid bundle both the original part of the bundle not sent and the part of the bundle which was received at the receiving node. In both cases the fragmented bundle is reassembled only at its destination.

The main disadvantage of the reactive fragmentation is that it is incompatible with the Bundle Authentication Block feature of the Bundle Security Protocol [64]. The usage of proactive fragmentation solves this problem, but requires determining the optimal bundle size, which is a non-resolved issue, highly dependent on the satellite visibility time and the contention mechanisms defined in the multiple access scheme used for sensor network within the nanosatellite coverage.

Related to the optimal size of a bundle, there is a lack of standard negotiation methods of bundle sizes that can be accepted by a bundle agent in satellite communications. Thus, too large bundles are dropped in proactive fragmentation.

In this chapter, I propose as main contribution of our work a message fragmentation assessment of DTN bundles in simulated environment characterized by high disruption and small payload transmission capabilities. I proposed a proactive fragmentation technique that considers an optimized frame size obtained through analysis and simulations of our proposed protocol ALOHAGP, which offers reliable delivery of DTN messages between sensor and nanosatellite node. In the analysis I balance the number of frames contained in the bundle with the probability of successfully reception of a given frame.

## 7.1 Distribution of the Number of Frames

Given the system described in chapter 6 and knowing the optimal access parameters evaluated there, we will obtain a probability density function of the number of frames that successfully arrive at Nanosatellite considering different visibility times (Figure 55). Using Matlab [65] program, we can fit the frame distribution obtained by simulation using a negative binomial distribution, this probability density function is given by:

$$f(x_i|r,p) = \frac{\Gamma(r+x_i)}{\Gamma(r)\Gamma(x_i+1)} p^r (1-p)^{x_i} \quad (17)$$

Where Γ is the gamma function, $x_i$ is the number of frames, p is the probability of success and r is the number of successes [66].
We chose this distribution because variance is much greater than mean ratio. We obtain a probability density (Theoretical) using a maximum likelihood estimate (MLE) considering a 95% confidence intervals, as it is shown in Figure 55.

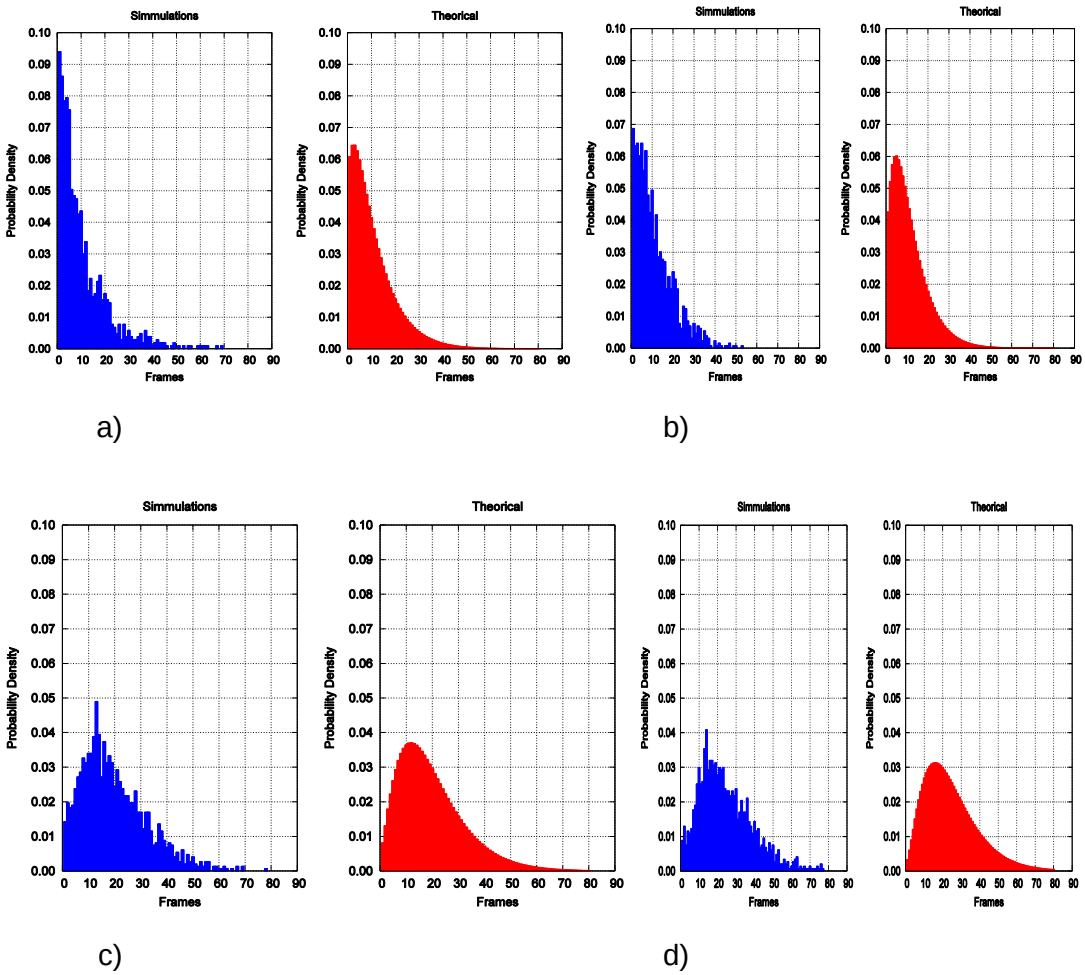


**Figure 55. Probability density vs number of frames with different visibility time a) 120s, b) 240s, c) 480s, d) 600s, obtained with simulation and fitted with theoretical results using a negative binomial distribution.**

The parameters obtained for this fitted negative binomial distribution are shown in Table 10. The r-, r+, p+ and p- show a 95% confidence interval.

**Table 10.** It shows r and p parameters of fitted negative binomial distribution with 95% confidence interval.

| Visibility time | r | r- | r+ | p | p- | p+ |
|---|---|---|---|---|---|---|
| 120 | 1.3949 | 1.2659 | 1.5239 | 0.1155 | 0.1045 | 0.1265 |
| 240 | 1.8526 | 1.6902 | 2.0150 | 0.1417 | 0.1298 | 0.1535 |
| 480 | 2.6429 | 2.4291 | 2.8567 | 0.1176 | 0.1085 | 0.1267 |
| 600 | 3.0324 | 2.7902 | 3.2745 | 0.11 | 0.1017 | 0.1184 |

We can use a multiple regression model to relate the visibility time (Tv) as a function of p and r parameters considering the values shown in Table 2. It was made using the R program [67], obtaining a probability density function of the number of frames x_i as a function of the visibility time. The p-value obtained for this regression is $\leq 0.05$. The multiple regression model used allow

us to obtain an equation relating r and Tv. Parameter p is observed constant while varying r and Tv: p=0.1155.
Thus, $r = f(T_v) = 3.39 * 10^{-3} * T_v + 1.01$ and the probability density of frame distribution will be given by:

$$f(x_i|T_v) = f(x_i|r,p) \quad (18)$$

## 7.2 Visibility Time Distribution

To obtain the visibility time distribution for the period of time defined in our scenario described before, we will use the STK [68] tool. We will consider two ground sensors located in two points with different latitude and longitude as shown in Table 11.

**Table 11.** Sensor parameters used in STK simulation.

| Sensor | Latitude (°) | Longitude (°) |
|---|---|---|
| A | -4.1 | -80.1 |
| B | 7.33 | 22.06 |

It can be seen in Figure 56 that during this period of time the satellite passes generate a circular coverage (footprint). The longest of visibility is given by the time it takes to traverse the greater arc formed within this circle.

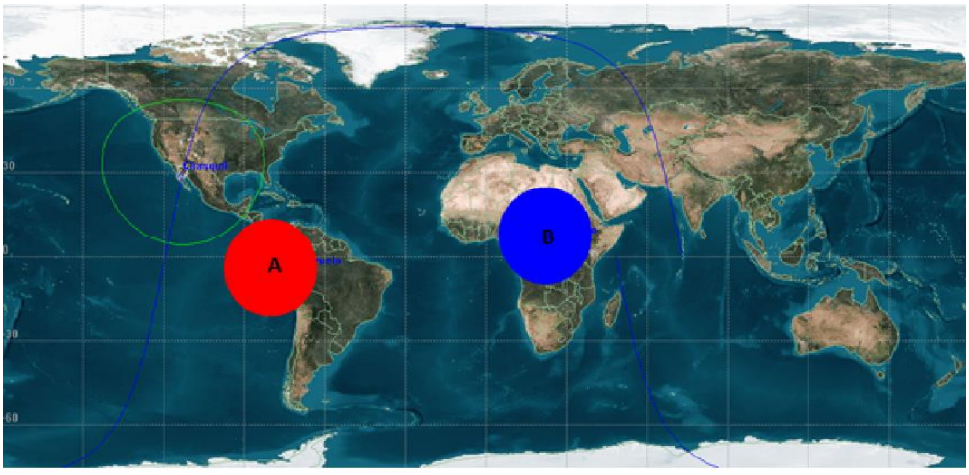


**Figure 56. Nanosatellite visibility area for two ground sensors: sensor A and sensor B**

Considering the visibility time obtained by STK for these two points, Figure 57 shows both the distribution and the probability density function of the visibility time (Tv).

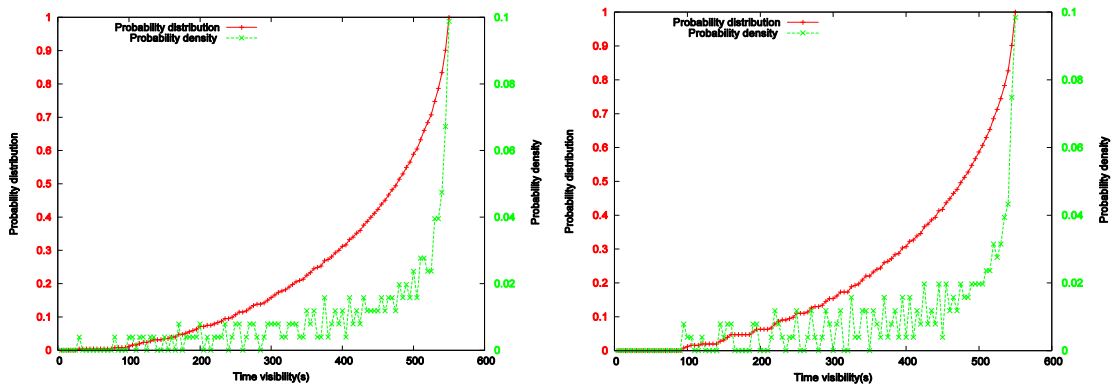


a) Sensor A b) Sensor B

**Figure 57. Probability distribution and density of visibility time for sensors a) Sensor A, b) Sensor B.**

Taking in consideration that the visibility area is circular (Figure 56), we consider that the visibility time ($T_v$) is directly proportional to the "visibility distance ($D_v$)". $D_v$ can be expressed as a function of the distance from the center ($D_c/2$) of the coverage circle as it is shown in Figure 58, where the more off-center visibility the less visibility time we have. We can establish that the visibility time is:

$$T_v = K\, D_v = K \sqrt{M^2 - {D_c}^2} \tag{19}$$

Where:
$T_v$: Visibility time <0…$T_m$>
$D_v$: Visibility distance
M: Coverage diameter
K: Constant value (inverse of the footprint speed)
$D_c/2$= Distance from the center.

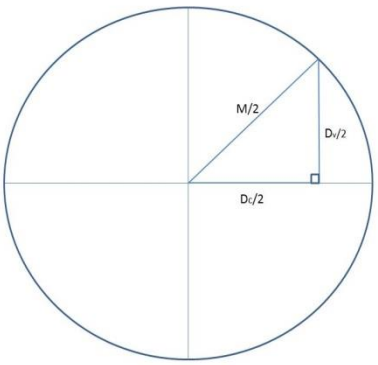


**Figure 58. Relation between visibility distance, coverage diameter and distance from the center for any visibility time.**

Considering that $T_m$ is the "Maximum visibility time (KM)" and $D_c/2$ is a random value distributed uniformly in the range [0…M/2], the probability distribution of having a visibility time $Y < T_v$ is given by:

$$P\ (Y <\ T_v) = \frac{T_m - \sqrt{{T_m}^2 - {T_v}^2}}{T_m} \tag{20}$$

And the probability density will be given by:

$$g(T_v) = \frac{T_v}{T_m \sqrt{{T_m}^2 - {T_v}^2}} \tag{21}$$

These theoretical distribution and probability density functions are shown in Figure 59 for the case of maximum visibility time for LEO orbit as described in our scenario. It is observed that the theoretical behavior of these functions matches with the simulation results that are presented in Figure 57.

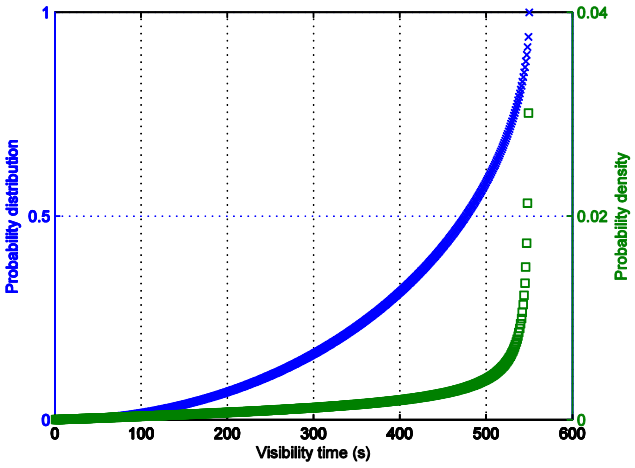


**Figure 59. Probability distribution and probability density of visibility time for a circular LEO orbit**

## 7.3 Probability distribution of the number of received frame

Our target is to obtain an optimal bundle size. The first step is to find a probability function $P(x_i)$, being $x_i$ each received frame, given a probability density of frame distribution $f(x_i,T_v)$ and a probability density of visibility time, $g(T_v)$, for all the visibility times, $T_v$.

$$P(x_i)\ =\ \int_0^{T_m} f(x_i, T_v) g(T_v)\, dT_v \tag{22}$$

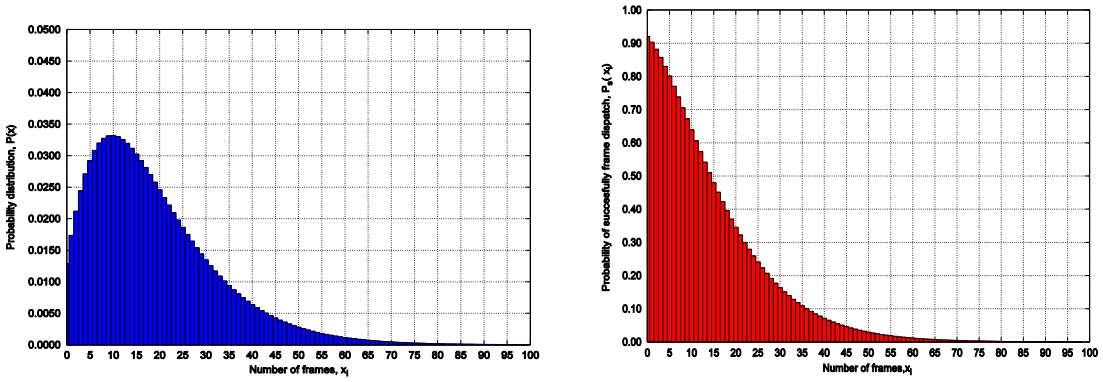


a) b)

**Figure 60. a) Probability distribution of the number of received frame in satellite LEO orbit. b) Probability of successfully frames dispatched.**

Taking in consideration the Equation 22, we could obtain the probability of successfully bundle reception when the bundle has a length of "$x_i$" frames as it is shown in Figure 60b obtained as:

$$P_s(x_i) = 1 - \sum_0^{i-1} P(\ x_j\ ) \tag{23}$$

## 7.4 Useful data sent per bundle

In Figure 61, we can observe the PDU and the header for each layer used in our simulations, using the values established in section 6.3. Considering a DTN schema this overhead is 51B and using CBHE [69] compressed bundle it is 22B [70]. The optimal ALOHAGP frame size (FS) used for N= 50 sensors is constant and equal to 304 B (see Figure 52) and it has an overhead of 30 B. Related to our previous analysis, tf = FS+30.

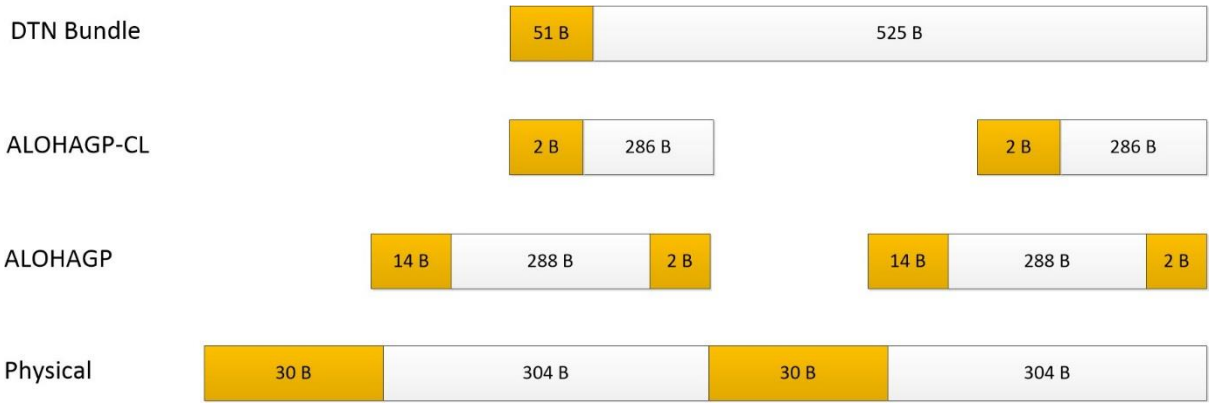

**Figure 61. PDU and header used in our simulation without CBHE when the bundle is fragmented in two frames.**

We could calculate the ratio of useful data sent per bundle ($C_u$), considering a bundle size with different ALOHAGP number of frames ($x_i$), as it is shown in Figure 61 and given by:

$$C_u(x_i) = F(x_i)/(FS + 30) \quad (24)$$

Where F(xi) is the mean useful bundle data per each frame when the bundle is fragmented into $x_i$ frames. We use the mean value as protocol headers are not uniformly distributed among the frames. Useful data $C_u$, may change depending on the DTN overhead. It is observed in Figure 62, that the DTN overhead with CBHE or without CBHE is important only for small bundle size (< 20 frames) because at higher number of frames the useful data sent per bundle is almost the same.

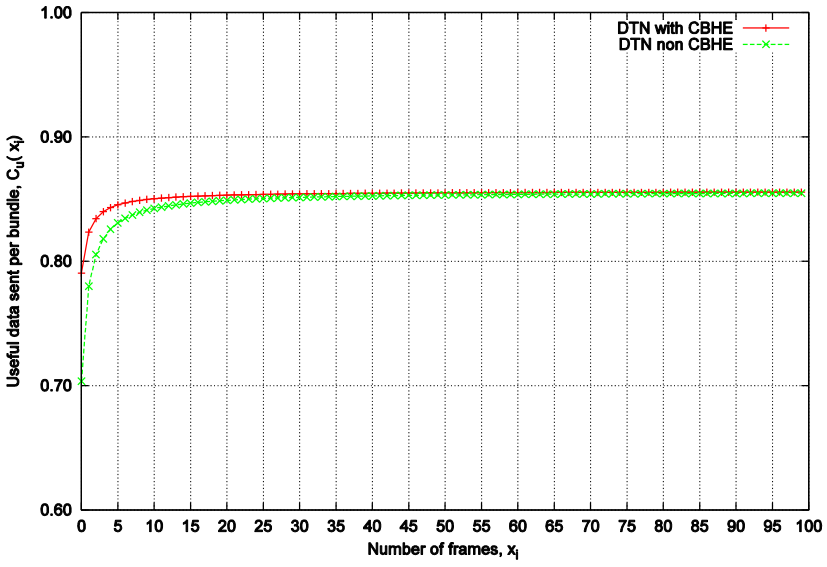


**Figure 62. Useful data sent per DTN bundle.**

## 7.5 Optimal bundle size

Finally, we could calculate the efficiency as a function of the bundle size (nº of frames per bundle) and probability of successfully reception of a given $x_i$ frame. Efficiency is given by:

$$E(x_i) = C_u(x_i) * P_s(x_i) \quad (25)$$

It is observed that the most efficient bundle size using DTN with CBHE is two frames per bundle giving us a bundle size of 572B (including 22B of bundle header). The most efficient bundle size if we use DTN without CBHE is three frames, which give us a bundle size of 858B (including 51B of bundle header).

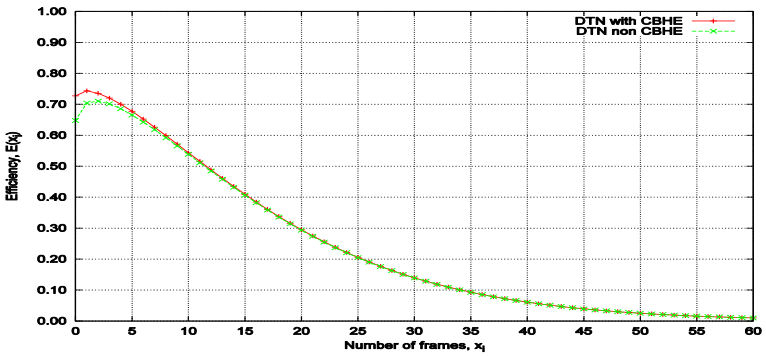


Figure 63. Efficiency vs Number of frames per bundle.

## 7.6 Message Fragmentation in DTN nanosatellite sensor network

### 7.6.1 Proactive Fragmentation

If we consider that a DTN bundle is fragmented using the optimal number of frames per bundle obtained in the last section (Figure 63), we can obtain the goodput values using CBHE and without CBHE as it is shown in Table 12 per each visibility time obtained in our simulation.
It can be seen in Table 12, that the mean goodput using CBHE is higher that the goodput without CBHE.

Table 12. Goodput vs visibility time using proactive fragmentation

| Mean goodput with CBHE (bps) | Mean goodput without CBHE (bps) | Mean visibility time (s) |
|---|---|---|
| 4838 | 4550 | 360 |

### 7.6.2 Reactive fragmentation

A different strategy which does not take into account the previous analysis of the sensor scenario and prior information about the satellite visibility time is the reactive fragmentation. In this case, the size of the fragmented bundle is the number of frames successfully received in the satellite of each sensor. Considering our simulations we can obtain the goodput on the nanosatellite, as shown in Table 13. We have considered a segment bundle with CBHE and without CBHE. One of the major problems is that reactive fragmentation is incompatible with the Bundle Authentication Block feature of the Bundle Security Protocol [64].

Table 13. Goodput vs visibility time using reactive fragmentation

| Goodput with CBHE (bps) | Goodput without CBHE (bps) | Visibility time (s) |
|---|---|---|
| 4996 | 4887 | 360 |

### 7.6.3 Comparative fragmentation

We can compare these two types of fragmentation strategies as it is shown in the Tables 12 and 13. We can observe that our proactive fragmentation proposal compared to reactive fragmentation using CBHE and not using CBHE are 97% and 93% respectively.

## 7.7 Summary

The use of DTN for Nanosatellite-based Sensor Networks in high disruption scenarios has some challenges related to the selection of the best fragmentation strategy and the optimal bundle size. In this chapter, I propose a message fragmentation assessment of DTN bundles by comparing the goodput (proactive effective throughput) in proactive and reactive bundle fragmentation.
Motivated by the incompatibility of the reactive fragmentation with the Bundle Authentication Block feature of the Bundle Security Protocol I propose a proactive fragmentation technique based on the determination of the optimal bundle size, dependent on the satellite visibility time and the contention mechanisms defined in the multiple access scheme used for sensor network within the nanosatellite coverage.
I perform an analysis and simulation of our ALOHAGP protocol to determine frame distribution arrival as a negative binomial distribution. Given a visibility time distribution for nanosatellite LEO orbits, I propose a new distribution function for the visibility time. Finally, I derive an optimal bundle size using a proactive fragmentation for this kind of scenarios. With this optimization I get efficiency very close (up to 97%) to the reactive fragmentation approach. Finally, in the next and last chapter I will show the main conclusions of the work achieved as part of this doctoral thesis.

# 8 Conclusions and Future Works

## 8.1 Conclusions

The motivation of this thesis is to contribute to the improvement of satellite communication services between a constellation of nanosatellites and ground stations (sensors, gateways) in a simple, efficient, optimal way, automatically and transparently integrated into Internet. In this thesis,

- I propose and evaluate a new communication architecture which is based on DTN to provide data service to a network of ground sensors, using satellite communications based on nanosatellites. It assumes a finite population and saturated traffic condition.
- I propose, analyze, evaluate and optimize a new ALOHAGP multiple access mechanism in terms of goodput, delay and fairness. I have found that is suitable to support data service for DTN nanosatellite based wireless sensor networks in a very efficient way.
- I investigate an optimal DTN message transfer employing a proactive fragmentation mechanism using cross layer optimization. I have found that a negative binomial distribution fits well a frame distribution arrival obtained from our simulations for this kind of scenario using ALOHAGP multiple access. Given a visibility time distribution for nanosatellite LEO orbits, we have proposed a new distribution function for the visibility time. Finally, we have derived an optimal bundle size using a proactive fragmentation for this kind of scenarios. With this optimization, we get efficiency very close to the reactive fragmentation approach.

These contributions meet the objectives raised in this thesis.

## 8.2 Future works

As future work, we will extend this work,

- To analyze a proactive fragmentation strategy knowing in advance the nanosatellite visibility time. This can be achieved by considering the predictive nature of the orbit of the satellite, where the satellite could inform through broadcast to all sensors within its coverage area about satellite's two-line element set (TLE).
- To investigate the presence of gateways and more satellites contacts.

# Publications

The author of this PhD dissertation has made a series of publications that can be classified as:

**Journals**

- H. Bedón, C. Miguel, A. Fernandez and J.S Park, "A DTN system for Nanosatellites Network using a new Aloha Multiple Access with Gateway Priority (ALOHAGP)", Smart Computing Review.
- H. Bedón, C. Miguel, A. Fernandez, F. Javier Ruiz, "Message Fragmentation Assessment in DTN Nanosatellite-based Sensor Networks", Ad Hoc Networks. Accepted (in review process).

**Book Chapter**

- J. Guzman, G. Comina, G. Rodriguez, H. Bedón, K. Surco, et al., "Global water pollution monitoring using a nanosatellite constellation (WAPOSAT)," Novel Ideas for Nanosatellite Constellation Missions, vol. 1, no 1, pp. 144-155, 2012.

**International Conferences**

- Bedón, H.; Negron, C.; Llantoy, J.; Nieto, C.M.; Asma, C.O.; , "Preliminary internetworking simulation of the QB50 cubesat constellation, "Communications (LATINCOM), 2010 IEEE Latin-American Conference on , vol., no., pp.1-6, 15-17 Sept. 2010
- Canales R, J.M.; Bedón, H.; Estela, J.; "First steps to establish a small satellite program in Peru," Aerospace Conference, 2010 IEEE, vol., no., pp.1-14, 6-13 March 2010.
- Seulki Lee , Tuan Anh Nguyen, Miseon Wi, Taehoon Eom, Jong Sou Park, Germán Comina, Hector Bedón; "Practical and Potential Applications of an Unmanned

Airship based on Automatic Control - Embedded Computer System Design", 11th International Conference on Computer Applications 2013 , 26-27 February, 2013, Yangon, Myanmar.

Otras publicaciones escritas por el autor, indirectamente relacionadas con esta tesis:

- Panta I, Sánchez J, Bedón H, Mondragón M; "Monitoreo en tiempo real y Predicción de Deslizamientos & Avalanchas en Zonas con Alto Riesgo en la Vertiente del Nevado Huascarán"; III Congreso Internacional de Ingeniería Física, 10-14 Septiembre del 2012. Medellin, Colombia.
- Kawashima R, Rustem A, Stancato F, Bedón H, Mugwe J, et al; "Results and future perspectives of the mission idea contest", 3rd Nanosatellite Symposium, 12-14 December de 2011, Kytakyushu,Japon.

# References


[1] H. Heidt, J. Puig-Suari, A. S. Moore, S. Nakasuka, and R. J. Twiggs, "CubeSat: A new Generation of Picosatellite for Education and Industry Low-Cost Space Experimentation," in *14TH Annual/USU Conference on Small Satellites*, 2000.

[2] "CubeSat Database - swartwout." [Online]. Available: https://sites.google.com/a/slu.edu/swartwout/home/cubesat-database. [Accessed: 30-Nov-2015].

[3] "Libertad 1 - Wikipedia, the free encyclopedia." [Online]. Available: https://en.wikipedia.org/wiki/Libertad_1. [Accessed: 30-Nov-2015].

[4] J. M. Canales R., H. Bedon, and J. Estela, "First steps to establish a small satellite program in Peru," in *2010 IEEE Aerospace Conference*, 2010, pp. 1–14.

[5] "Satélites: PUCP-Sat-1 Satellites: PUCP-Sat-1Satelliten: PUCP-Sat-1 » PUCP | Instituto de Radioastronomía." [Online]. Available: http://inras.pucp.edu.pe/proyectos/pucp-sat-1/?lang=es. [Accessed: 30-Nov-2015].

[6] "UAPSAT 1." [Online]. Available: http://www.uap.edu.pe/uapsat/AcercaDe.aspx. [Accessed: 30-Nov-2015].

[7] A. Castro, R. Walker, F. Emma, F. Aguado, R. Tubio, and W. Balogh, "The Humsat system and the ESA GEOID Initiative," *ESA Bulletin*, pp. 45–50, 2012.

[8] J. Guzman, G. Comina, G. Rodriguez, H. Bedon, K. Surco, C. Negron, J. Sanchez, M. Mondragon, and T. Tuesta, "Global water pollution monitoring using a nanosatellite constellation (WAPOSAT)," in *Novel Ideas for Nanosatellite Constellation Missions*, 2012, pp. 144–155.

[9] Von Karman Institute, "QB50 Project," 2014. [Online]. Available: https://www.qb50.eu/.

[10] "JPL | Cubesat | MarCO." [Online]. Available: http://www.jpl.nasa.gov/cubesat/missions/marco.php. [Accessed: 30-Nov-2015].

[11] P. Banazadeh, J. Lazio, D. Jones, D. P. Scharf, W. Fowler, and C. Aladangady, "Feasibility analysis of XSOLANTRA: A mission concept to detect exoplanets with an array of CubeSats," in *2013 IEEE Aerospace Conference*, 2013, pp. 1–20.

[12] "Loon for All – Project Loon – Google." [Online]. Available: http://www.google.com/loon/. [Accessed: 30-Nov-2015].

[13] "Connecting the World from the Sky." [Online]. Available: https://fbcdn-dragon-a.akamaihd.net/hphotos-ak-ash3/t39.2365-6/851574_611544752265540_1262758947_n.pdf. [Accessed: 30-Nov-2015].

[14] "Samsung wants to deliver the internet via thousands of satellites | ExtremeTech." [Online]. Available: http://www.extremetech.com/extreme/212240-samsung-wants-to-deliver-the-internet-via-thousands-of-satellites. [Accessed: 30-Nov-2015].

[15] "Welcome to your planet - Planet Labs - Planet Labs." [Online]. Available: https://www.planet.com/. [Accessed: 30-Nov-2015].

[16] N. Abramson, "Multiple access in wireless digital networks," *Proc. IEEE*, vol. 82, no. 9, pp. 1360–1370, 1994.

[17] L. E. Miller, “Performance analysis of exponential backoff,” *IEEE/ACM Trans. Netw.*, vol. 13, no. 2, pp. 343–355, Apr. 2005.
[18] J. Goodman, A. G. Greenberg, N. Madras, and P. March, “Stability of binary exponential backoff,” *J. ACM*, vol. 35, no. 3, pp. 579–602, Jun. 1988.
[19] Z. J. Haas, “On optimizing the backoff interval for random access schemes,” *IEEE Trans. Commun.*, vol. 51, no. 12, pp. 2081–2090, Dec. 2003.
[20] J.-B. Seo and V. C. M. Leung, “Analysis of an Exponential Backoff Algorithm for Multipacket Reception Slotted ALOHA Systems,” in *2010 IEEE International Conference on Communications*, 2010, pp. 1–5.
[21] A. U. H. Sheikh, “Analysis of finite population buffered slotted ALOHA protocols using tagged user analysis (TUA),” in *IEEE GLOBECOM 1998 (Cat. NO. 98CH36250)*, 1998, vol. 3, pp. 1652–1657.
[22] J. H. Sarker and H. T. Mouftah, “Maximizing Throughput with Multiple Power Levels in a Random Access Infrastructure-Less Radio System,” in *2009 IEEE International Conference on Communications*, 2009, pp. 1–6.
[23] J. H. Sarker and H. T. Mouftah, “Mitigating the effect of jamming signals in wireless ad hoc and sensor networks,” *IET Commun.*, vol. 6, no. 3, p. 311, 2012.
[24] S. Burleigh, V. Cerf, R. Durst, K. Fall, A. Hooke, K. Scott, and H. Weiss, “The interplanetary internet: A communications infrastructure for Mars exploration,” *Acta Astronaut.*, vol. 53, no. 4–10, pp. 365–373, Aug. 2003.
[25] W. Ivancic, W. M. Eddy, D. Stewart, L. Wood, P. Holliday, C. Jackson, and J. Northam, “Experience with Delay-Tolerant Networking from Orbit,” in *2008 4th Advanced Satellite Mobile Systems*, 2008, pp. 167–172.
[26] J. Wyatt, S. Burleigh, R. Jones, L. Torgerson, and S. Wissler, “Disruption Tolerant Networking Flight Validation Experiment on NASA’s EPOXI Mission,” in *2009 First International Conference on Advances in Satellite and Space Communications*, 2009, pp. 187–196.
[27] A. Jenkins, S. Kuzminsky, K. K. Gifford, R. L. Pitts, and K. Nichols, “Delay/Disruption-Tolerant Networking: Flight test results from the international space station,” in *2010 IEEE Aerospace Conference*, 2010, pp. 1–8.
[28] N. Magaia, P. R. Pereira, A. Casaca, J. J. P. C. Rodrigues, J. A. Dias, J. N. Isento, C. Cervello-Pastor, and J. Gallego, “Bundles fragmentation in Vehicular Delay-Tolerant Networks,” in *2011 7th EURO-NGI Conference on Next Generation Internet Networks*, 2011, pp. 1–6.
[29] M. Pitkanen, A. Keranen, and J. Ott, “Message fragmentation in opportunistic DTNs,” in *2008 International Symposium on a World of Wireless, Mobile and Multimedia Networks*, 2008, pp. 1–7.
[30] P. Ginzboorg, V. Niemi, and J. Ott, “Fragmentation algorithms for DTN links,” *Comput. Commun.*, vol. 36, no. 3, pp. 279–290, Feb. 2013.
[31] L. Wood, W. M. Eddy, and P. Holliday, “A bundle of problems,” in *2009 IEEE Aerospace conference*, 2009, pp. 1–17.
[32] W. D. Ivancic, P. Paulsen, D. Stewart, W. Eddy, J. McKim, J. Taylor, S. Lynch, J. Heberle, J. Northam, C. Jackson, and L. Wood, “Large File Transfers from Space Using Multiple Ground Terminals and Delay-Tolerant Networking,” in *2010 IEEE Global Telecommunications Conference GLOBECOM 2010*, 2010, pp. 1–6.
[33] C. V. Samaras and V. Tsaoussidis, “Adjusting transport segmentation policy of DTN Bundle Protocol under synergy with lower layers,” *J. Syst. Softw.*, vol. 84, no. 2, pp. 226–237, Feb. 2011.
[34] “UNISEC.” [Online]. Available: http://www.unisec.jp/flash/index-e.html. [Accessed: 01-Dec-2015].
[35] Ramon Martinez Rodriguez-Osorio and Enrique Fueyo Ramírez, “A Hands-On Education Project: Antenna Design for Inter-CubeSat Communications [Education Column],” *IEEE Antennas Propag. Mag.*, vol. 54, no. 5, pp. 211–224, Oct. 2012.
[36] H. Bedon, C. Negron, J. Llantoy, C. M. Nieto, and C. O. Asma, “Preliminary internetworking simulation of the QB50 cubesat constellation,” *Commun. (LATINCOM),*

*2010 IEEE Latin-American Conf.*, 2010.
[37] "Water Management | UNESCO-IHE." [Online]. Available: https://www.unesco-ihe.org/water-management. [Accessed: 01-Dec-2015].
[38] "WHO | Water."
[39] "Water Quality | Water, Sanitation and Hygiene | UNICEF." [Online]. Available: http://www.unicef.org/wash/index_43106.html. [Accessed: 01-Dec-2015].
[40] "UN-Water: Home." [Online]. Available: http://www.unwater.org/. [Accessed: 01-Dec-2015].
[41] "Monitor Global - Tudo sobre Espaço, Ciência e Tecnologia." [Online]. Available: http://monitorglobal.com.br/novo/. [Accessed: 02-Dec-2015].
[42] "HOTSPOTS -University of Hawaii." [Online]. Available: http://modis.higp.hawaii.edu/. [Accessed: 02-Dec-2015].
[43] "Real-Time Internet Monitor | Akamai." [Online]. Available: https://www.akamai.com/us/en/solutions/intelligent-platform/visualizing-akamai/real-time-web-monitor.jsp. [Accessed: 02-Dec-2015].
[44] N. E. S. R. L. US Department of Commerce, "CarbonTracker CT2013B - ESRL Global Monitoring Division."
[45] E. P. A. (EPA), "Reports & SAFER-Data."
[46] "US Geological Survey Real-Time Water Quality Data For the Nation." [Online]. Available: http://nrtwq.usgs.gov/. [Accessed: 02-Dec-2015].
[47] G. Comina, S. Holmin, P. Ivarsson, F. Winquist, and C. Krantz-Rülcker, "COD monitoring of waste water using an electronic tongue," in *2nd SENSPOL Workshop response to new pollution challenges*, p. 22.
[48] "Development of a Portable Water Quality Analyzer," *Sensors & Transducers Journal*, 2010. [Online]. Available: http://www.sensorsportal.com/HTML/DIGEST/P_659.htm. [Accessed: 02-Dec-2015].
[49] "Cubesatshop.com." [Online]. Available: http://www.cubesatshop.com/. [Accessed: 02-Dec-2015].
[50] L. Wood, W. Ivancic, W. Eddy, D. Stewart, J. Northam, and C. Jackson, "Investigating operation of the Internet in orbit: Five years of collaboration around CLEO," p. 2, Apr. 2012.
[51] V. Cerf, S. Burleigh, A. Hooke, L. Torgerson, R. Durst, K. Scott, K. Fall, and H. Weiss, "Delay-Tolerant Networking Architecture," *IETF Request for Comments, RFC 4838*. 2007.
[52] L. Wood, W. M. Eddy, W. Ivancic, J. McKim, and C. Jackson, "Saratoga: a Delay-Tolerant Networking convergence layer with efficient link utilization," in *2007 International Workshop on Satellite and Space Communications*, 2007, pp. 168–172.
[53] C. Caini, P. Cornice, R. Firrincieli, M. Livini, and D. Lacamera, "TCP, PEP and DTN performance on disruptive satellite channels," in *2009 International Workshop on Satellite and Space Communications*, 2009, pp. 371–375.
[54] C. Casetti, M. Gerla, S. Mascolo, M. Y. Sanadidi, and R. Wang, "TCP westwood: end-to-end congestion control for wired/wireless networks," *Wirel. Networks*, vol. 8, no. 5, pp. 467–479, Sep. 2002.
[55] "The Network Simulator - ns-2." [Online]. Available: http://www.isi.edu/nsnam/ns/. [Accessed: 05-May-2014].
[56] "Global Educational Network for Satellite Operations / Education / ESA." [Online]. Available: http://www.esa.int/Education/Global_Educational_Network_for_Satellite_Operations. [Accessed: 02-Dec-2015].
[57] J. Martin Canales, G. Rodriguez, J. Estela, and N. Krishnamurthy, "Design of a Peruvian small satellite network," in *2010 IEEE Aerospace Conference*, 2010, pp. 1–8.
[58] "TCP Evaluation Suite." [Online]. Available: http://nrlweb.cs.ucla.edu/tcpsuite/. [Accessed: 02-Dec-2015].
[59] H. Bedon, C. Miguel, A. Fernandez, and J. Sou Park, "A DTN System for Nanosatellite-based Sensor Networks using a New ALOHA Multiple Access with Gateway Priority,"

*Smart Comput. Rev.*, vol. 3, no. 5, pp. 383–396, Oct. 2013.

[60] J. Ott, M. Demmer, and S. Perreault, "Delay Tolerant Networking TCP Convergence Layer Protocol."

[61] K. A. Bartlett, R. A. Scantlebury, and P. T. Wilkinson, "A note on reliable full-duplex transmission over half-duplex links," *Commun. ACM*, vol. 12, no. 5, pp. 260–261, May 1969.

[62] H. Boiardt and C. Rodriguez, "Low Earth Orbit nanosatellite communications using Iridium's network," *IEEE Aerosp. Electron. Syst. Mag.*, vol. 25, no. 9, pp. 35–39, Sep. 2010.

[63] K. Scott and S. Burleigh, "Bundle Protocol Specification," *IETF Request for Comments, RFC 5050*. 2007.

[64] S. Symington, S. Farrell, H. Weiss, and P. Lovell, "Bundle Security Protocol Specification," *IETF Request for Comments, RFC 6257*. 2011.

[65] "MATLAB - The Language of Technical Computing." [Online]. Available: http://www.mathworks.com/products/matlab/. [Accessed: 06-May-2014].

[66] "Negative Binomial Distribution - MATLAB & Simulink." [Online]. Available: http://www.mathworks.com/help/stats/negative-binomial-distribution.html#brn2ivz-105. [Accessed: 06-May-2014].

[67] "The R Project for Statistical Computing." [Online]. Available: http://www.r-project.org/index.html. [Accessed: 06-May-2014].

[68] "AGI - software to model, analyze and visualize space, defense and intelligence systems." [Online]. Available: http://www.agi.com/products/stk/modules/default.aspx/id/stk-free. [Accessed: 05-May-2014].

[69] S. Burleigh, "Compressed Bundle Header Encoding (CBHE)," *IETF Request for Comments, RFC 6260*. 2011.

[70] L. Clare, S. Burleigh, and K. Scott, "Endpoint naming for space delay / Disruption Tolerant Networking," in *2010 IEEE Aerospace Conference*, 2010, pp. 1–10.